The Therapeutic Potential of Mesenchymal Stem Cells & FGF8 in Chronic Demyelinating Diseases

Pablo Cruz Martinez

Tesis doctoral

Esta tesis doctoral ha sido llevada a cabo en el Instituto de Neurociencias de Alicante
(Consejo Superior de Investigaciones Científicas - Universidad Miguel Hernández), para la
obtención del grado de Doctor en Neurociencias de la UAB (Universidad Autónoma de Barcelona)

Director de tesis: Dr. Salvador Martínez Pérez
Codirector: Dr. Jonathan Richard Jones Barberá

Tutor UAB: Dr. Enrique Claro Izaguirre

Instituto de Neurociencias
Universidad Autónoma de Barcelona
-2015-

El Director, Codirector y Tutor de esta tesis doctoral AUTORIZAN:

La presentación de la Tesis Doctoral titulada: "THE THERAPEUTIC POTENTIAL OF MESENCHYMAL STEM CELLS & FGF8 IN CHRONIC DEMYELINATING DISEASES", realizada por D. Pablo Cruz Martinez, bajo su inmediata dirección y supervisión, para la obtención del grado de Doctor en Neurociencias por la Universidad Autónoma de Barcelona.

Y para que así conste a los efectos oportunos, firman el presente certificado, en San Juan de Alicante, a 27 de Mayo de 2015.

Director de tesis   **Co-Director**

Dr. Salvador Martinez Pérez   Dr. Jonathan Richard Jones Barberá

Tutor UAB   **Doctorando**

Dr. Enrique Claro Izaguirre   D. Pablo Cruz Martinez

AGRADECIMIENTOS

Desde estas líneas pretendo expresar mi más sincero agradecimiento a todas aquellas personas que durante estos años de trabajo han estado a mi lado, apoyándome y que de una forma u otra han contribuido no sólo a que esta tesis doctoral sea hoy una realidad, sino también a ayudarme a crecer como persona y científico.

En primer lugar quiero agradecer de manera muy especial a toda mi familia. Sin lugar a dudas, es la pieza más importante de mi vida, y sin ellos no habría podido llevar a cabo esta tesis doctoral.

Especial agradecimiento merecen mis padres, cuyo amor incondicional y apoyo, hacen que me sienta feliz cada día. Gracias por todos los esfuerzos y sacrificios que habéis hecho a lo largo de la vida, para intentar ofrecerme siempre lo mejor. Nunca podré agradeceros lo suficiente todo lo que hacéis por mí. Simplemente sois los mejores padres que uno pueda tener y me siento orgulloso de ser vuestro hijo. Esta tesis doctoral quiero dedicárosla a vosotros.

A ti Lucía, por ser como eres y estar a mi lado siempre que te necesito. Si pudiera elegir, te elegiría 100 veces como hermana. Sé que siempre estaremos juntos y nos tendremos el uno al otro. A mis abuelos, por todo el amor, cariño y apoyo que siempre me habéis dado, por haberme cuidado tanto, y estar siempre a mi lado. A mis tíos y primos, por poder contar con vosotros siempre que os he necesitado. Y a todos los miembros de mi familia. Gracias de corazón.

Tras mi familia, a la primera persona que quiero agradecer por haber confiado en mí y abrirme las puertas de su laboratorio, es a mi director de tesis, Salvador Martínez. Gracias por tu dedicación, criterio y aliento, así como por la libertad que me has dado para trabajar en todo momento. Gracias por preocuparte por mi formación, permitiéndome ir a tantos cursos y congresos. Siempre que te he necesitado has estado ahí y me has tratado con gran respeto y cariño. Ha sido un privilegio poder contar con tu guía y ayuda.

Cuando me encontraba finalizando mis estudios de máster en Reino Unido, contacté con él para realizar el doctorado en su laboratorio, sin conocer a nadie, ni tener ningún tipo de referencia. Lo único que sabía era que me atraían mucho las líneas de investigación que estaban desarrollando, y que quería hacer la tesis en su grupo. Uno tiene siempre esa incertidumbre de si habrá tomado la decisión correcta, y que tipo de gente encontrará en su nuevo destino. A día de hoy, he de decir que tuve muchísima suerte de encontrarme con Salvador y esa gran familia que su grupo forma. No soy capaz de imaginar otro laboratorio en el que uno se pueda sentir mejor y haya más compañerismo que en este. Hacen que lo más difícil parezca realmente fácil.

Quiero continuar mostrando mi gratitud y más sincero cariño a una persona muy especial, mi codirector de tesis, Jon. Por tener siempre la puerta abierta para resolver dudas, atender quejas y en general, solucionar todo tipo de problemas que han surgido en el desarrollo de este trabajo. Para mí no solo ha sido el mejor codirector de tesis y mentor que uno pueda tener, sino que me ha demostrado en todo momento que es un amigo al que siempre podré recurrir. Gracias por darme la oportunidad de haber trabajado a tu lado.

Me gustaría también dar las gracias a una persona muy especial, Roberta, por todo tu amor y apoyo, por las críticas constructivas y por tu ayuda en la elaboración de esta tesis. Gracias por confiar siempre en mí, estando a mi lado y haciendo que todo sea mucho más sencillo. Sin ti esta tesis doctoral habría sido muy diferente.

Igualmente quiero agradecer a Alicia por toda su ayuda, enseñanzas y por poder contar con ella para cualquier cosa que haya surgido. Es una de las personas de las que más he aprendido y ha sido un placer el poder trabajar con ella.

Gracias a mis compañeros Edu "Junior" y Alejandro "Xispi" por ser mis guías y gurús electrofisiológicos, así como un par de grandes amigos con los cuales he vivido tantas experiencias y anécdotas durante estos años. Igualmente a Emilio Geijo y a Laura por darme la oportunidad de realizar esta parte de mi tesis en su laboratorio, así como por su ayuda.

A todo el equipo técnico y de soporte del laboratorio (Mónica, Olga, Paqui, Marusa y Carol), por prestarme vuestra ayuda siempre que la he necesitado, por estar disponible en cualquier momento para resolver una duda o consulta y por ponerme las cosas tan fáciles. Especialmente, gracias a Carol por su paciencia y ayuda con los Western. Sinceramente, ha sido un placer poder trabajar con todas vosotras.

A Eduardo de Puelles y Diego Echevarría, por acogerme con los brazos abiertos en su laboratorio, por crear ese ambiente de paz y armonía cada día y por hacerme sentir que podía contar con vosotros para cualquier cosa. Sois dos grandes investigadores y mejor persona. También palabras de agradecimiento y afecto al profesor Constantino Sotelo, por formar parte de esta gran familia y por su gran aportación científica.

Al resto de compañeros de doctorado, del "Puelles corner", Juan Antonio, Valentina, Pili y Jesús, al "Jonas" Abra, a los "Xispas" Edu y Alejandro, a Maria, Victor, y a los estudiantes de máster, Aitor, Rita y Cristina. Gracias también al resto de compañeros del laboratorio, Arancha, Almudena, Raquel, Mari Paz, Ana, Elena, Loli, Diego Pastor y Carlos, así como a diferentes personas que han ido pasando por el laboratorio a lo largo de estos años. Gracias por todo vuestro apoyo, por las risas y los viajes, por los congresos, Neuroabengibre, por esas charlas en las comidas y todos esos momentazos, y en definitiva, por hacer tan entrañable cada día que hemos compartido juntos durante esta travesía. Ha sido una experiencia única e irrepetible, y sé que será difícil o casi

imposible encontrar compañeros como vosotros en ningún otro sitio.

A todos mis amigos de Cofrentes, Valencia, Cambridge, y tantos otros lugares… por formar parte de mi vida y haber estado siempre junto a mí, sois los mejores amigos que uno pueda imaginar.

Al Dr. Robin Franklin y al Dr. Chao Zhao por permitirme realizar una estancia en su laboratorio del "Stem Cell Institute" de Cambridge, y por sus sabios consejos. Así como a todas las maravillosas personas que allí conocí.

A mis antiguos directores de tesis de máster, el Dr. Selim Cellek y la Dra. Jenny Carmichael, por vuestra ayuda, dedicación y por acceder a ser los dos evaluadores externos de esta tesis.

A mi tutor de la UAB, Enrique Claro, por toda su ayuda y simpatía.

A los miembros del tribunal de esta tesis por querer formar parte de ese día tan especial.

A todo el personal del Instituto de Neurociencias de Alicante y al equipo del animalario. Igualmente a toda la gente de la Universidad Autónoma de Barcelona, la Universidad Miguel Hernández y la Universidad de Cambridge por el soporte y ayuda. Todos habéis formado parte de este viaje.

Y por último, a todas aquellas personas, que aunque no aparecen aquí con nombres y apellidos, han estado presentes de alguna forma durante el desarrollo de este trabajo y han hecho posible que hoy vea la luz.

A todos mi eterno agradecimiento.

TABLE OF CONTENTS

ABSTRACT

Several researchers have demonstrated the therapeutic potential of mesenchymal stem cells (MSCs) in various neurodegenerative disorders, including demyelinating diseases. However, this effect was generally observed only locally, in the surrounding area where the MSCs were transplanted. Moreover, current treatments modifying the pathological mechanisms are capable of ameliorating the disease symptoms, but are frequently insufficient to repress the progressive loss of myelin and promote functional recovery. Thus, in order to achieve general remyelination in various brain structures simultaneously, bone marrow-derived MSCs were transplanted into the lateral ventricles of chronic demyelinated mice. In this manner, the first section of this work shows that the cells may secrete soluble trophic factors into the cerebrospinal fluid (CSF) and boost the endogenous oligodendrogenic potential of the subventricular zone (SVZ). The results indicated an enhanced recruitment of oligodendrocyte progenitor cells (OPCs) within the corpus callosum (CC) over time, which was correlated with an increase in myelin content. Electrophysiological studies, together with electron microscopy analysis corroborated that the newly-formed myelin was functional. Whereas the number of astrocytes seemed to be unaffected, an enhancement in the proliferation of neural stem progenitor cells (NSPCs) was detected in the SVZ, possibly due to their contact with the tropic factors released in the CSF. Hence, the findings of this study revealed that MSCs intraventricular-injection is a feasible method to elicit a paracrine effect in the oligodendrogenic niche of the SVZ, which is prone to respond to the secreted factors and therefore promoting oligodendrogenesis and functional remyelination. Similarly, the second part of this work reveals that the fibroblast growth factor 8 (FGF8), a key molecular signal for early embryonic development of the central nervous system, was capable of activating mouse post-natal OPCs *in vitro*. The results demonstrated that FGF8 is a novel factor to induce OPCs activation, migration, and increase their proliferation, without impairing their differentiation. In conclusion, both strategies were proven as very interesting alternative treatments for demyelinating diseases.

LIST OF FIGURES

LIST OF TABLES

LIST OF ABBREVIATIONS

ACSF	Artifical Cerebrospinal Fluid
AIGF	Androgen-induced Growth Factor
APC	Antigen Presenting Cell
BBB	Blood Brain Barrier
BSA	Bovine Serum Albumin
CAP	Compound Axon Potentials
CC	Corpus Callosum
CM	Conditioned Medium
CNS	Central Nervous System
CSF	Cerebrospinal Fluid
DMT	Disease-modifying Drugs
EAE	Experimental Autoimmune Encephalomyelitis
ECM	Extracellular Matrix
EM	Electron Microscopy
ERK	Extracellular Signal Regulated Kinase
FGF	Fibroblast Growth Factor
FGFR	Fibroblast Growth Factor Receptor
GFAP	Glial Fibrillary Acidic Protein
ICC	Immunocitochemistry
IF	Immunofluorescence
IHC	Immunohistochemistry
LV	Lateral Ventricle
MAPK	Mitogen-activated Protein Kinase
MBP	Myelin Basic Protein
MHV	Mouse Hepatitis Virus
MOG	Myelin Oligodendrocytic Protein
MS	Multiple Sclerosis
MSC	Mesenchymal Stem Cell
NSPC	Neural Stem Progenitor Cell
OPC	Oligodendrocyte Progenitor Cell
PDGF	Platelet Derived Growth Factor

PI3K	Phospatidylinositol-3 kinase
PLP	Proteolipidic Protein
PNS	Peripheric Nervous System
PVWM	Perivascular White Matter
SGZ	Subgranular zone
SVZ	Subventricular Zone
Th	T Helper
V-SVZ	Ventricular Subventricular Zone
WM	White Matter

Chapter I

- INTRODUCTION -

1.1 Organisation of the vertebrate nervous system

The nervous system is the most complex system that vertebrates developed throughout evolution, regulating crucial functions ranging from sensory perception and motor coordination to cognitive features such as learning and memory. The mammalian nervous system can be subdivided into two distinct morphological and functional entities, the CNS, including the brain and the spinal cord, and the PNS, which contains the cranial and spinal nerves as well as the connections between the CNS and the target organs of the body. The CNS is a control center that integrates all input signals from the PNS to process the information and eventually evoke an appropriate response. The PNS, on the other hand, provides the sensory and motor wiring to convey and elicit the answers to the rest of the body in a voluntary (somatic nervous system) or involuntary manner (autonomic nervous system) (Kandel et al., 2000).

The major cellular components of the nervous system are the neurons, which conduct electrical impulses to another neuron or to other cell types by synaptic communication; and the glial cells, which are much more abundant than neurons, having important developmental, supportive and trophic roles critical for the normal function of the nervous tissue. Virchow first described that there were cells other than neurons. He thought that it was the connective tissue of the brain, which he called "nervenkitt" (nerve glue), i.e., neuroglia (Virchow, 1846). The name survived, although the original concept radically changed. The characterization of the major glial cell types was the result of microscopic studies, and especially the techniques of metallic impregnation developed by Ramon y Cajal and Rio Hortega (Rio Hortega, 1928; Ramon y Cajal, 1913b). Our understanding of the role of the glia in the CNS function has drastically progressed in recent years. We know now that glial cells are subdivided into astrocytes, microglia and the myelin forming cells (oligodendrocytes in the CNS and Schwann cells in the PNS) (Figure 1). Each of these cell types performs different essential tasks in the CNS. Astrocytes form a selective filter around the brain capillaries, the blood brain barrier (BBB), that prevents toxic substances and pathogens in the blood from entering the CNS, while other substances are allowed to enter freely. They also support neurons by providing energy, specific substrates and facilitate the formation, maintenance and function of synapses (Allen and Barres, 2009). Following injury, these cells are major regulators of neuronal and myelin repair. The microglia are the resident macrophages of the brain and spinal cord, and thus act as the

first and main form of active immune defense in the CNS, being responsible of eliminating dead cell debris (Graeber et al., 2011). Two types of glial cells (oligodendrocytes and Schwann cells) produce myelin sheaths used to insulate nerve axons, thereby allowing the fast saltatory conduction of the action potential, increasing the speed of its propagation in function of the diameter of the axon (Hartline and Colman, 2007). Moreover, the myelin sheath provides trophic support to the axon during all its life (Nave and Trapp, 2008).
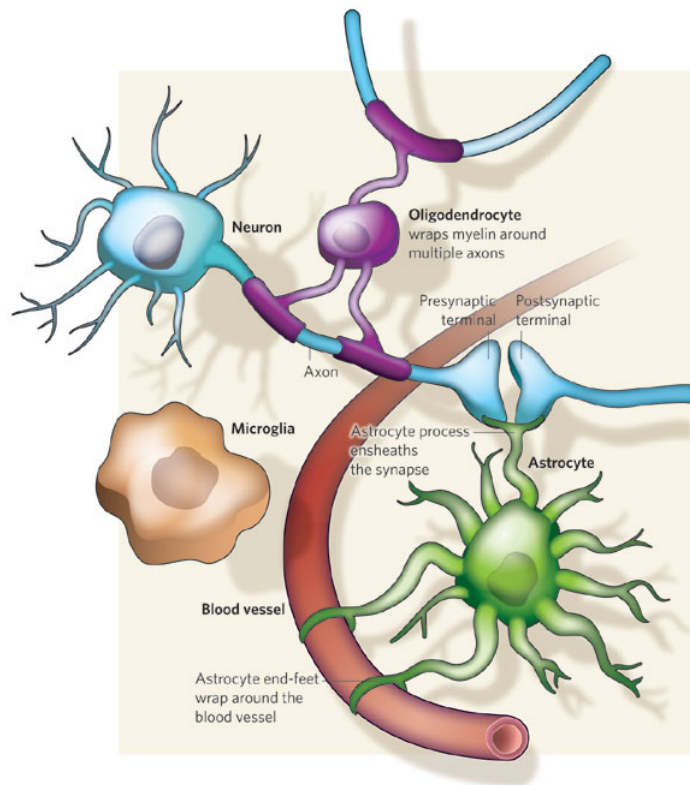
Figure 1. Cells of the central nervous system. Schematic drawing of different glial cells, their interactions with neurons and the surrounding blood vessels. (Allen and Barres, 2009).

1.2 Myelin

During evolution, different organisms have demonstrated a need to increase the conduction speed of the electrical impulse, which can be accomplished by two different mechanisms. One way is to increase the diameter of an axon, which effectively decreases the internal resistance and thus a faster axon potential propagation. The second strategy is to insulate the axonal membrane, reducing the leaking of the current and thus increasing the distance along the axon that a given local current can flow passively. This strategy is evident in the myelination of axons (Purves et al., 2001). Although the myelin sheaths of the CNS and PNS differ in their cellular origins, anatomical details and molecular constituents, they are

thought to function similarly (Berthold and Rydmark, 1995; Peters et al., 1991). Myelin is a multilamellar spiral of specialized membrane that ensheaths axons larger than 1 μm in diameter. It arises from glial cells as an outgrwoth that is elaborated around the axons and later becomes compacted by withdrawal of cytoplasm to form a tightly wound, membranous sheath comprising a number of lamellae (Figure 2). Its unique composition, rich in lipids (70-85% of the dry mass) and low content of water, allows electrical insulation of axons. Its segmental structure is responsible for the saltatory conduction which allows the fast nerve conduction in the thin fibres of the vertebrate nervous system. Myelin also participates in the regulation of axonal maturation as well as the maintenance and survival of axons (Griffiths et al., 1998; Waxman, 1997). The importance of the myelin is illustrated by the neurological deficits caused by demyelinating deseases such as multiple sclerosis (MS) and leukodystrophies in the CNS and peripheral neuropathies in the PNS.

MYELINATED FIBERS IN
THE VERTEBRATE
CENTRAL NERVOUS SYSTEM
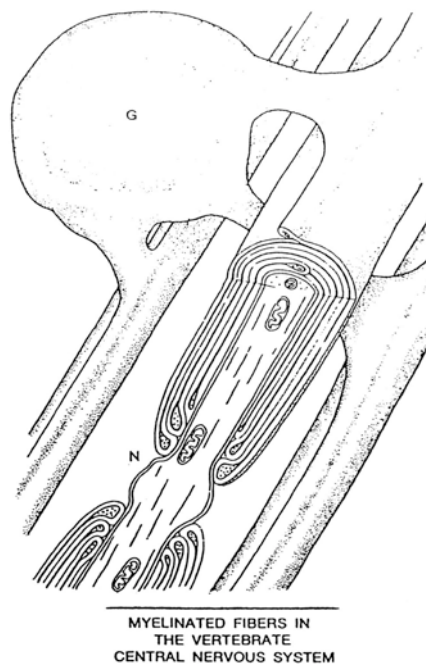
Figure 2. Mature oligodendrocyte wrappig an axon. An oligodendrocyte (G) sends a glial process forming compact multilamellar spiral of myelins around an axon. Cytoplasm is trapped occasionally in the compact myelin. In transverse sections, this cytoplasm is confined to a loop of plasma membrane, but along the internode length, it forms a ridge that is continuous with the glia cell body. In the longitudinal plan, every myelin unit terminates in a separate loop near a node (N). Within these loops, glial cytoplasm is also retained. Adapted from Bunge, 1968. See also Baumann and Pham-Dinh, 2001.

1.2.1 CNS myelination

In the CNS, myelination is driven by the oligodendrocytes. These cells extend many processes to form several myelin sheaths, and in the optic nerve one oligodendroyte can myelinate up to 30-50 axon segments (Peters et al., 1991; Bunge, 1968). The oligodendrocyte progenitor cells (OPCs) are derived from the neuroepithelium of the ventricular areas of both spinal cord and brain, being able to differentiate into mature oligodendrocytes (Nave and Trapp, 2000). The mature CNS retains a population of adult OPCs that are ubiquitously distributed in the brain parenchyma and which are thought to be activated later for repair of demyelinated axons. The sequential expression of developmental markers, identified by a panel of cell-specific antibodies, divides the oligodendrocyte lineage into distinct phenotypic stages characterized by proliferative capacities, migratory abilities and changes in cell morphology (Figure 3). Early OPCs can be identified by their expression of platelet derived growth factor receptor alpha (PDGFR-α) and the chondroitin sulphate proteoglycan NG2. Possibly upon axonal contact but also by cell-intrinsic mechanisms the cell transits to a myelinating state where the O4, GalC and PLP/DM20 markers start to be expressed (Levine et al., 2001).
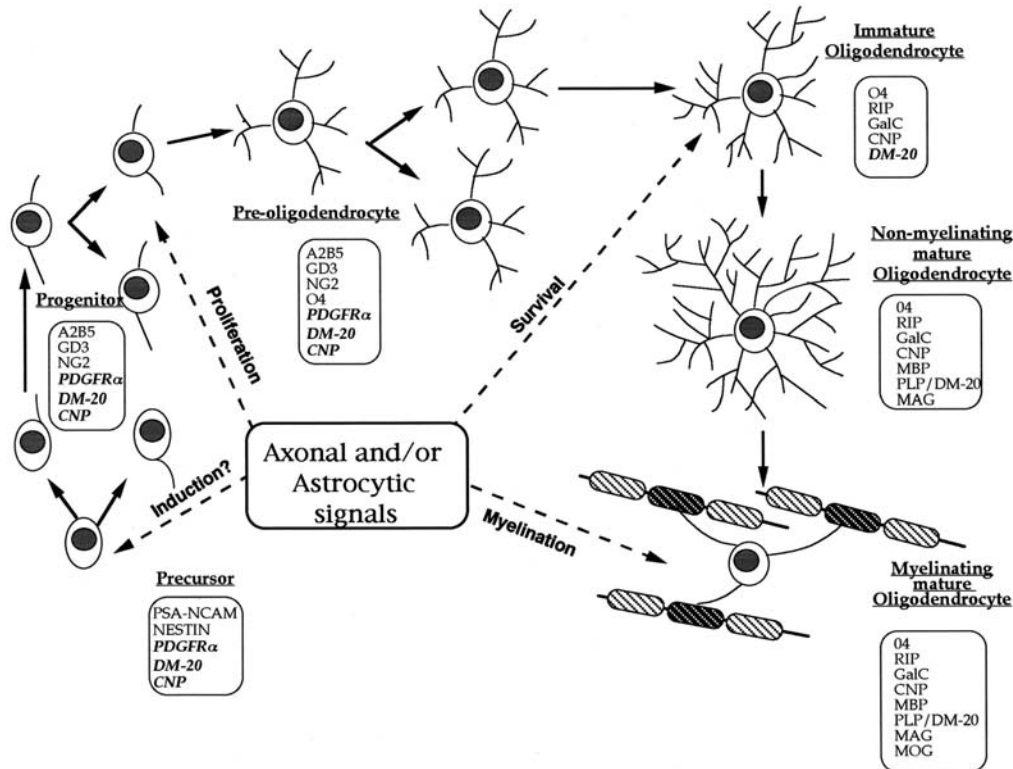
Figure 3. Schematic illustration of the oligodendrocyte stages. Morphological and atigenic progression from precursor cells to myelinating mature oligodendrocytes. Timing of neuronal and astrocytic signaling is

indicated. Stage-specific markers are boxed. RNAs are in italics. (Baumann and Pham-Dinh, 2001). See also Lubetzki et al., 1997; Hardy & Reynolds, 1991.

In the mouse CNS the myelination starts perinatally, peaks at third posnatal week and continues until at least P60 (Vincze et al., 2008; Baumann and Pham-Dinh, 2001). In humans myelination starts during mid-gestation although little myelin exists in the brain at the time of birth. During infancy, myelination occurs quickly, leading to a child's fast development, until the age of 40 months approximately (Parazzini et al., 2002).

1.3 Demyelinating diseases

The term demyelination refers to the loss of myelin with relative sparing of axons. This is the result of a wide range of diseases that either damage myelin sheaths or the cells that form them. These diseases must be distinguished from those that damage the myelin sheaths in concert with the destruction of axons, which are not considered "demyelinating" since the axonal degeneration occurs first and degradation of myelin is secondary, as it occurs for example in amyotrophic lateral sclerosis. Additionally, there are CNS and PNS demyelinating diseases and disorders, as the myelin is antigenically different (CNS myelin derives from oligodendroglia while PNS myelin arise from Schwann cells). Regarding CNS demyelinating diseases, which will be the focus of this thesis, they can be caused by several factors such as inflammatory processes, autoimmune reactions (i.e., MS), infectious factors, metabolic/genetic alterations (leukodystrophy), cerebrovascular affections, neurodegenerative conditions and injuries. However, this classification is rather simplistic and in many occasions there is an overlap in pathogenesis between some of the different categories. In all cases, the loss of myelin ultimately causes irreversible neurological deficits, as the oligodendrocytes are crucial both for the correct transmission of the nerve impulse as well as the metabolic support of the axons (Jaramillo-Merchán et al., 2013; Reeves & Swenson, 2008; Love, 2006).

1.3.1 Multiple sclerosis

Demyelinating diseases and disorders affect millions of people worldwide. Of these diseases, MS, also known as disseminated sclerosis or encephalomyelitis disseminata, is the most common, with 2.5 million people affected worldwide. It is a chronic, inflammatory, and multifocal demyelinating disease where demyelination occurs in the

white matter (WM) of the brain and in the spinal cord, with progressive neurodegeneration. It is caused by an autoimmune response to self-antigens in a genetically susceptible individual. Although the aetiology is still unknown, there is proof that a combination of multiple genetic, environmental, virus or metabolic factors are involved, which altogether leads to a self-sustaining autoimmune disorder in the CNS. MS is more common in young adults in the western hemisphere, the onset being normally at the age of 20–50 and a mean age of onset of 30, affecting twice as many women as men (Milo & Miller, 2014; Nylander & Hafler, 2012).

The pathology of the disease lies entirely in the CNS and is characterized by a sequence of events that include inflammation of localized areas surrounding venules that extend to the myelin sheaths, demyelination, axonal loss and gliosis in the brain and spinal cord. Traditionally, MS has been considered a T cell-mediated autoimmune reaction against the major constituents of myelin sheaths, such as myelin basic protein (MBP) and proteolipidic protein (PLP) (Greer, 2013). However, it has been demonstrated that the pathogenesis is far more complex, involving all arms of the innate and adoptive immune system with slowly progressive neurodegeneration in addition to acute inflammation (Milo & Miller, 2014). More recently, it was also proposed that OPCs themselves contribute to the postinjury inflammatory milieu by producing cytokines that directly enhance their repopulation of areas of demyelination and hence their ability to contribute to remyelination (Moyon et al., 2015). MS seems to begin with the activation of autoreactive CD4+ T helper type 1 (Th1) cells directed against CNS antigens in the periphery. Once these cells become activated, they start to upregulate surface cell adhesion molecules and cytokine receptors as well as secrete pro-inflammatory cytokines. This causes changes in the endothelial cells, enabling adherence of the activated cells to the endothelium and facilitating their penetrance through the BBB (De Riccardis et al., 2015). In addition, the participation of another subset of CD4+ cells, termed Th17 cells, was discovered. Thus, once the autoreactive T-cells have entered into the CNS, they can be reactivated by resident antigen presenting cells (APC) such as microglia, resulting in their recruitment. Also, brain resident and peripheral inflammatory cells are then activated as a consequence of the T-cells, ultimately leading to plaque formation (Figure 4) (Milo & Miller, 2014; Nylander & Hafler, 2012; Brinkmann et al., 2010; Fletcher et al., 2010). It is this plaque formation from with MS derives its name, as the plaques are scar tissue and "sclerosis" means scar. MS plaques are formed in different white matter (WM) regions such us the

corpus callosum (CC), optic nerves and tracts, around the ventricles, subpial regions of the spinal cord and brainstem, as well as in grey matter areas. The plaques are mainly composed of perivenular infiltrates such as T-cells, monocytes/macrophages, and plasma B cells, and characterized by demyelinated or even transected axons, reduced number of oligodendrocytes, and astrocyte proliferation with the result of a glial scar (C Lucchinetti et al., 2000).
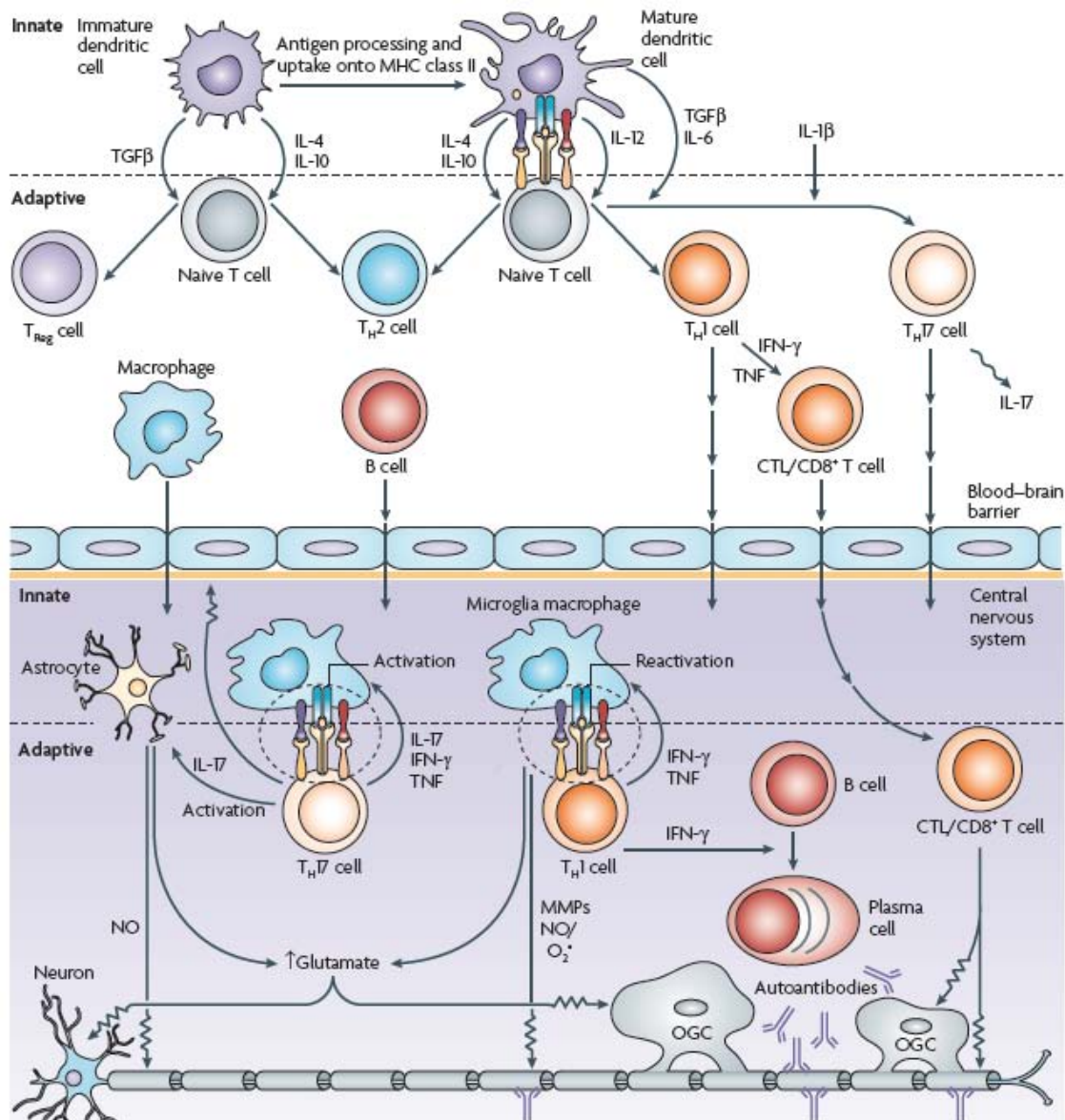
Figure 4. Simplify schema of the pathophysiology of multiple sclerosis. Immature dendritic cells are the central players in innate immune responses and are involved in the maintenance of peripheral tolerance, presumably by promoting regulatory T cell responses. Abnormally activated (mature) antigen-presenting dendritic cells can be found in patients with multiple sclerosis (MS), and effective regulation and immune tolerance is partially lost. This favours the clonal expansion of self-cross-reactive T cells in lymph nodes. The nature of the antigen, the co-stimulatory signals and the cytokine environment in the lymph nodes directs the differentiation of cells towards CD4$^+$ T helper 1 (T$_H$1), T$_H$2, T$_H$17 or regulatory T (T$_{Reg}$) cells and CD8$^+$

cytotoxic T lymphocytes (CTLs). Primed autoreactive cells recirculate to blood and, after reactivation by phagocytes at leptomeningeal vessels, penetrate the blood–brain barrier to invade the central nervous system (CNS), where they are reactivated, clonally expanded and terminally differentiated by self antigen presented on dendritic cells. The presence of autoreactive T_H1 and T_H17 cells, CTLs and plasma B cells in the CNS, together with abnormally activated astrocytes and microglia, lead to an increased production of inflammatory cytokines, reactive oxygen species, excitotoxicity, autoantibody production and direct cytotoxicity, which are all involved in demyelination and axonal, neuronal and blood–brain barrier damage that is present in patients with MS. Abbreviations: IFN, interferon; IL, interleukin; MHC class II, major histocompatibility complex class II; MMPs, matrix metalloproteinases; NO, nitric oxide; TGFβ, transforming growth factor-β; TNF, tumour necrosis factor. Adapted from Brinkmann et al., 2010.

Typically, MS is grouped into four major categories based on the course of the disease. The most common form is the "relapsing-remitting" course, affecting approximately 85% of MS patients. The second most common is the "primary progressive", affecting approximately 10% of MS patients, whose symptoms continue to worsen gradually from the beginning. The "secondary progressive" form of MS refers to when the disease course continues to worsen with or without periods of remission and which may be developed in cases of relapsing–remitting MS. "Progressive-relapsing" MS is the last and rarest form, with a prevalence lower than 5%, being progressive from the onset, with intermittent flare-ups of worsening symptoms during the disease progression and with no periods of remission (Figure 5) (Milo & Miller, 2014; Goldenberg, 2012; Lucchinetti et al., 2000; Rubin & Reingold, 1994).
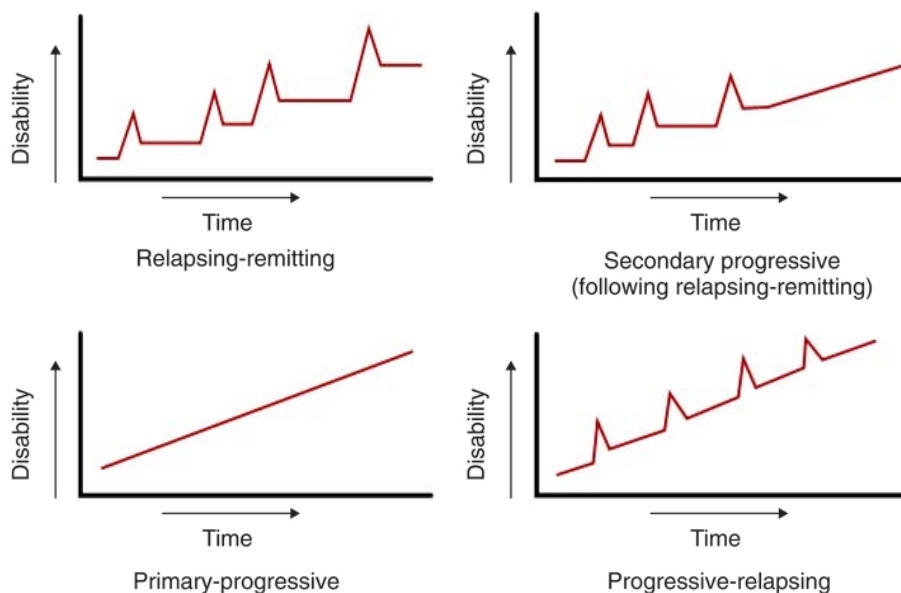
Figure 5. Multiple sclerosis types. Relapsing-remitting: Unpredictable attacks which may or may not leave permananent deficits followed by periods of remission. Secondary progressive: Initial relapsing-remiting multipe sclerosis that suddenly begins to have decline without periods of remission. Primary progressive: Steady increase in disability without attacks. Progressive-relapsing: Steady decline since onset with super-imposed attacks. Adapted from Rubin & Reignold, 1994.

Additionally, MS generally progresses through two phases, depending on the type of demyelinating lesions: acute and chronic. In the acute phase, the nearby oligodendrocyte progenitor cells invade the lesion, differentiate into mature oligodendrocytes as early as 7 days after the injury and remyelinate (Chari et al., 2003; Health & Complete, 2003). The chronic phase, on the other hand, affects the migratory and differentiating mechanisms of these progenitors, resulting in sustained demyelination (Williams et al., 2007), due to the lack of factors that stimulate regeneration and/or to the presence of molecules that repress remyelination (Kuhlmann et al., 2008). Thus, OPCs stimulation to migrate and differentiate will be vital in a remyelinating therapy in order to favor neuronal survival (Irvine & Blakemore, 2008).

Regarding the clinical symptoms of the disease, these are entirely attributable to the CNS pathology and patients usually present a wide variety of neurological symptoms that can arise alone or in combination, as isolated attacks or as a part of a gradual progression. These may include: visual disturbances, paresthesias or numbness, motor weakness, bowel and bladder incontinence, sensory disturbances including dizziness, spasticity, neuropathic pain, sexual dysfunction, vertigo, depression and less common cognitive impairments (Milo & Miller, 2014; Goldenberg, 2012; Steinman, 1996). It is very difficult to predict the course of MS, although there seems to be a relation between MS focality (local or multifocal) and prognosis. Thus, life expectancy is considered to be the same as the general population in most of the cases, however, when the presentation is multifocal and in severe cases that lead to medical complications the life expectancy can be reduced by an average of 7–10 years (Milo & Miller, 2014; Miller et al., 2005). The diagnosis of MS is primarily clinical and relies on the demonstration of symptoms and signs attributable only to WM damages distributed in time and space, along with the exclusion of other disorders that may mimic MS. There is no single laboratory test diagnostic for MS and although several sets of criteria have been proposed, the diagnosis criteria of MS was formalized as the so-called McDonald Criteria and updated to reflect the increased reliance on imaging for lesion identification (Figure 6) (Milo & Miller, 2014; Rocca et al., 2013).
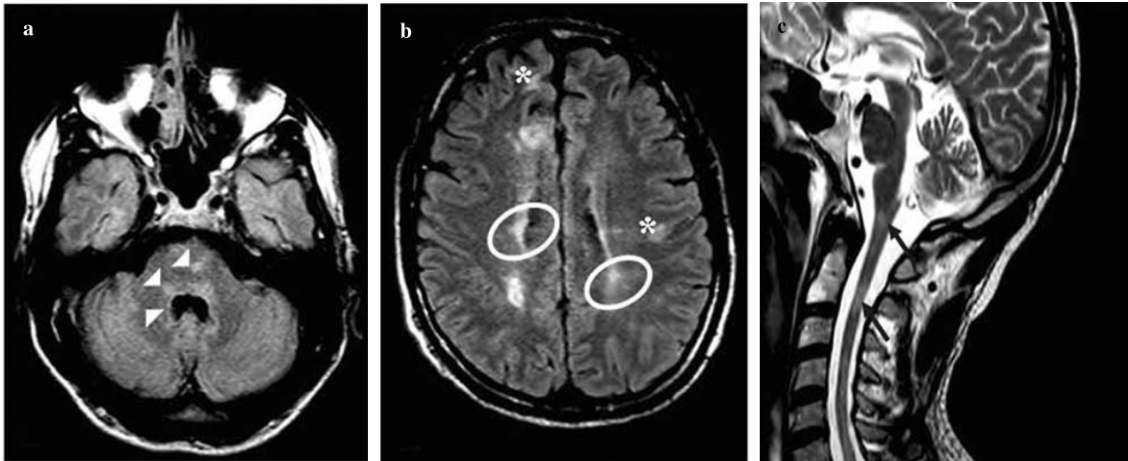
Figure 6. Contribution of magnetic resonance imaging to the diagnosis of multiple sclerosis. Axial fluid-attenuated inversion recovery images of the brain (a, b) and T2-weighted images of the cervical spinal cord (c) of a patient with a clinically isolated syndrome of the central nervous system at onset. Lesions can be seen in at least two of four locations typical for multiple sclerosis: (1) periventricular (circles), (2) subcortical (asterisks), (3) infratentorial (arrowheads), (4) spinal cord (arrows). On the basis of the 2010 revision of the McDonald criteria, this case fulfils criteria for dissemination in space (DIS). (Rocca et al., 2013).

As of yet there is no cure for MS, and current treatments focuses on reducing lapse risk, slowing the progression, preserving neurological function and managing symptoms. Typical MS treatments use disease-modifying drugs (DMTs), which have a variable degree of efficacy, tolerability, likelihood of adherence and secondary effects (Wingerchuk & Carter, 2014). These include treatments for the attacks such as corticosteroids or plasma exchange (plasmapheresis), those which focus in modifying the progression, such us immune-suppressive cytokines interferon beta-1a and interferon beta-1b, the immune-modulating drug glatiramer acetate, the immune-suppressant mitoxantrone, dimethyl fumarate, the monoclonal antibody natalizumab which decrease the ability of immune cells to cross the BBB and fingolimod, that reduces lapse rate. Finally, it is possible to find treatments that ameloriate signs and symptoms such as physical thearpy, muscle relaxants, drugs to reduce fatigue among others (Wingerchuk & Carter, 2014; RJ Franklin et al., 2012; Goldenberg, 2012). However, all kinds of MS treatments have only minor effects in the progressive forms of MS, and although current treatments ameliorate the pathological mechanisms, there is no efficient method to repress progression and restore lost function. Thus, the medical and scientific community is expecting for new therapeutic approaches capable of modifying the disease rather than being purely palliative (Jaramillo-Merchán et al., 2013; McKernan et al., 2010; Kassis et al., 2008).

1.4 Remyelinating response to myelin damage

It is generally considered that the CNS has a limited capacity for regeneration after traumatic injuries and degenerative or demyelinating diseases. It has instead an endogenous regenerative capacity to regain structure and function (Rivera & Aigner, 2012). In MS, macrophages phagocyte the myelin sheaths in response to the autoimmune attack, leading to multi-foci demyelinated areas. After an acute inflammatory mediated demyelination, the affected regions can be effectively remyelinated, although with a thinner and shorter myelin sheath than would be expected for a given diameter of axon, unlike what happens during developmental myelination (Figure 7) (RJ Franklin & Hinks, 1999).
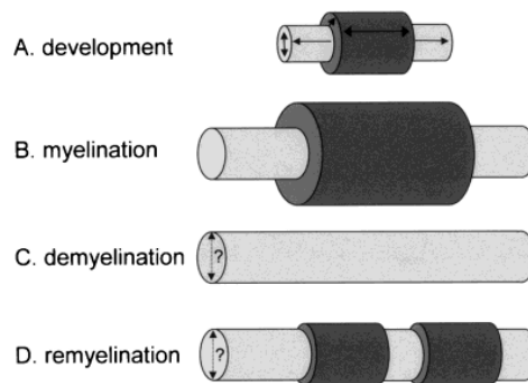
Figure 7. Schematic illustration of the relationship between the length and thickness of the myelin sheath and axon size. (A) As the axon increases the length and thickness, the myelin sheaths change proportionally. (B) In the adult there is a constant relationship between the axon diameter and myelin sheath size. After a demyelinating event (C), there is no proportional change in the myelin sheaths dimensions (D), resulting in a much thinner and shorter sheaths. (RJ Franklin & Hinks, 1999).

During the progression of the disease, as well as during aging, remyelination begins to fail. In the chronic MS plaques, the nude axons are more likely to degenerate, leading to irreversible neurological dysfunctions, characteristics of MS (Figure 8) (RJ Franklin et al., 2012; RJ Franklin, 2002). Hence, while remyelination can be a highly efficient repair process, it shows clinically significant failure in MS and other diseases.
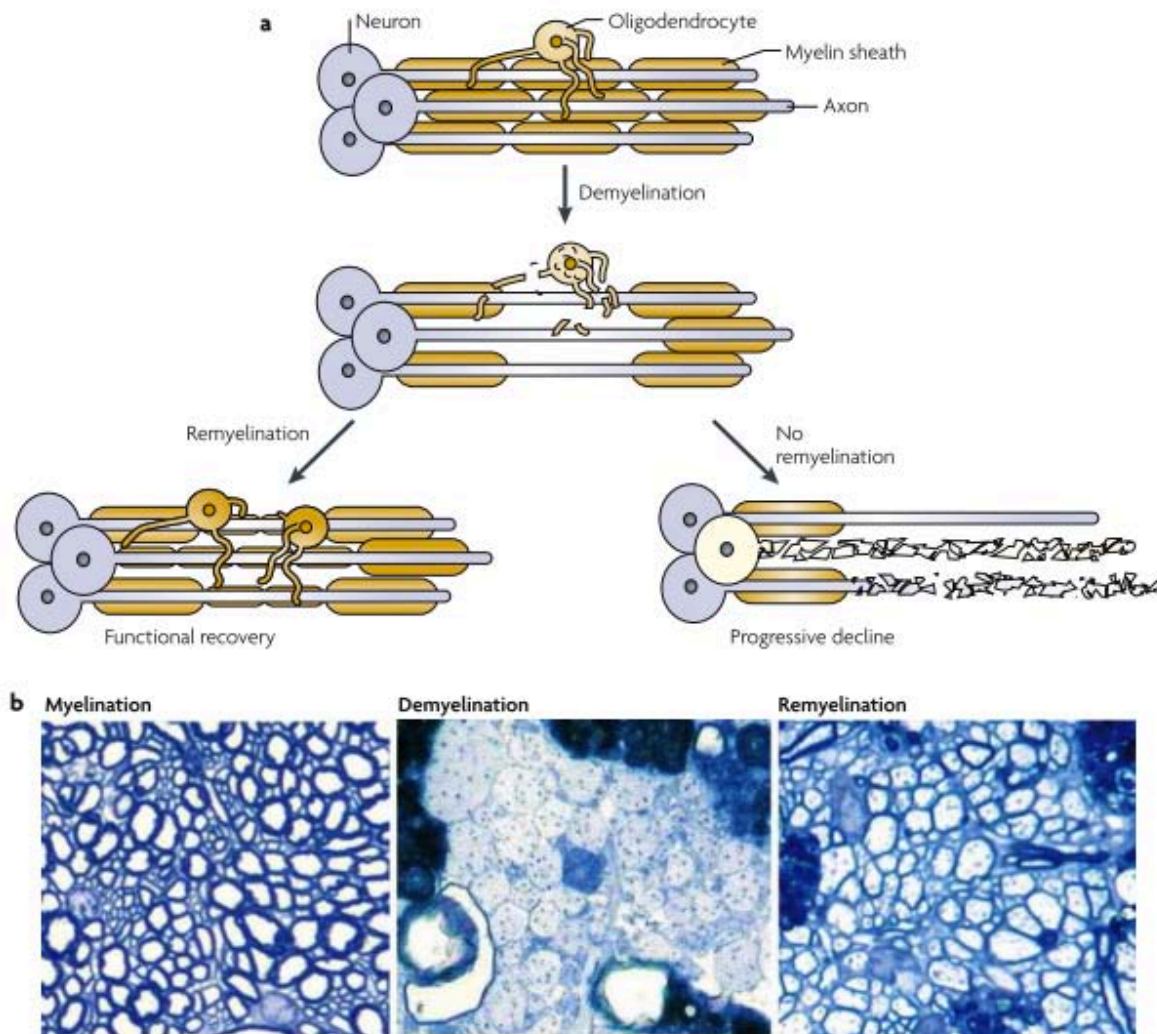
Figure 8. Demyelination/Remyelination process. (A) When a demyelinating event occurs in the CNS, the nude axon has two posible fates. In many cases, after an acute phase there is spontaneous remyelination induced by mature oligodendrocytes. This leads to functional recovery. However, in certain circumstances chronic plaques are formed due to remyelination failure, leaving the axons susceptible to degeneration. This leads to the degeneration of the entire neuron and consequently to the progressive neurodegenerative process. (B) An effective method to visualize the remyelination is to examine semi-thin sections by light microscopy. The transverse axonal section showed in this figure belongs to an adult rat cerebellum. The images correspond to a normally myelinated area (left), a demyelinated area with debris-filled macrophages (middle), and a remyelinated area with shorter and thinner myelin sheaths (right). Adapted from RJ Franklin & Ffrench-Constant, 2008.

The use over the last decades of different animal models to study the demyelinating/remyelinating process has increased our knowledge about the underlying mechanism of this event (Ransohoff, 2012). However, the reasons why adult remyelination does not recapitulate the full program of developmental myelination is still unclear. There is an enormous interest in understanding the factors that lead to this failure as this will

enable us to develop efficient therapeutic approaches (RJ Franklin, 2002; Rivera & Aigner, 2012).

1.4.1 The oligodendrogenic program

Myelination of vertebrate CNS axons by oligodendrocytes represents one of the clearest and best orchestrated processes. After a demyelinating event, the number of oligodendrocytes in the lesion is greater than it was before demyelination. This implies that there must exist a mechanism by which new oligodendrocytes are generated (RJ Franklin, 2002). Currently it is clear that these oligodendrocytes arise from a population of adult CNS stem/precursor cells, termed adult oligodendrocyte precursor or progenitor cells (OPCs). The process by which OPCs remyelinate can be divided into three steps: (1) OPCs activation, (2) recruitment/migration and (3) differentiation into mature myelinating oligodendrocytes (DM Chari et al., 2003). Upon demyelination, OPCs are activated by the mitogens secreted by the astrocytes and microglia which induce the expression of oligodendrogenic transcription factors such as Olig2, Nkx2.2 and SOX2 (Menn et al., 2006; S. Wang et al., 2013). The recruitment phase of activated OPCs is the next step in the remyelinating process, where OPCs migrate to the demyelinated areas in addition to the ongoing proliferation. Once the progenitors contact with the bare axons, they activate the processes to produce myelin membranes that finally wrap around the axons to form the myelin sheaths (RJ Franklin, 2002; Kotter et al., 2006).

In such a scenario, where remyelination involves very well define and controlled stages, it is posible to identify at which moment the remyelinating process fails. Thus, remyelination can be limited due to an inadequate provision of OPCs (recruitment failure) or because of a differentiation block of OPCs (Kuhlmann et al., 2008). With aging both process become more protracted, leading to a decrease in remyelination efficacy (Sim et al, 2002). Another posible cause of the failure is that successives steps of demyelination and remyelination, which are characteristic of MS, can exhaust the OPC reservoir, considerably affecting the number of recruited OPCs (RJ Franklin, 2002). Finally, the failure to repopulate the demyelinated areas can arise because of an inappropiate microenvironment governing their recruitment, because the OPCs become less responsive to these factors and even for the myelin debris generated during the demyelination, which can impair the OPC diferentiation (Figure 9) (Kotter et al., 2006).
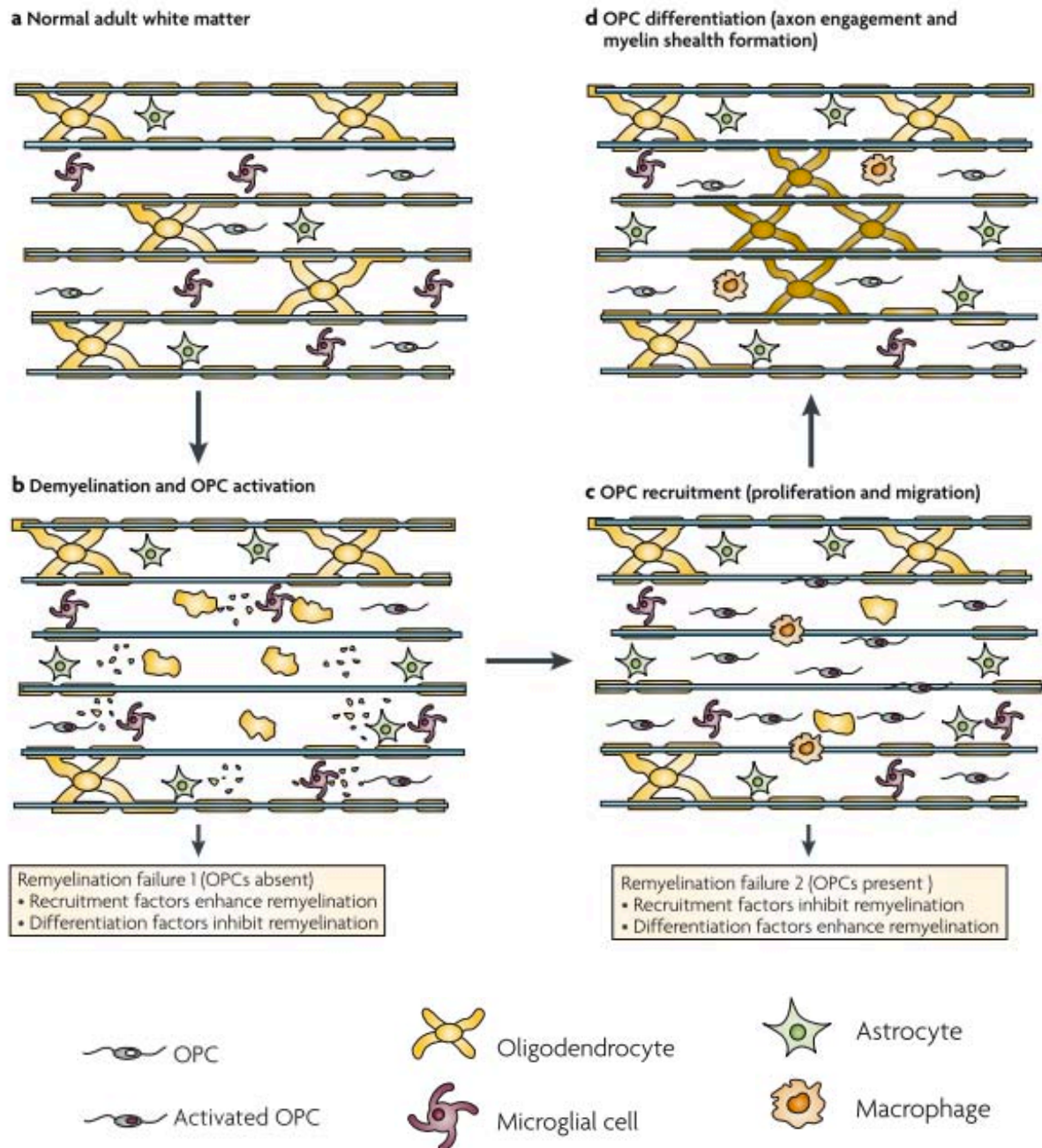
Figure 9. Phases and impairments of remyelination. (A) Along the normal adult white matter several cell types can be detected, such as progenitor and mature oligodendrocites, microglia and astrocytes. After a demyelinating event, OPCs become activated (B) by the mitogens secreted in the microenvironment by inflammatory cells and astrocytes. (C) This results in the proliferation and migration of the OPCs which start to populate the nude axons. Additionally, macrophages start to clean the myelin debris. (D) The last stage corresponds to OPCs recruitment, which engage the axons and differentiate to produce new myelin sheaths. Remyelination failure can occur as a result of the failure in OPC recruitment or due to the impairment on the differentiation phase. Adapted from RJ Franklin & Ffrench-Constant, 2008.

1.4.2 Oligodendrogenesis in the Adult Subventricular Zone (SVZ)

Whereas the birth of new neurons in the adult mammalian brain is apparently limited to the dentate gyrus of the hippocampus and the lateral ventricle (LV) wall, newly produced

oligodendrocytes are derive from OPCs, which are ubiquitous distributed throughout the brain parenchyma (Miller & Mi, 2007; Polito & Reynolds, 2005) as well as from multipotent neural stem/progenitor cells (NSPCs) present in the SVZ (Figure 10B). The SVZ of the adult mammalian brain contains slowly dividing astrocytic neural progenitors, which express glial fibrillary acidic protein (GFAP), known as type-B cells. These germinal astrocytes give rise to actively proliferating transient amplifying type-C cells, which in turn generate immature neuroblasts termed type-A cells. Menn and colleagues demonstrated that some type-B cells, possibly via intermediate precursors similar to type-C cells that express the oligodendrocyte lineage transcription factor 2 (Olig2) (Gonzalez-Perez & Alvarez-Buylla, 2011), were capable of giving rise to OPCs which in turn would differentiate into mature myelinating oligodendrocytes (Figure 10A) (Ming & Song, 2011; Menn et al., 2006). Alternatively, some groups found that neuroblasts (type-A cells), which normally generate interneurons in the OB, could be re-specified during migration to generate glial cells, as it is the case after lysolecithin-induced demyelination of the CC and SVZ cell grafting into the CC (Cayre et al., 2006; Nait-Oumesmar et al., 1999). Furthermore, in patients suffering from MS as well as in experimental models of demyelinating diseases, it has been observed that SVZ-derived NSPCs respond to demyelinating lesions enhancing basal oligodendrogenesis at the expenses of neurogenesis (Rivera & Aigner, 2012; Gonzalez-Perez & Alvarez-Buylla, 2011). These newly generated OPCs have been observed migrating towards the CC, the striatum, the fimbria fornix and to the cortex (Figure 10B) (Menn et al., 2006; Kessaris et al., 2005).
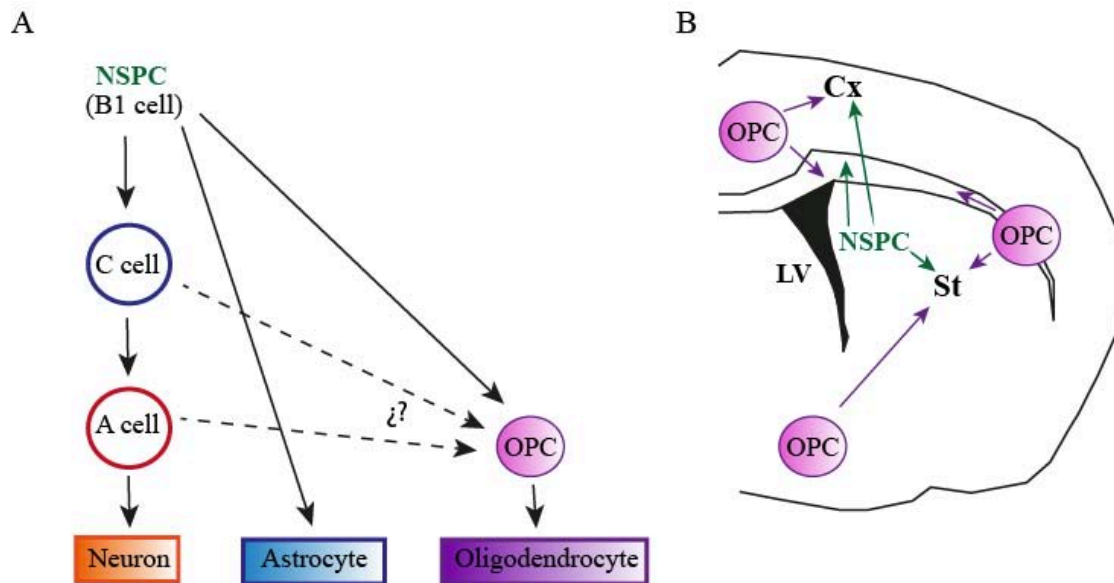
Figure 10. Schematic of NSPC lineage fate and OPC behavior after a demyelinating lesion. (A) B1 astrocytes are the quiescent neural stem/progenitor cells of the adult ventral-SVZ (V-SVZ). Under normal circumstances, they give rise to transient amplifying type-C cells, which in turn produce neuroblasts (type-A cells), with a small subpopulation giving rise to highly migrating OPCs (possibly via intermediate precursor as the type-C cells or more unlikely via migrating type-A-cells). OPCs finally differentitate into mature myelinating oligodendrocytes. (B) After demyelination, both NSPCs and OPCs attempt to repair the lesioned white matter area by proliferating, migrating and finally restoring the myelin sheaths. This causes a shift in the fate of SVZ-derived NSPC, from neuronal lineage to oligodendrogenic. The newly generated OPCs are capable of migrating and remyelinating the cortex, fimbria/fornix, corpus callosum and striatum, however, the migration of local OPCs residing outside the V-SVZ (e.g., pia matter, fimbria or cortical layer) could be more relevant when demyelination occur in more distant areas. Adapted from Maki et al., 2013.

1.5 Animal models of multiple sclerosis (MS)

There are several well-characterized MS animal models that allow studying from different angles the pathology of MS as well as look for new therapeutic strategies. Thus, depending on which clinical aspects and mechanistic hypotheses are being modeled it would be better to use one model or another. Immune-mediated, viral, genetic and toxic models are the main ones that are now used to understand the mainfold aspects of MS (Ransohoff, 2012). Experimental autoimmune encephalomyelitis (EAE) is the most commonly used experimental model. EAE has been used for about 85 years to model MS, and nowadays the model has been finely tuned. EAE is induced by either the systemic administration of myelin proteins such as MBP, PLP, myelin oligodendrocytic protein (MOG), peptides of these proteins in adjuvant or by the adoptive transfer of encephalitogenic T cell blasts into naïve recipients, all resulting in distinct models featuring different aspects of the diseases

(Constantinescu et al., 2011; SD Miller et al., 2010). Above all the models, EAE has contributed enormously to our understanding of the autoimmune and inflammatory processes as well as to the cytokine biology (Waksman, 1999). Additionally, the mechanics of several treatments have been elucidated using this model (Yednock et al., 1992). Although, this model may be the most suitable to decipher the underlying inflammatory mechanims in MS and has contribute to major advances, it has also some major drawbacks to take into consideration (reviewed in Ransohoff, 2012):

- While in humans with MS the major affected areas are found in the cerebral and cerebellar cortex, EAE is mainly a disease of the subpial spinal cord WM.
- Disssapointing conducted researchs to find out the potential benefits of neuronal and oligondendrocyte growth and survival factors.
- Demyelination and remyelination processes can not be well studied in this model as lesions occur stochastically with regard to timing and localization.
- It is not the most appropiate model to investigate the MS progression.
- The model makes it difficult to study B cells, which have been proven to have a very important role in MS.
- Most forms of EAE are generated by immunization mechanism that trigger CD4+ T cell responses, of instead of CD8+ T cells which predominate in MS.

Viral vector have been also used to induce demyelination in the CNS. Two of the most used are the picornavirus TMEV and certain strains of the coronavirus mouse hepatitis virus (MHV). Whereas MHV provides a model where the viral infection is controlled by well-defined mechanims that provide sequence of inflammatory demyelination in the absence of detectable pathogen gene expression (Rivera-Quiñones et al., 1998), TMEV has been very useful to study the origin of certain behavioral signs that arise after a demyelinating event (Miller et al., 1997).

1.5.1 Cuprizone model

Understanding remyelination may hold the key to understand how to treat MS, yet this cannot be addressed using the EAE mouse model. On the other hand, toxicity-induced demyelination overcomes the limitations of timing and lesion localization and provides a perfect way to study the remyelinating processes. One of particular interest is the copper

chelating agent Bis(cyclohexanone)oxaldihydrazone (cuprizone). In the cuprizone model the toxin causes dysfunction of mitochondrial complex IV, specifically affecting the oligodendrocytes (Mahad et al., 2008). This model offers the advantage of being helpful to elucidate the molecular and cellular mechanism that occurs during de- and mainly remyelinating processes independently of the participation of peripheric immune cells, as the BBB is intact (Bakker & Ludwin, 1987; Kondo et al., 1987). Thus, microgliosis and astrogliosis, driving inflammatory but also reparative processes in the face of an intact BBB, are prominent features of this animal model (Gudi et al., 2014). Additionally, the cuprizone model produces highly reproducible demyelination of distinct brain regions. Among them the CC is the most commonly used to investigate the mechanism of remyelination (Steelman et al., 2012). First of all, the CC is a large area that is greatly affected both in MS patients and in the experimental model and secondly, it is near one of the two neurogenic niches in the adult, making it feasible to study the activationg of the NSPCs of these areas and the oligodendrogenic program that they may undergo (Jaramillo-Merchán et al., 2013). Moreover, cuprizone treatment can be halted at any time to allow the study of spontaneous remyelinating processes, which is not possible or more difficult with viral or autoimmune models (Hibbits et al., 2009). When the cuprizone diet is kept for 5-6 weeks the CC and other WM tracts are demyelinated in a process that mimic the "acute phase" of MS, and in which spontaneous remyelination occurs when diet is changed to normal chow. However, if the cuprizone administration is prolonged until 12 weeks or more, the remyelination is highly restricted, leading to the so-called "chronic phase" of the disease. This provides an excellent tool for researchers to investigate both MS phases separatedly, which is not possible with other animal models (Kipp et al., 2009).

Another toxin-induced model is produced by microinjections of lysophosphatidylcholines, also called "lysolecithins" into specific regions of WM tracts causing immediate demyelination followed by remyelination. While the strength of this model lies in isolating the demyelination/remyelination as discrete events with spatial and temporal predictability, similar to the cuprizone model, the major limitation is the lack of an autoimmune response (Miller & Fyffe-Maricich et al., 2010). Thus, there is a great interest in using these toxin-induced models to identify new strategies to enhance remyelination, which is deemed crucial for neuroprotection and therefore a major line of defense against progressive MS.

1.6 Novel remyelinating therapies

Since the early 1990s, when beta-IFN 1b was shown to reduce the relapse rate in patients with "relapsing-remitting" forms of MS, we have been witnesses of the development of several types of DMTs which beneficially modify the course of MS (the principal ones are reviewed in previous sections) (Cross & Naismith, 2014). However, and despite the enormous benefit that they have provided, these molecular therapies might not be sufficient to target all different aspects of MS pathogenesis. In addition to the fact that MS is a multifactorial disease, it is also progressive, and thus both the microenvironment and the pathogenic parameters change during the course of the disease. For that reason it is unlikely that a single drug would be able to drive MS treatment into the next frontier. Ideally, an effective treatment for MS should target the autoimmune/inflammatory side, the neurodegenerative aspect and finally activate repairing mechanisms such as remyelination (Rivera & Aigner, 2012). Regarding this, there are two major approaches that have been tested in animal models: transplantation of different exogenous cells that could remyelinate, and stimulation of the endogenous repairing machinery (precursor and progenitor cell populations) by transplantating cells that stimulate the existing cell niches (reviewed in RJ Franklin & Ffrench-Constant, 2008).

Experimental studies with the aim of enhancing remyelination by exogenous cell transplantation were initiated in the early 1980s, showing that transplantion of glial cells in the developing CNS were capable of myelinating WM tracts in rodents with myelin mutations or toxin-induced focal demyelinations (Blakemore & Crang, 1985; Lachapelle, et al., 1984; Duncan at el., 1981). Since then, several studies have focused in these approaches, transplanting different cell types such as primary OPCs (Windren et al., 2004; Zhang et al., 1999; Groves et al., 1993), Schwann cells (Bachelin et al., 2005; Honmou et al., 2005; Blackemore et al., 1985), olfactory ensheathing cells (Barnett et al., 2000; Imaizumi et al., 1998; RJ Franklin et al., 1996), neural stem cell lines (Hammang et al., 1997) and embryonic-stem-cell-derived glial precursors (Brustle et al., 1999), all of which have been reported to produce new myelin after the transplant. However, despite these promising results there are significant hurdles associated with exogenous cell transplantation (Lindvall & Kokaia, 2010). First, it may be illogical to transplant exogenous remyelinating cells into an environment that contains resident progenitors that are themselves impaired to remyelinate by the diseased microenvironment. Second, MS is

a multifocal chronic disease and therefore would probably require direct intralesional injection throughout the disease course, as evidence from some studies indicate the limited capacity of the glial cells to migrate. This is a relative invasive technique that would require repetitive cell transplantations in multiple points (Divya M Chari & Blakemore, 2002). Additionally, it is necesary to control the proliferation and differentiation process of the transplanted cells in order to avoid uncontrolled cell proliferation that may lead to tumor formation or aberrant differentiation and migration, which appears as a very difficult challenge. In many cases, these type of transplants have shown to attenuate the disease symptoms to a certain degree. However these could be due to an immunomodulatory effect which reduce the content of infiltrating immune cells and pro-inflammatory cytokines, rather than to direct remyelination (Einstein et al., 2007, 2006). Finally, there is the issue of the source of these cells. As there would be problems with the availability of these cells, either surgical specimens or fetal material would be required. Another option could be stem cell lines, which possess the advantage of being able to provide unlimited quantities of progenitors as well as to partially match human leukocyte antigen types for each patient (Nistor et al., 2005).

The second alternative approach to achieve remyelination would be to mobilise the endogenous precursor and progenitor stem cell populations to enhance the regenerative/remyelinating process. It has been already mentioned in the preceding sections that insufficient OPC recruitment and more commonly OPC differentiation failure are the two main reasons of remyelination impairment (Angeles et al., 2002; Claudia Lucchinetti et al., 1999). However, the underlying biology of these processes are different and sometimes mutually exclusive. This, makes it difficult to find a single candidate factor to enhance both phases of the remyelinating process. For instance, PDGF induces OPC proliferation and migration however, *in vitro* it seems to inhibit the final stages of differentiation when myelin is produced (Wang et al., 2007). This means that pro-recruitment factors may not promote and even impair remyelination, where the primary limitation is OPC differentiation and viceversa. In this context, stem cell therapies which may stimulate both processes, via the secretion of several trophic factors, appears as an attractive and promising strategy.

1.6.1 The potential use of mesenchymal stem cells (MSCs)

Both in our lab (Jaramillo-Merchán et al., 2013) and others have shown the therapeutic potential of mesenchymal stem cells (MSCs) (El Akabawy & Rashed, 2015; Barhum et al., 2010; Bai et al., 2009; Lu et al., 2009; Gerdoni et al., 2007). MSCs were initially identified as a subpopulation of bone marrow cells with osteogenic potential (Friedenstein et al., 1976, 1970, 1968). We know now that MSCs are abundant and reside in the bone marrow and most connective tissues (Meirelles et al., 2006; Minguell et al., 2001) being highly accessible and simple to expand *in vitro* (Jadasz, et al., 2012; Martino et al., 2010), in contrast to NSPCs and OPCs. Other advantages of MSCs are that they have been proven to be relatively safe in non-human primates and humans as well as exhibit low immunogenicity compared with other types of stem cell treatments (Darlington et al., 2011). MSCs are capable of giving rise to different cell types with mesenchymal lineage such us adipose tissue, cartilage, tendons, muscle and bones. In bone marrow, the MSCs also present stromal properties, as they control the activity and fate of hematopoietic stem cells, most probably through paracrine mechanisms (Minguell et al., 2001). Thus, this dual nature as stromal and stem cells may represent an advantage to adapt in a neural microenvironment that occur in neurological diseases such as MS. All this make MSCs transplantation therapies a very attractive alternative to develop an autologous cell-based therapy for demyelinating diseases.

During the last decades, researchers have performed great efforts to evaluate the therapeutic properties of MSCs transplantations into the diseased CNS. In animal models of demyelination, MSCs have shown the capacity to promote functional remyelination (Jaramillo-Merchán et al., 2013). Despite early studies which proposed that MSCs could transdifferentiate into mature neurons and/or oligodendrocytes (MSC plasticity) (Krampera et al., 2007), this has been later proven to be untrue, being their primary function to boost endogenous OPCs population for remyelination, exerting a neuroprotective effect and also modulating the immunological response (Figure 11) (El Akabawy & Rashed, 2015; Jaramillo-Merchán et al., 2013; Barhum et al., 2010; Bai et al., 2009; Lu et al., 2009; Gerdoni et al., 2007). It has been also shown that *in vivo* MSCs appear to be perivascular and propose that during local injury, MSC are released from their perivascular location, become activated and set up a favorable microenvironment by secreting bioactive molecules (Caplan & Correa, 2011). In the EAE model, treatment with MSC induces anti-

inflammatory Th2 polarized immune response at the expense of pro-inflammatory Th1, and promote endogenous repair (Bai et al., 2009). In addition, it has been reported that MSC conditioned medium (MSC-CM) can enhance remyelination with hepatocyte growth factor as a critical component (Bai et al., 2012) and also instruct an oligodendrocytic fate on adult NSPCs *in vitro* (Rivera et al., 2006).
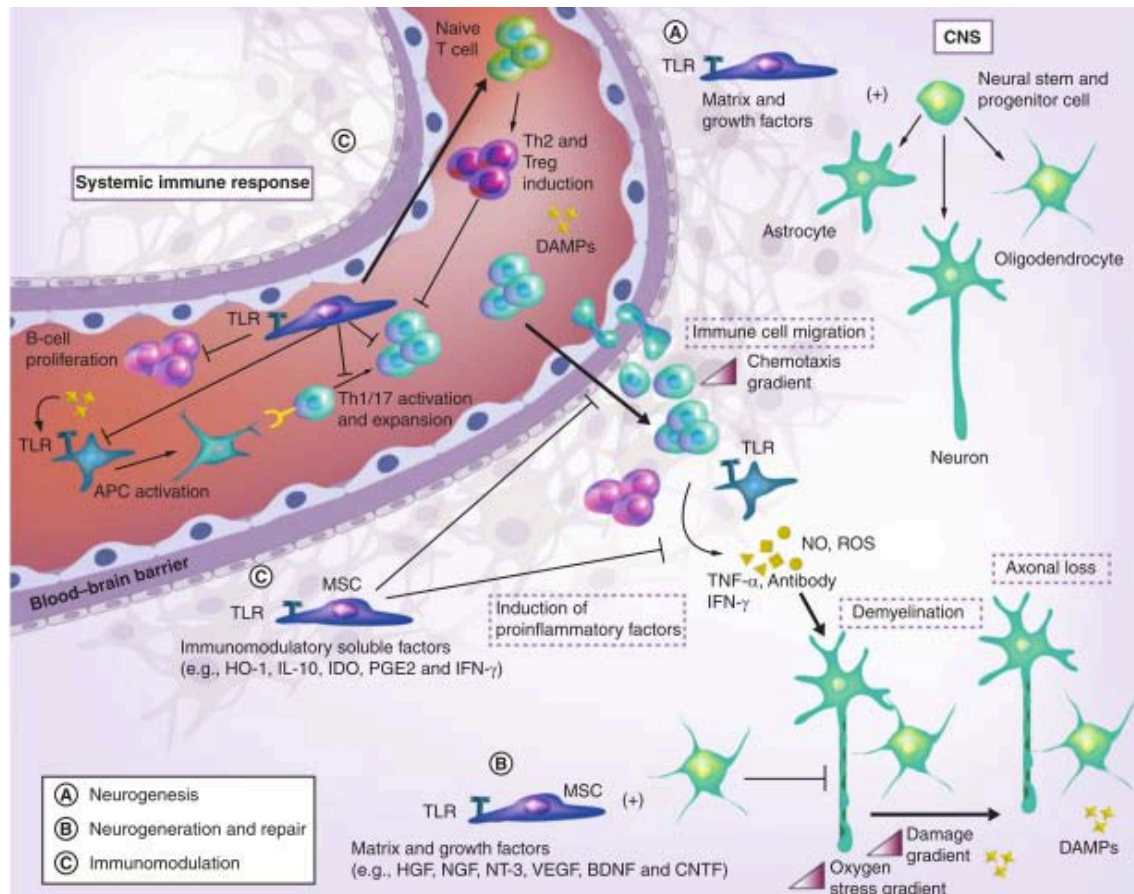
Figure 11. Therapeutic activities of MSCs in the diseased nervous system. The mechanisms proposed for the pathophysiology of MS have been extrapolated mainly from EAE models. The autoimmune-mediated proinflammatory process would arise as a response of autoreactive lymphocytes in the body or damage gradients caused by oligodendrocyte and axonal lesions in the CNS. Briefly, TLRs would recognize both DAMPs and PAMPs and activate innate immune cells to produce proinflammatory cytokines and chemokines, acting as APCs for naive T cells. This activates proinflammatory Th1 and Th17 cells, which secrete soluble factors, increasing the chemotaxis gradients, ultimately resulting in their migration into the CNS. Autoantibodies, cytokines such as IFN-g and TNF-a and hypoxia-inducible factors including NO and ROS are responsible for demyelination and finally the axonal injury/loss. Additionally to this type of damage, proinflammatory damage gradients can also activate innate and adaptive immune response in the CNS to release neurotoxic soluble factors. Proposed therapeutic activity of MSCs include (A) neurogenesis, and subsequently oligodendrogenesis, and/or stimulate endogenous OPCs differentiation and maturation that might enhance remyelination in vivo, (B) regeneration and repair of myelin and axons and (C) immunemodulation of the systemic and CNS inflamatory response. Pathologic mechanisms underlying multiple sclerosis pathophysiology are depicted as dashed boxes, and proposed mechanims of MSCs are illustrated with encircled letters. Abbreviations: DAMP, Damage-associated molecular pattern; EAE, Experimental autoimmune encephalitis; HO-1, Heme-oxygenase 1; IDO, Indoleamine 2,3-dioxygenase;

MSC, Mesenchymal stem cell; NO, Nitric oxide; NT-3, Neurotrophin 3; PAMP, Pathogen-associated molecular pattern; ROS, Reactive oxygen species; TLR, Toll-like receptor. (Salem & Thiemermann, 2010).

Although pre-clinical and clinical trials suggest MSC transplantation as a promising therapy for MS, more studies and long-term clinical trials are necessary to provide final conclusions. As of April 2015, the NIH website (http://clinicaltrials.gov) lists 13 MSC-based therapies in multiple sclerosis. Currently, there are over 215 open studies and 195 closed clinical trials (results retrieved 26th April 2015) in a search of www.clinicaltrials.gov on the search term "mesenchymal stem cells" and excluding trials with an unknown status.

1.6.1.1 Mesenchymal stem cell secretome

The wide range of secreted soluble factors produced by the MSCs, generally refered to as the MSC secretome, has a considerably therapeutic potential for the treatment of several diseases, including demyelinating disorders. Thus, harnessing the secretome will have important implications for clinical approaches. To this end, different groups have identified a spectrum of cytokines, growth factors, chemokines, extracelular matrix (ECM), proteases hormones and lipid mediators secreted by MSCs (Paul & Anisimov, 2013; Zimmerlin et al., 2013; Bai et al., 2012; Ranganath et al., 2012; Meirelles et al., 2009; Rivera et al., 2008, 2006). However, it must be considered that once the MSCs have been transplanted, it is more challenging to control and study the secretome expression and that it is most likely to be different from that observed *in vitro*. Meirelles and colleagues reviewed the main bioactive molecules secreted by MSC that may exert a paracrine effect upon transplantation (Figure 12) (Meirelles et al., 2009).
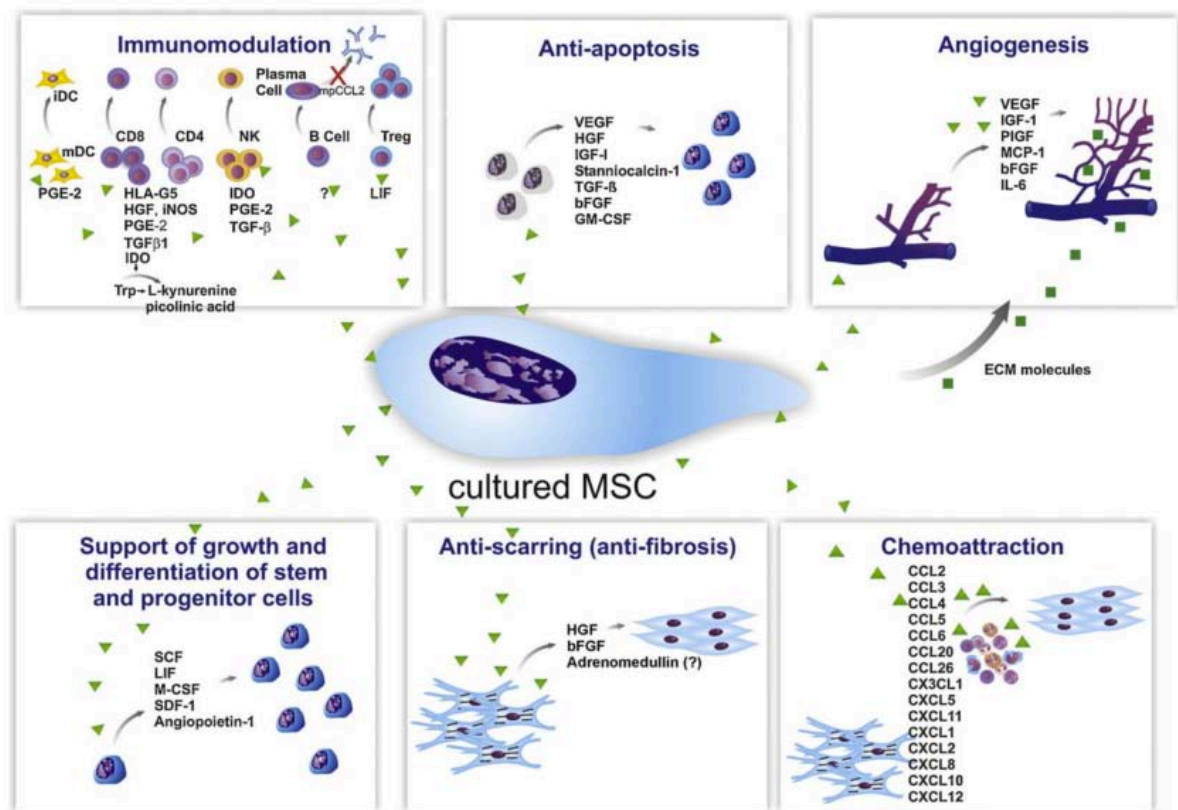
Figure 12. Main soluble factors secreted by MSCs. The secretion of a wide range of bioactive molecules is believed by many scientist to be the main mechanims by which MSCs exert their beneficial therapeutic effect. It can by divided into 6 categories: Immunomodulatory, anti-apoptotic, angiogenic, support of the growth and differentiation of local stem and progenitor cells, antiscarring and chemoattracting. Although new factors are discovered every day, the main modulators of the paracrine effect of MSCs are depicted here for illustrative purposes. Regarding the immunomodulation, MSCs inhibit the proliferation of CD8+ and CD4+ T lymphocytes and natural killer (NK) cells, suppress the immunoglobulin production by plasma cells, stimulate the proliferation of regulatory T cells and finally inhibit the maturation of dendritic cells (DCs). The rest of the effects induced by the soluble factors are depicted in the figure (Meirelles et al., 2009).

Despite the progress made in recent years regarding the elucidation of the MSCs secretome, there are still some questions that remain elusive: 1) Do scientist have the required technology to study the MSC secretome in vivo? Which are the most effective approaches to achieve this? 2) How do the composition and sustainability of the MSC change *in vitro* and after transplantation, and how is this is influenced by the dynamic of local microenvironment? (3) What are the ways to control the secretome properties over time after transplantation? These and other challenges remain, and harnessing the MSCs secretome for meaningful therapeutic outcomes will be necessary in the near future (Ranganath et al., 2012).

1.7 Fibroblast growth factors (FGFs)

Fibroblast growth factors (FGFs) are a family of soluble protein ligands that regulates a plethora of developmental processes, including brain patterning, branching morphogenesis and limb development, as well as tissue homeostasis and metabolism. Additionally, several mitogenic, cytoprotective and angiogenic therapeutic applications of FGFs have been explored (reviewed in Beenken and Mohammadi, 2009). There are 18 mammalian FGFs (FGF1–FGF10 and FGF16–FGF23), with different receptor binding affinities and biological functions including neural induction, patterning, survival, proliferation, diferentiation, axon pathfinding and synapse formation (Mohammadi et al., 2005; Itoh and Ornitz 2004; Eriksson et al., 1991). The molecular weight of FGFs proteins range 17-34kDa. They present similar tridimensional structure and alternative splicing modulates their receptor affinity. Transductional mechanims of FGF signaling pathways is mediated via transmembrane tyrosine-kinase FGF receptors (FGFR1-4). Heparine sulphate proteoglycans (HSPGs) act as co-factors in the activation of the FGFRs by FGFs. The FGFs act through highly conserved Ras-ERK mitogen-activated protein kinase (MAPK) signaling cascade or through the phospatidylinositol-3 kinase (PI3K-AKT) pathway, promoting proliferation, survival, and/or motility in various cell types, including oligodendrocytes (Mitew et al., 2013; Furusho et al., 2011; Turner & Rose 2010; Gotoh 2008; Bottcher & Niehrs 2005; Thisse & Thisse 2005; Chandran et al., 2003). Such a diverse set of activities requires a tight control of the transduction signal which is achieved through the expression of genes that function in the FGF-feedback regulation such as the Sproutys, Sef and MAP kinase phosphatase 3 which are responsible for the attenuation of FGF signals, limiting its activities in time and space (Thisse & Thisse, 2005).

1.7.1 Fibroblast growth factor 8 (FGF8)

Fibroblast growth factor 8 (FGF8) was originally identified as an androgen-induced growth factor (AIGF) being isolated from the mouse mammary carcinoma cell line SC-3 in response to androgen stimulation (Tanaka & Takeda, 1992). The gene structure of FGF8 is more complicated than that of most FGF genes, since there are at least four exonic forms in FGF8 that correspond to the usual first exon of other *Fgf* genes. Despite the existence of such isoforms, *in situ* hybridization and immunohistochemistry (IHC) analysis have not revealed major differences in the spatial and temporal localizations of the FGF8 isoforms,

being postulated that they are functionally redundant (Blunt et al., 1997; Crossley & Martin 1995; Macarthur et al., 1995). FGF8 is known to be implicated in early vertebrate brain patterning, and its inhibition causes early embryonic death with absence of the entire mesencephalic and cerebellar primordia (Nakamura et al., 2008; Partanen 2007; Reifers et al., 1998; Crossley & Martin 1996, 1995) as well as important thalamic and telencephalic malformations (Martinez-Ferre & Martinez 2009; Storm et al., 2006). FGF8 is capable of binding to all its four receptors, with different affinities among them (Ornitz et al., 1996; Kouhara et al., 1994). When the growth factor binds to its receptor, phosphorylation of the Extracellular signal Regulated Kinase 1/2 (ERK1/2) usually occurs, activating the RAS-MAPK intracellular pathway (TsangM & Dawid 2004; Corson et al., 2003; Chirsten & Slack 1999; McKinnon et al., 1990) Several studies have demonstrated the importance of the FGF8 in the treatment of several neurodegenerative diseases, since *in vitro* generation of dopaminergic neurons, cells that are lost in Parkinson´s disease, requires the presence of this inductive growth factor (Parmar & Li, 2007; X. Wang et al., 2004; Goridis & Rohrer 2002). However, our knowledge about the role of FGF8 in the CNS diseases remains poorly understood.

Another interesting growth factor of this family that has attracted some attention during the past years, due to its effects in some CNS cell populations, is the fibroblast growth factor 2 (FGF2), also known as basic fibroblast growth factor (bFGF) and which is found in the MSCs secretome. FGF2 when combined with PDGF-AA, is known to induce proliferation in OPCs (Bogler et al., 1990; McKinnon et al., 1990), while mature oligodendrocytes in the presence of this growth factor revert to a progenitor state (Fressinaud et al., 1995; Grinspan et al., 1993). The survival of newly generated OPCs as well as oligodendrocytes is likely to be via the prosurvival PI3K/Akt signaling pathway, which is a downstream effect of FGFR2 activation (Bryant et al., 2009). Moreover, FGF2 is typically used in combination with other factors to mantain neurospheres cultures *in vitro* in an undifferentiated state, promoting their proliferation. In addition, Azim and colleagues shown that intraventricular injection of FGF2 induce NSPCs to follow an oligodendrocytic fate, and even though FGF2 did not notably block OPC differentiation, increasing the number of oligodendrocytes in the perivascular white matter (PVWM) and cortex, it markedly disrupted myelination in the PVWM (Azim et al., 2012). Similarly, Zhou and collaborators have reported that FGF2 inhibits OPCs differentiation during development and limits remyelination following chronic demyelination (Zhou et al., 2004). The key

evidence that FGF2 may have a direct detrimental effect on mature oligodendrocytes comes from previous culture studies showing that exposure of pure cultures of mature oligodendrocytes to FGF2 results in loss of myelin-like membranes (Bansal and Pfeiffer, 1997), as well as the negative effects of FGF2 on myelination that may be mediated via FGFR1, and not FGFR2 signaling (Fortin et al., 2005). Thus, whereas this factor is promising due to its mitotic effect in OPCs and the promotion of an oligodendrocityc determination in NSPCs, all the studies indicate that there is also a negative effect in terms of OPCs differentiation and myelin production. On the other hand, it has been proven that OPCs cultured in the presence of FGF8 expressed significantly more MBP compared to FGF2 (Fortin et al., 2005), revealing that these two at-first similar growth factors, may have a distinct effect, possibly due to its different binding receptor affinity.

Chapter II

- AIM & OBJECTIVES -

2.1   Project aim

The general aim of this work is to investigate the therapeutic potential of bone marrow-derived mesenchymal stem cells (MSCs) in a murine chronic demyelinating model. In particular, the present study focuses on the analysis of the effect that intracerebroventricular injections of MSCs may have on remyelination and whether the trophic factor support exerted by the stem cells in the CSF could be stimulating the endogenous oligodendrogenic program in the ventricular-subventricular zone (V-SVZ). In addition, the main objective of the second section of this thesis is to study the effect that the fibroblast growth factor 8 (FGF8) may exert on post-natal OPCs *in vitro*. As this factor is a known morphogen during embryonic development, the rationale is that FGF8 may be used to induce OPCs mobilization, proliferation, differentiation and/or remyelination.

2.2   Project objectives

Section I

1. **To investigate whether the transplanted MSCs could change the oligodendrocyte and astrocyte numbers within the demyelinated corpus callosum (CC) over time.** The CC is by far the largest fiber tract in the brain, being a common target in MS (Ozturk et al., 2001; Warlop, et al., 2008). Thus, the number of oligodendrocytes will be calculated at different stages of differentiation within the CC over time as well as the astrocyte content, using immunohistochemical techniques (IHC).

2. **To assess the myelin content in the corpus callosum over time and its correlation with the oligodendrocyte numbers.** In order to elucidate if the increase of oligodendrocytes over time correlates with a real increase of myelin content in the CC, the myelin density will be quantified both *in vivo* in a longitudinal study by magnetic resonance imaging (MRI) and *in vitro* using a combination of IHC and 3D Imaris reconstruction software.

3. **To study the functionality of the newly formed myelin as well as its ultrastructure.** In order to characterize the functional consequences of the MSC treatment, electrophysiological recordings of the axonal conduction velocity in the callosal axons will be performed. Moreover, further assessment of the integrity of

the myelin ultrastructure will be performed, calculating its thickness as well as the g-ratio of myelinated and unmyelinated axons by electron microscopy (EM) analysis.

4. **To analyze the trophic factor content of the cerebrospinal fluid (CSF) as well as the behaviour of the injected MSCs.** MSCs are known to be the source of multiple immunomodulatory agents and trophic factors involved in repair and regenerative processes. In this study, the trophic factor content of the CSF will be analysed by qPCR three months after MSCs transplantation, as they may be the potential candidates for the remyelinating effects observed. Furthermore, the precise location, viability and phenotypic characteristics of the transplanted MSCs will be studied by IHC, MRI and Western Blot (WB).

5. **To unravel the mechanisms underlying the remyelination processes observed.** In order to elucidate whether the NSPCs located within the V-SVZ are capable of responding to the secreted soluble factors in the CSF, BrdU proliferating assay will be performed *in vivo*, just after MSC transplantation. Furthermore, it will be analysed whether the MSCs are capable of activating survival and proliferation signalling pathways in the NSPCs *in vitro*. To this end, NSPCs will be cultured in the presence of MSC conditioned medium (MSC-CM) and the activation of the PI3K/Akt and MAPK/Erk1/2 signaling cascades analysed by WB.

Section II

1. **To study the effect of FGF8 in the proliferation and differentiation of oligodendrocyte progenitor cells (OPCs) *in vitro*.** Post-natal OPCs will be cultured in the presence of FGF8. BrdU incorporation analysis, IHC and quantitative PCR (qPCR) will be performed in order to study their proliferation and differentiation due to the morphogen effect.

2. **To investigate the capability of FGF8 to stimulate OPCs migration throughout the binding of FGF8 to its FGF receptors *in vitro*.** Migration studies will be performed in matrigel cultures, where OPCs will be placed at a certain distance of a FGF8-soaked heparin bead. In order to confirm this migrating property, the FGF-receptor inhibitor SU5402 will be used in the cultures to counteract the effect of FGF8.

Chapter III

- MATERIAL & METHODS -

3.1 Animals models

All experiments have been performed in compliance with the Spanish and European Union laws on animal care in experimentation (Council Directive 86/609/EEC) and have been analysed and approved by the Animal Experimentation Committee of the Universidad Miguel Hernández. Green fluorescent protein (GFP) (C57BL/6-Tg(ACTB-EGFP)1Osb/J) transgenic mice were used as donors, whereas C57BL/6 wild type mice were used as hosts. Both animal strains were bred and maintained in the animal facilities at the Universidad Miguel Hernández.

3.1.1 Cuprizone treatment to obtain the chronically demyelinated model

The approach used was similar to our previously published reports (Cruz-Martinez et al., 2014 [Appendix 1]; Jaramillo-Merchán et al., 2013). Six-week old C57BL/6 mice were given a diet with 0.2% cuprizone (w/w) (Sigma, Cat. No. C9012) for 12 weeks ad libitum in order to obtain a chronic version of toxicity-induced demyelination. Finely powdered cuprizone (Sigma-Aldrich, St. Louis, MO) was mixed in the rodent chow and administered to the mice using specially designed feeders. After 12 weeks, the mice were used for different experiments and returned to normal chow until their sacrifice, which was depending on the test at 0, 15, 30, 60, 90 or 120 days.

3.2 Tissue culture

3.2.1 Mesenchymal stem cells (MSCs) isolation & culture

The isolation and culture of MSCs was performed as in our previous studies (Cruz-Martinez et al., 2014 [Appendix 2]; Jaramillo-Merchán et al., 2013; Pastor et al., 2012; Jones et al., 2010). Femurs were dissected from 2-3 month old mice, which were sacrificed by cervical dislocation. Bone marrows (BM) of either transgenic-GFP or C57BL/6 wild type mice were extracted and cells were collected by cutting both ends of femurs and flushing them into a 15-ml conical tube (Sarstedt) with complete medium (CM), containing Dulbecco's Modified Eagle Medium (DMEM), (High Glucose) with GlutaMAX (Bioscience, Cat. No. 32430-027, 1X), fetal bovine serum (Biochrom, Cat. No. S0115, 15%) and Penicillin/Streptomycin (Gibco, Cat. Num. 15140-122, 1%). The obtained cell suspension (3 animals per falcon tube) was centrifuged at 1000 rpm for 5 min and the supernatant was removed. The pellet was then

resuspended into 5 ml of the complete medium (CM) and plated in T-25 flasks (Sarstedt). The first media change was performed less than 72 hours after plating the cells in the flask. The stem cells were maintained for 3–4 weeks (passages 2–3) growing in T-75 flasks (Sarstedt), changing the media every 2-3 days and replating when needed, before proceeding to the surgical interventions. It was checked that the MSCs were positive for CD44 and CD90, typical surface markers of these cells, and negative for hematopoietic surface antigens like CD45.

3.2.1.1 Preparation of MSC conditioned medium (MSC-CM)

The isolation and culture of MSCs was performed following the above mentioned protocol. MSC-CM was collected after 24h of plating the MSCs at 60-70% of confluence in a T-75 flask with fresh culture medium (complete medium). The MSC-CM was then filtered using a 0.22 μm filter.

3.2.2 Neural stem progenitor cells (NSPCs) isolation & culture

NSPCs were isolated and cultured in a similar fashion as published in (Hutton and Pevny, 2008; Wachs et al., 2003). The brains of the C57/BL6 mice (P0-P1) noeonates were carefully removed from the skull and placed in a clean culture dish containing ice-cold Neurobasal medium (Fisher, Cat. No. 11570556). Using fine-tipped forceps and a microsurgical knife, the meninges were carefully removed and the SVZ was microdissected. Using a sterile transfer pipette, the SVZ was then transferred using a sterile transfer pipette to a non-treated polystyrene dish containing cold Neurobasal medium, where the tissue was cut into smaller pieces using a 1.75 mm angled phaco slit knife (Eagle Labs). The pieces were then transferred to a 15-mL conical tube (Sarstedt) containing 2 mL of 1mg/ml Collagenase XI (Sigma, Cat. No. C7657)/3mg/ml Dispase (Gibco, Cat. No. 17105-041), minimizing the amount of Neurobasal transferred with the sample. The tissue was incubated at 37°C for 20 min in a cell culture incubator, mixing every ~5 min by mechanical trituration, with different sized pipette tips. The obtained cell suspension (5 animals per falcon tube) was centrifuged at 1000 rpm for 5 min and the supernatant was removed. The resulting pellet was resuspended in 5ml of Neurobasal medium (Life Technologies; Cat. No. 21103-049) supplemented with B27 1X (Gibco, Cat. No. 17504-044), 20ng/ml EGF (Roche; Cat. No. 11376454001), 2ng/ml bFGF

(Roche, Cat. No. 11104616001), 0.7U/ml Heparin (Sigma, Cat. No. H3393), 2mM L-glutamine (Gibco, Cat. No. 25030-024) and 1% Penicillin/Streptomycin (Gibco, Cat. No. 15140-122), and plated in non-coated T-25 flasks (Sarstedt), changing ½ of the culture medium every 2-3 days. After 5-7 days, neurospheres with variable sizes (50-100 μm in diameter) were formed in the culture. Neurosphere cell suspension was collected and centrifuged at 1000g for 5 min, the supernatant was discarded, and the pellet resuspended in 2 ml of Accutase (Sigma-Aldrich, Cat. No. A6964) at 37 °C for 5 min. The cell suspension was gently pipetted, 4 ml of Neurobasal was added and centrifuged again at 1000g for 5 min. The pellet was then resuspended in 10 ml of supplemented Neurobasal medium and subcultured into new T-75 flask (Sarstedt). The culture was maintained for another 12 days, when the neurospheres were collected for experiments.

3.2.3 Treatment of NSPCs with MSC-CM

To study the phosporylation state of MAPK (Erk1/2) and AKT, neurospheres were obtained as in the above-mentioned procedure. NSPCs cultures from 2-3 T-75 flasks were collected, the cell suspension was divided into 2 15-ml conical tubes and centrifuged at 1000g for 5 min. The supernatant was discarded and both pellets resuspended in 4 ml of MSC-CM and the control medium [Dulbecco's Modified Eagle Medium (DMEM), (High Glucose) with GlutaMAX] respectively. One mililiter of each conical tube was added in a Petri dish (Sarstedt), with a total of 8 Petri dishes and placed into a cell culture incubator at 37ºC and 5% CO_2. The culture was stopped at 15´, 30´ and 1 hour by pippetting the cell suspension of each Petri dish into an eppendorf, placing it in ice and centrifuging at 1000g for 5 min at 4ºC, discarding the supernatant and resuspending the pellet in lysis buffer. Subsequently, the suspension was processed for protein analysis by Western Blot. For further analysis, the NSPC cultures were analysed at 15 minutes.

3.2.4 Oligodendrocyte Progenitor Cells (OPCs) isolation & culture

The protocol used was similar to previous publications (Morello et al., 2011; Lee et al., 2007; Yang et al., 2005). The brains of C57/BL6 mice (P0-P1) neonates were carefully removed from the skull, and using fine-tipped forceps under a dissection microscope, the meninges were carefully removed from the tissue. Placing the meninges-free brains into one clean Petri

dish on ice, the forebrains were microdissected and diced into 1 mm fragments, placing them in a clean dish containing ice-cold DMEM medium (Sigma, Cat. No. D6546). The pieces from every 4 neonates were pippetted into a 15-ml conical tubes, and 1ml of 1mg/ml Collagenase XI (Sigma, Cat. No. C7657)/3mg/ml Dispase(Gibco, Cat. No. 17105-041) solution was added. The tissue was incubated at 37°C for 20 min, mixing every 5 min by mechanical trituration, with different size pipette tips. The obtained cell suspension was centrifuged at 1000 rpm for 5 min and the supernatant removed. The resulting pellet was resuspended in 5ml of DMEM (Sigma, Cat. No. D6546) supplemented with fetal bovine serum (Biochrom, Cat. No. S0115, 15%) and Penicillin/Streptomycin (Gibco, Cat. Num. 15140-122, 1%). The resulting cellular suspension was then placed on previously poly-L-lysine coated T-25 flasks (Sarstedt), changing the culture medium every 2-3 days. After 7–10 days, the culture consisted mainly in astrocytes with a small number of OPCs growing on top. In order to purify the culture, the flasks were placed on a horizontal orbital shaker at 200 rpm and 37ºC in order to remove microglial cells. The medium was discarded from the flasks by aspiration, adding fresh culture medium. Tightening the plug-seal caps and securing the flasks to the orbital shaker, the flaks were shaken again at 200 rpm overnight at 37 ºC . The next day, the flasks were removed from the shaker and sterilized the surface by spraying with 70% ethanol to prevent contamination. The cell suspension from each flask was collected and plated onto uncoated Petri dishes (Sarstedt) for 1h to further remove residual contaminating microglia/astrocytes. The cell suspension was then replated in DMEM with 10% FBS (Biochrom, Cat. No. S0115), Penicillin/Streptomycin (Gibco, Cat. Num. 15140-122, 1%), 10 ng/ml PDGF-AA (Sigma, Cat. No. SRP3228) and 10 ng/ml bFGF (Roche, Cat. No. 11104616001) for 7 days to stimulate the proliferation of OPCs, changing the culture medium every 2-3 days. This resulted in a cell culture of mainly OPCs. Some of these OPCs were used for the matrigel culture experiments, whereas the rest were used for immunocytochemistry and quantitative PCR analysis.

3.2.5 Treatment of OPCs with FGF8

Purified OPCs were obtained as mentioned above and the resulting pellet was resuspended in three different culture medium: differentiating medium (DMEM with 15% FBS, 1% penicillin/streptomycin), undifferentiating medium (DMEM with 10% FBS, 1%

penicillin/streptomycin, 10 ng/ml PDGF-AA and 10 ng/ml bFGF) and differentiating medium + 500 ng/ml FGF8 (R&D, Cat. No. 423-F8-025). The resulting cell suspensions was plated at the same concentration in different poly-L-lysine coated Petri dishes for qPCR and onto coated coverslips for immunocytochemistry analysis. The cultures were kept in each specific mediums for 7 days, refreshing the medium every 2-3 days. In the case of the proliferation assay, BrdU (1μg/ml) was added to the culture 24 hours before fixing the cells.

3.2.6 Matrigel cultures

OPCs obtained by the aforementioned protocol were also used to perform matrigel culture experiments. This experiment was conducted in collaboration with another independent researcher of our group. The method used was similar to that previously published (Aarum et al., 2003). A total of 20.000 oligodendrocyte progenitor cells were re-suspended in 5 ml of DMEM (Sigma, Cat. No. D6546) and 20 ml of matrigel basement membrane matrix (BD Bioscience, 10 ml). DMEM supplemented with 15% FBS (Biochrom, Cat. No. S0115) was used as culture medium, as in the differentiation protocol of OPCs. The re-suspended cells were spread on a tissue culture dish (Becton Dickinson Labware), solidified during 25 min at 37ºC and culture medium was added. Afterwards the cell-matrigel was cut in small squares of 125 mm^2 and put on a solidified matrigel drop. Heparin acrylic beads (Sigma) were first rinsed in phosphate-buffered saline (PBS) four to six times and then soaked in FGF8 solution (5000 ng/ml; R&D) at 4ºC overnight. The beads were then rinsed three times in PBS and put on the solidified matrigel drop 500 mm from the place where cellsmatrigel was located. Control beads were soaked only in PBS and implanted in the same manner. FGF inhibitor (SU5402) was diluted in culture medium to a final concentration of 20 mM and soaked in Affigel blue beads (Bio-Rad), using the same procedure as described for FGF8-soaked beads. Then, 25 ml of a 1:1 matrigel:culture medium mix was added, covering the drop where cells and beads were placed. After 2 h at 37ºC, the culture medium was added. Finally, 24h and 48h afterwards, the migrating and/or non-migrating-cells were observed under a dissecting microscope. To confirm an FGF8-mediated attracting effect, the proximal/distal rate was calculated in control and FGF8-embedded cultures. This was performed similar to a previous publication (Vernerey et al., 2013). Thus, the images of the cell clusters were analyzed by imaging software to draw a 45º arc from the cluster towards the beads. The number of cells

counted inside this arc (proximal cells) was divided by the number of cells outside the arc (distal cells), obtaining a proximal/distal rate. Values greater or less than 1 indicated more or less cells, respectively, near the bead.

3.3 Surgical procedures

3.3.1 MSCs transplantation & experimental groups

A total of 42 mice were injected with MSCs [n=12 for immunohistochemistry (IHC), n=6 for immunofluorescence (IF) & Imaris analysis software, n=6 for magnetic resonance imaging, n=4 for electrophysiology, n=4 for electron microscopy (EM), n=6 for BrdU proliferation assay, n=4 for electroporation]. For the sham-operated group a similar number of animals were used for each type of experiment. The protocol used was similar to previous publications with some modifications (Cetin et al., 2006). Before starting the surgery, the surgical area was disinfected by wiping with 70% ethanol and the tools sterilized. The animals were weighed individually in order to calculate the appropriate dose of anesthesia/analgesia, which consisted in a mixture of ketamine and xylazine at a dose of 80–100 mg ketamine (Richter Pharma) and 10 mg xylazine (Laboratorios Calier) per kilogram body weight, given intraperitoneally. To inject the mixture, the animals were restrained with one hand with abdomen facing up and the injection was performed intraperitoneally through a needle inserted into the lower left abdominal quadrant (needle size, 22–23 G). The mice normally fell asleep (but still be sensitive to nociceptive stimuli) within 2–3 min and surgical anesthesia (lack of response to nociceptive stimuli) reached within 10–15 min. The fur of the skull of the animals was shaved, the skin cleaned with 70% ethanol and the mice placed in the stereotaxic apparatus (Stoelting, Wheat Lane Wood Dale, IN, USA). The injections were performed in both LV at the following stereotaxic coordinates (Kopf, model 900 small animal stereotaxic instrument; anteroposterior relative to bregma, mediolateral and dorsoventral from the surface of the brain): +0.5, 0.75 and 2.5 mm, respectively. The x, y and z coordinates that would be used for the injection were calculated and a small incision with a 27-G needle held at a flat angle was cut (avoiding injuring the brain surface by pointing the needle downward). The MSCs were injected using a 5 μl Hamilton syringe (Reno, NV, USA). A volume of 2μL, containing approximately 300.000 cells, was injected in a 4-minute time lapse into each LV. The needle

was left in place after injection for 2 minutes and then withdrawn slowly. After the injection, the incision was sutured and 30 ml of sterile PBS per kilogram body weight were injected subcutaneously to avoid dehydration. Mice were kept warm either under a heat lamp or on a temperature-controlled heat blanket (in the electroporation experiments) until they fully recovered. Aftery recovery, buprenorphine (RB Pharmaceuticals) was injected at a dose of 0.1 mg per kilogram body weight. The animals were returned to a clean cage, adding a small dish with wet food pellets in the cage for easy access to food. Injections of additional analgesic, meloxicam (Norbrook) at a dose of 1 mg per kilogram body weight on the first and second days after the surgery were carried out. The recovery of the animals was monitored closely on a daily basis for at least 1 week, assessing any signs of distress, lack of grooming, reduced locomotion, wound healing. For the IHC analysis, the mice were sacrificed at 30, 60 and 90 days after the surgical intervention, whereas for MRI mice were euthanized at 0, 15, 30, 60 and 90 days after the surgery. For the BrdU analysis mice were analysed 1 month post-injection, and 20 days post-injection in the case of the electroporations. As for the remaining tests (electrophysiology and EM), the mice were sacrificed 2 and 4 months after the intervention.

3.4 Molecular biology techniques

3.4.1 Western Blot analysis for NSPCs protein extract

Proteins were processed for Western blot analysis to determine the relative levels of p-AKT and p-ERK1/2. Neurospheres were lysed with 10mM TRIS-HCl buffer (pH7.4) containing 0.5% TX-100, 0.5% Igepal, 150mM NaCl, 50mM MgCl2, 1mM EGTA, (all from Sigma), and the proteases inhibitor cocktail tablet, and phosphoStop tablet (both from Roche). Samples were sonicated and centrifuged at 12.000 rpm for 30 min at 4ºC; the supernatant collected in aliquots and stored at -20ºC. The protein concentration was determined using the BCA protein assay kit from Pierce (Rockford, IL). Sample proteins were separated by electrophoresis in 10% SDS-polyacrylamide minigels and transferred to nitrocellulose membranes (Protran, Whatman GmbH). Membranes were blocked with 5% BSA (Sigma) in (TBS-T) Tris buffer saline (TBS) (0.2 M Tris-HCl, 137 mM NaCl, from Sigma, at pH 7.6) with 0.025% Tween 20 (Sigma), and incubated with primary antibodies diluted in blocking solution overnight at 4ºC: rabbit anti-Akt phosphorylated (Ser 473, 1:1000, Cell Signalling), rabbit anti-ERK1/2 di-

phosphorylated (Thr 44/42, 1:1000, Cell Signalling). After extensive washing with (TBS-T), membranes were incubated with the HRP-conjugated goat anti-rabbit 1:5000 diluted in 1% milk blocking solution for 90 min at RT. The membranes were revealed with the Luminata Forte HRP substrate (Millipore) and images taken with a LAS-1000 apparatus (Fuji). Membranes were subsequently washed with TBS-T in order to perform the loading control, using mouse monoclonal anti-β actin (1:15000, Sigma) as primary antibody and HRP-conjugated horse anti-mouse (1:7000, Vector Laboratories, CA) as secondary. For signal development Luminata Classic HRP substrate (Millipore) was used. Quantifications and data analysis were performed using ImageJ software (http://rsbweb.nih.gov/ij) as described by (Hu & Beeton, 2010).

3.4.2 Western Blot analysis for cerebrospinal fluid (CSF) protein extract

Animals were anesthetized three months after MSC-injection and placed in the stereotaxic device. Subcutaneous tissue was scraped off the skull with a scalpel, and a small burr hole (from 1 mm to 2 mm diameter) was drilled where the old incision was made, as it was still visible. The CSF was withdrawn through a needle, placing it into the LVs as explained before, and 200 µL of CSF from each animal were draw, making sure that the sample did not contain traces of blood. Animals were then sacrificed by cervical dislocation and used for other experiments. Control CSF was obtained from age-matched animals (SHAM) in a similar fashion. The samples were procesed as before, following a standard Western Blot protocol, analyzing in this case the GFP protein content. Rabbit anti-GFP (1:5000, Molecular Probes) was used as a primary antibody and HRP-conjugated goat anti-rabbit (1:7000, Vector Laboratories, CA) as a secondary antibody. The antibodies for the control charge were the same as before.

3.4.3 Quantitative real time PCR (qPCR)

3.4.3.1 CSF analysis

CSF of MSC-transplanted as well as SHAM mice was extracted as previously explained and analysed for gene expression of neurotrophic factors NT3, NT4, PDGF, IGF, VEGF, BDNF, FGF2, NGF, and GDNF. Total mRNA of the cells was isolated using the Trizol protocol (Invitrogen). A total of 5 µg of mRNA was reverse-transcribed, and approximately 100 ng of

cDNA was amplified by Real Time PCR using Power SYBR Green Master mix (Applied Biosystems). All the samples were run in triplicate using the StepOne Plus Real-Time PCR system (Applied Biosystems) and analysed with the StepOne Software. Analyses were carried out using the delta C(T) method and calculated relative to GAPDH. The results were normalized with respect to the control condition, which presented a value of 1, using the same approach as in previous report (Jones et al. 2012). The sequences of the primers used are shown in Table 1. The resulting PCR products were placed in a QIAxcel apparatus (Qiagen) and analysed using the QIAxcel gel analysis software (QIAxcel Biocalculator).

3.4.3.2 OPCs gene expression

For the OPCs experiments, total mRNA of these cells was isolated using the Trizol protocol (Invitrogen). A total of 5 µg of mRNA was reverse-transcribed, and approximately 100 ng of cDNA was amplified using the same method previously commented. PDGFR-α, NG2 and Olig2 gene expression were analysed. All the samples were run in triplicate. Analyses were also carried out using the delta C(T) method and calculated relative to GAPDH. The results were normalized as in the aforementioned protocol. Primers sequences are shown in Table 1.

Table 1. List of primers used for the qPCR.

Gene	Forward Primer	Reverse Primer
GAPDH	AGGTCGGTGTGAACGGATTTG	GGGGTCGTTGATGGCAACA
PDGFR-α	TCCATGCTAGACTCAGAAGTCA	TCCCGGTGGACACAATTTTTC
NG2	GGGCTGTGCTGTCTGTTGA	TGATTCCCTTCAGGTAAGGCA
Olig2	CTAATTCACATTCGGAAG	AAAAGATCATCGGGTTCT
NT3	AGTTTGCCGGAAGACTCTCTC	GGGTGCTCTGGTAATTTTCCTTA
NT4/5	TGAGCTGGCATATGCGAC	CAGCGCGTCTCGAAGAAGT
PDGF	GCAAGACCAGGACGGTCATTT	GGCACTTGACACTGCTCGT
FGF2	AGTGTGTGCTAACCGTTACCT	ACTGCCCAGTTCGTTTCAGTG
BDNF	TCATACTTCGGTTGCATGAAGG	GTCCGTGGACGTTTACTTCTTT
NGF	GCACTACACCCATCAAGTTCA	TCCTGAGTCATGCTCACAAGT
GDNF	CGCCGGTAAGAGGCTTCTC	CGTCATCAAACTGGTCAGGATAA
VEGF	CGCAGCTACTGCCATCCAAT	GTGAGGTTTGATCCGCAT
IGF-1	GGAGCTGTGATCTAAGGAGGC	GGGCTGATACTTCTGGGTCTT

3.5 BrdU proliferation assay

MSC-transplanted and SHAM mice were given 5-bromo-2-deoxyuridine (BrdU) (Sigma, Cat. No. B5002) in the drinking water (1 mg/ml) daily for up to two weeks just after transplantations, followed by another 2 weeks with BrdU-free drinking water. BrdU-containing water bottles were shielded from light to prevent BrdU degradation and the water was replaced twice per week. Mice were then sacrificed and brain sections were obtained as previously described. Sections were double immunostained for BrdU/Nestin/DAPI. Sixteen 14-μm sections that were 84-μm apart were selected, containing the SVZ (n=6 in each treatment group). The total number of double immunostained cells (BrdU/Nestin+) per section and per SVZ was then calculated.

3.6 Histological techniques

3.6.1 Paraffin microtome sections

To fixate the brain tissue, the mice were anesthesized using isoflurane and perfused intracardially with ice-cold 4% filtered paraformaldehyde (PFA) in phosphate buffer solution (PBS; pH 7.4). Animals were decapitated using large scissors, the skin down the midline from the neck up was removed and subsequently the scissors inserted in the foramen magnum of the skull and continued along the midline rostrally. The skull was peeled back with straight forceps, and the brain rapidly removed using a small spatula, placing it immediately in a flask containing 4% PFA. Brains were kept in 4% PFA overnight rocking at 4ºC. After fixation, the samples were dehydrated and paraffin-embedded overnight. The paraffin was then changed every 1h around 5-7 times, the brains were finally oriented and the paraffin was allowed to solidify. 14μm coronal serial sections were obtained using a microtome (Microm HM335E), mounted on six parallel series and processed for staining or IHC.

3.6.2 Klüver-Barrera staining

Several microtome series were used to study the areas of demyelination in the cuprizone-treated mice. The sections were incubated with Luxol Fast Blue (1% in 95% ethanol with 0.5% acetic acid) and counterstained with Cresyl Violet according to the standard Klüver-Barrera protocol (Sheehan and Hrapchak, 1980). Sections were incubated in Luxol Fast Blue (Fisher, Cat. No. 212170250) staining solution overnight at 60ºC, the excess solution removed using 96% EtOH in water, rinsed in distilled water, treated with lithium carbonate solution (0.05%) for 30 seconds followed by 70% EtOH until the gray matter was clear and WM sharply defined. When the staining was completed, the slides were placed in distilled water and counterstained in (Cresyl Violet Acetate) for 5 min, dehydrated in an ethanol series, cleared in xylene and mounted for microscopy.

3.6.3 Immunohistochemistry (IHC)

For IHC, sections were deparaffinised in xylol for 2h, rehydrated through a descending series of EtOH solutions: 2 X 10 min in 100% EtOH, 2 X 10 min in 96% EtOH in water, 2 X 10 min in 70% EtOH in water and 1 X 10 min in water. Afterwards, antigen retrieval was performed

when necessary with a Dako Autostainer (Dako). In the case of BrdU antigen, DNA was denatured by incubating sections in 2N HCl (Sigma-Aldrich, Cat. Num. 30721) for 30 minutes at 37 °C, and the acid neutralized by immersing sections in 0.1M borate buffer (Sigma-Aldrich) for 2 x 5 min, before incubation in PBS-T. Samples were then blocked with 5% Bovine Serum Albumin (BSA) (A2058) + 10% serum (same species as the secondary antibody) diluted in PBS 1X for 2h. After the blocking step, the slides were incubated overnight at 4ºC with different primary antibodies (Table 2). Even when the transplanted MSCs and the electroporated GFP-plasmid express GFP, immunostaining was performed on this protein in order to amplify the signal in both cases. After washing in PBS-T for 30 min, the slides were incubated with the appropriate fluorescent labelled secondary antibody for 1h or biotinylated secondary for 2h at RT (Table 2) followed by an incubation with streptavidin conjugated with Cy2 or Cy3 (1:500, Amersham) for 1h at RT in the case of the biotinylated secondary. 6-Diamidino-2-phenylindole (DAPI; 2ng/ml; Molecular Probes) was used to stain nuclei. For non-fluorophore-conjugated antibodies, biotinylated secondary antibodies were visualized using the streptavidin-biotin-peroxidase method (Vectastain ABC Kit, Vector laboratories), stained with the cromogen 3-3′-diaminobenzidine tetrahydrochloride (DAB Substrate Kit for peroxidase, Vector laboratories) and counterstained with cresyl violet (Acros Organics, Belgium). Controls of immunostaining were performed in two slides of each sample following the same procedure, but eliminating primary or secondary antibodies. Finally, the slides were mounted with either Mowiol-NPG solution (fluorescence) (Millipore, Cat. No. 475904) or with Eukitt mounting medium (EMS, Cat. No. 15322).

3.6.4 Immunocytochemistry (ICC)

OPCs for ICC were cultured on top of poly-L-lysine coated coverslips. After the specific treatment the cells were fixed in 4% ice-cold paraformaldehyde (pH 7.4) and processed for ICC following a standard protocol. Coverslips were rinsed 3 x 10 min in PBS 1X, incubated 1h with PBS-T (0.05% Triton in PBS) and blocked with 5% BSA (Sigma, Cat. No. A2153-506) + 10% serum (same specie as secondary antibody) diluted in PBS 1X for 2h. In the case of BrdU antigen, DNA was denatured by incubating sections in 2N HCl (Sigma-Aldrich, Cat. Num. 30721) for 15 minutes at 37 °C, and the acid neutralized by immersing sections in 0.1M borate buffer (Sigma-Aldrich) for 2 x 5 min, before incubation in PBS-T. After the blocking

step, the coverslips were incubated overnight at 4ºC with different primary antibodies (Table 2). After washing in PBS 1X for 30 min, the slides were incubated with the appropriate fluorescent labelled secondary antibody 1h or biotinylated secondary 2h at RT (Table 2) followed by an incubation with streptavidin conjugated with Cy2 or Cy3 (1:500, Amersham) 1h at RT. 40,6-Diamidino-2-phenylindole (DAPI; 2ng/ml; Molecular Probes) was used to stain nuclei.

Table 2. List of primary and secondary antibodies used for the histological analysis.

Primary Antibody	Dilution	Company
anti-NG2 rabbit-polyclonal IgG	1:150	Chemicon
anti-CC1 mouse monoclonal IgG	1:50	Calbiochem
anti-BrdU sheep polyclonal IgG (IHC)	1:150	Abcam
Anti-BrdU mouse monoclonal IgG (ICC)	1:200	Dakocytomation
anti-PDGFR-α rabbit monoclonal IgG	1:100	Santa Cruz Biotechnology
anti-MBP mouse monoclonal IgG	1:100	Chemicon
Anti-Nestin mouse monoclonal IgM	1:200	Chemicon
Anti-Olig2 rabbit polyclonal IgG	1:200	Chemicon
Anti-GFP chicken polyclonal IgY	1:500	AVES
Anti-O4 mouse monoclonal IgM	1:500	Chemicon
Anti-GFAP rabbit polyclonal IgG	1:500	Calbiochem
Anti-CD44 rat polyclonal IgG	1:250	BD Biosciences
Anti CD-45 rat monoclonal IgG	1:500	BD Biosciences
Secondary Antibody	**Dilution**	**Company**
Rabbit anti-Chicken biot	1:200	Abcam
Rabbit anti-Sheep biot	1:200	Vector Labs
Goat anti-Mouse biot	1:200	Vector Labs
Goat anti-Mouse Alexa 488	1:500	Molecular Probes
Goat anti-Mouse Alexa 594	1:500	Molecular Probes
Donkey anti-Rabbit Alexa 488	1:500	Molecular Probes
Donkey anti-Rabbit Alexa 594	1:500	Molecular Probes
Goat anti-Rat biot	1:200	Vector Labs
Goat anti-Rat Alexa 488	1:500	Molecular Probes

3.7   Microscopy & cell quantification analysis

3.7.1 Oligodendrocyte & astrocyte quantifications in brain slides

Inmunostained brain sections were divided into rostral (coronal sections where CC fibers are crossing the midline of the brain) and caudal (coronal sections corresponding to the caudal

fibers in the posterior forceps) for cell quantification analysis. Brain sections were observed under a fluorescence microscope (Leica DM6000D; Leica Microsystems, Wetzlar, Germany). Micrographs were taken with DFC350/FX and DC500 Leica cameras. To quantify the number of Olig2+, NG2+, CC1+, PDGFR-α+ and GFAP+ cells, six to nine 14-μm sections that were 168-μm apart in the rostral CC and six in the caudal CC, were randomly selected (n = 4 per group for each time point). The average cell number per section was calculated by counting labelled cells in 5 non-overlapping, randomly selected, medial to lateral bilaterally distributed files per section at 40X magnification in the rostral CC and 3 non-overlapping, randomly selected, medial to lateral distributed files per section at 40X magnification in each hemisphere of the caudal CC forceps (Figure 15M).

3.7.2 Cell quantifications in cell cultures

To quantify the number of OPCs, mature oligodendrocytes as well as proliferating oligodendrocytes (BrdU incorporation) in the case of the FGF8 experiment, the average cell number per culture treatment was calculated by counting double labelled cells (Olig2/PDGFR-α/DAPI or Olig2/NG2/DAPI) and (BrdU/NG2/DAPI) or single labelled cells (O4/DAPI or Olig2/DAPI) in 5 random 20X fields (n = 4 per treatment). Quantifications were performed using a Leica fluorescence microscope (Leica DMR, Leica Microsystems) and micrographs were taken with a DFC350/FX Leica camera.

3.7.3 Confocal microscopy

For the BrdU proliferation assay, MBP immunostaining (Imaris analysis) and the postnatal electroporations, a Leica DM5500 laser scanning confocal microscope was used. Ten to twelve z-stack images (1-μm Z-step) were obtained and all the focal planes were merged to visualize the maximum projection. Nine to twelve 14-μm sections that were 168-μm apart and which contained either the SVZ or the CC, were selected for each specific experiment.

3.8 Magnetic resonance imaging (MRI)

Twenty-four hours before the surgical intervention, the MSCs were pre-cultured in 7 μg/ml of Feraspin XL (Viscover). This product consists in nanoparticles containing iron and enveloped in dextran, allowing its diffusion to the cells. For the detection of SPIO labeled cells, the

protocol used was identical to our previously published works (Cruz-Martinez et al., 2014 [Appendix 2]; Jones et al., 2014). Using this method, grafted cells were tracked *in vivo* by MRI. Thus, mice were anesthetized in an induction chamber with 3–4% isoflurane (Esteve Veterinary, Milan, Italy) in medical air and maintained with 1–2% isoflurane during the process. Anesthetized animals were placed in a custom-made animal holder with movable bite and ear bars and positioned fixed on the magnet chair. This allowed precise positioning of the animal with respect to the coil and the magnet and avoided movement artifacts. The body temperature was maintained at ~37 ºC using a water blanket, and the animals were monitored using a MRI compatible temperature control unit (MultiSens Signal conditioner, OpSens, Quebec, Canada). Experiments were carried out in a horizontal 7 Tesla scanner with a 30 cm diameter bore (Biospec 70/30v; Bruker Medical, Ettlingen, Germany). The system had a 675 mT/m actively shielded gradient coil (Bruker Medical; BGA 12-S) of 11.4 cm inner diameter. A ^{1}H mouse brain receive-only phase array coil with integrated combiner and preamplifier, no tune/no match, in combination with the actively detuned transmit-only resonator (Bruker BioSpin MRI) was employed. Data were acquired with a Hewlett-Packard console running Paravision software (Bruker Medical) operating on a Linux platform.

T2-weighted anatomical images to position the animal were collected in the three orthogonal orientations using a rapid acquisition relaxation enhanced sequence (RARE), applying the following parameters: field of view 40 × 40 mm, 15 slices, slice thickness 1 mm, matrix 256 × 256, effective echo time 56 ms, repeti- tion time 2 s, RARE factor of 8, 1 average and a total acquisition time of 1 min 4 s. To detect superparamagnetic iron oxide labeled cells, a T2* multigradient echo images were acquired in the three orthogonal orientations with the following parameters: repetition time: 1,500 milliseconds, echo time: 3 milliseconds, flip angle: 30º, field of view: 20 x 20 mm, 20 slices, slice thickness: 0.5 mm, matrix: 256 x 256, two averages and a total acquisition time of 12 minutes 48 seconds. As a result, the cells were observed at different time points (0-15-30-60-90 days), studying the location of the transplanted MSCs within the brain, as they appear as black spots due to the iron nanoparticles. In addition, the demyelinated areas can also be visualized and myelin quantified using the image analysis software Image J (http://imagej.nih.gov/ij/) and the Franklin and Paxinos atlas (Franklin & Paxinos, 2001). This allows the quantification of myelin density in

the same individual at different moments before and after transplantation, in a longitudinal study (Willenbrook et al., 2012).

3.8.1 Myelin density quantifications

To correlate the MRI results with the histological data, the 3D structure of the CC was also divided into rostral and caudal sections (see Microscopy & Cell quantification analysis section). In order to extract T2 signal intensity from WM and for each subject, a ratio of mean T2 signal intensity of WM to a reference region (cortex) was implemented. Myelin content within the CC was quantified by measuring the mean grey level with ImageJ software, obtaining the T2 ratio from every section, using a similar method as described by (Chandran et al., 2012). Finally, the average of all sections was calculated for the rostral and caudal CC in both sham-operated and stem cell-treated mice.

3.9 Electrophysiological recording procedures

Axonal conduction-velocity measurements were performed similarly as previously described (Crawford et al., 2010). Animals were sacrificed by cervical dislocation at 2 or 4 months after transplantation or the equivalent age for sham-treated, wild type and cuprizone controls (non-surgical procedure), the head wiped with 70% ethanol and then decapitated using large scissors. The brains were rapidly extracted following the same procedure as explained in previous sections, and immediately placed in a flask containing ice-cold artificial cerebrospinal fluid (ACSF) containing 124mM NaCl, 2.5mM KCl, 1.25mM NaH_2PO_4, 2.5mM $MgCl_2$, 0.5mM $CaCl_2$, 26mM $NaHCO_3$ and 10mM glucose (pH=7.4, osmolarity $\leq$ 300 mOsm/kg). During the whole process the skull and brain were rinsed with ice-cold ACSF, bubbled with carbogen (95% oxygen and 5% carbon dioxide, PH). Using a spatula, the brain was placed into a petri dish with ice-cold ACSF, so that the ventral side of the brain was in contact with a filter paper. The olfactory bulbs and the cerebellum were removed by making a cut with a sterile razor blade. The brain was then place in dry filter paper with the spatula, with the caudal part touching the filter. While the brain dried, a few drops of glue were placed onto the vibratome base plate near a block of agar, spreading the glue out so that it formed a thin layer covering a few square centimeters. Once dried, the brain was placed onto the base plate with the caudal parto ver the glue and the ventral part in close contact with the block of agar.

The base plate was rapidly placed into the vibrating-knife microtome (Leica, model VT1000S, Wetzlar, Germany) containing ice-cold ACSF bubbled with carbogen. Four coronal slices that were 400-mm thick, corresponding approximately to Plates 25-31 and 40-46 in the atlas of Franklin and Paxinos (Franklin & Paxinos, 2001), were obtained and placed in a submersion type recording chamber that was filled with extracellular solution at 37ºC and bubbled with carbogen, containing 124mM NaCl, 5mM KCl, 1.25mM NaH_2PO_4, 1mM $MgCl_2$, 1.2mM $CaCl_2$, 26mM $NaHCO_3$ and 10mM glucose (pH=7.4, osmolarity $\leq$ 300 mOsm/kg). The slices were incubated in this solution at 37º during 30 min and thereafter kept at RT during 1h until use.

The CC was stimulated as shown in Figure 21A with a 200 μm diameter concentric metallic electrode (Frederick Haer & Co, Cat. No. CBBRC75), with a round tip and inner filaments of platinum and iridium that were 25 μm in diameter. The stimulus was continuously performed using pulses of 0.1 ms of duration. Two simultaneous extracellular recordings were obtained with borosilicate glass microelectrode (0.2–5MΩ) filled with extracellular solution; the two electrodes were placed at a certain distance from each other as well as from the stimulating electrode (Figure 21A). The recordings were obtained at room temperature (24.3–26.3ºC) in voltage clamp configuration, with a two channel Multiclamp 700B amplifier (Axon Instruments, Molecular Devices, USA), filtered at 4 KHz and digitized at 20 KHz with a 16-bit resolution analogue to digital converter Digidata 1200B (Axon Instruments, Molecular Devices, USA). All recordings were performed under visual control using an upright microscope (Olympus BX50WI). Images were obtained for each position with a (SONY CCD-Iris, Japan) camera. The generation of pulses (Iso-Flex, A.M.P.I. instruments, Jerusalem, Israel) and data acquisition was controlled by Clampex 10.3 software (Axon Instruments) at a frequency of 20kHz. To eliminate the background noise (50Hz) a Hum-Bug (Quest Scientific, Digitimer, England) was used. To enhance the signal-to-noise ratio, all the recordings were conducted on waveforms that were the average of fifteen succesive sweeps.

3.9.1 Axonal conduction velocity measurement

For the recordings analysis Clampfit10.1 software (Axon Instruments) was used. The conduction velocity was measured from the distance between the tips of both electrodes and

the difference in the latency of the propagated action potential for both (fast-conducting axons) and (slow-conducting axons) components (Figure 21A, B).

3.10 Electron microscopy (EM)

The following part of the project was performed in collaboration with Dr. Susana González Granero, from the group of Dr. Jose Manuel García Verdugo, at the Cavanilles Institute (University of Valencia, Spain). Mice were perfused with a 2% paraformaldehyde, 2.5% glutaraldehyde fixative solution. The brains were dissected out and postfixed in the same solution. Coronal 200 mm sections were cut on a vibratome (Leica VT-1000) and were post-fixed with 2% osmium, rinsed, dehydrated and embedded in Durcupan resin (Sigma, St Louis, MO, USA). Semithin sections (1.5 µm) were cut, using an ultramicrotome (Leica EM UC-6) with a diamond knife (Histo; Diatome), and stained lightly with 1% toluidine blue to select the regions of interest. Later ultra-thin sections (0.08 µm) were cut, using an ultramicrotome (Leica EM UC-6) with diamond knife (Ultra 45º; Diatome), stained with lead citrate (Reynolds solution) and examined under a transmision EM (FEI Tecnai G2 Spirit BioTwin) using a digital camera (Morada, Soft Imaging System, Olympus).

Three telencephalic areas, enriched in myelinic axons, were studied: cingulate cortex (cg), in anterior levels of the telencephalon (from Bregma 1.10 to -0.10 mm), dorsal hippocampal commissure (dhc) and alveus of the hippocampus (alv), two regions of the posterior levels. Three levels for each region and animal were analysed and 100 myelinic axons from non-overlapping electron micrographs were measured per level for G-ratio analysis. G-ratios of axons were quantified using ImageJ software, where it was implemented a plug-in (http://gratio.efil.de/), which allowed for semiautomated analysis of randomly selected sets of axons (Goebbels et al., 2010).

3.11 Postnatal GFP electroporations *in vivo*

Animals were deeply anesthesized and stereotaxically injected with 2 µl of the plasmid solution (pCX-GFP with a final concentration of 18 µg/µl) in one LV, following the same procedure as explained in previous sections. Similar protocol as previously described (Barnabé-Heider et al., 2008) was performed. After the injection, conductive gel (Siemens)

was applied on the skin of the skull and electroporated (200V, 5 pulses, 50 ms per pulse, 950 ms intervals) using round (0.5-cm diameter) electrodes and a square electroporator CUY21 EDIT (Nepagene, Chiba, Japan). Immediately after electroporation, MSCs were injected in MSC-treated group, following the same surgical procedure as explained before. Mice were sutured and kept under observation for 24h. Twenty days after electroporation, mice were sacrificed, the brains were carefully extracted and prepared for immunofluorescence (IF).

3.12 Rotarod test

The rotarod test was performed on an 8500 Rota-rod (Letica Scientific Instruments, Barcelona, Spain). The lane was 500 mm wide, and the rod had a diameter of 30 mm. After 12 weeks of cuprizone intake, C57BL/6 chronic demyelinated mice and C57BL/6 wild type at the same age, were trained daily for 1 week on the rotarod. Afterwards, they were analysed during the next five consecutive days, taking note of the maximum speed achieved, by increasing the speed at a constant rate of 4 to 40 rpm in a 1-min interval until the animal fell from the rod.

3.13 Imaris analysis software

Confocal z-stack images for MBP immunostaining were obtained with a Leica DM5500 laser scanning confocal microscope as detailed in previous sections. 18 randomly selected areas correspondind to the rostral CC, and 12 to the caudal CC, were analysed (n=6 MSC, n=8 SHAM). Three-dimensional reconstruction Imaris software (Bitplane) was used to project the z-stacks in the three dimensional view. The resulting files were loaded into Imaris and using surface rendering, fluorescence thresholding, and masking of unwanted immunolabeling, tools found in IMARIS, we were able to obtain an accurate 3D structure of each CC MBP immunostained section. To this end, images were processed using the "Surpass Module" of Imaris, which is able to piece together the suite of z-stack confocal images to create a three dimensional reconstruction on a region of interest. Finally, volume ratios were calculated for each z-stack (intensity sum normalized by volumen) as the relative volumen of myelin.

3.14 Statistical analysis

Statistical analysis of mean values was performed using Sigmaplot v12.0, GraphPad Prism and SPSS softwares. Statistical significance between control and experimental groups were

calculated using Student's t-test for independent samples, one-way ANOVA and Bonferroni's multiple comparison post hoc test where applicable, establishing the level of significance at $P<0.05$. Values are expressed as mean ± standard error of the mean (SEM).

Chapter IV

- RESULTS -

Section I

4.1 Twelve weeks cuprizone-intake predominantly affects the corpus callosum (CC) leading to chronic demyelination

In order to detect the degree of demyelination, Klüver-Barrera staining, together with IHC for MBP were performed. Although different patches of demyelination were observed in the fimbria/fornix and septum, the CC was rather homogenously affected among mice (Figure 13A-D, H). Moreover, these lesions presented a high concentration of OPCs NG2+ cells (Figure 13E-G), which is a major feature of the response after a demyelinated insult in the brain parenchyma.
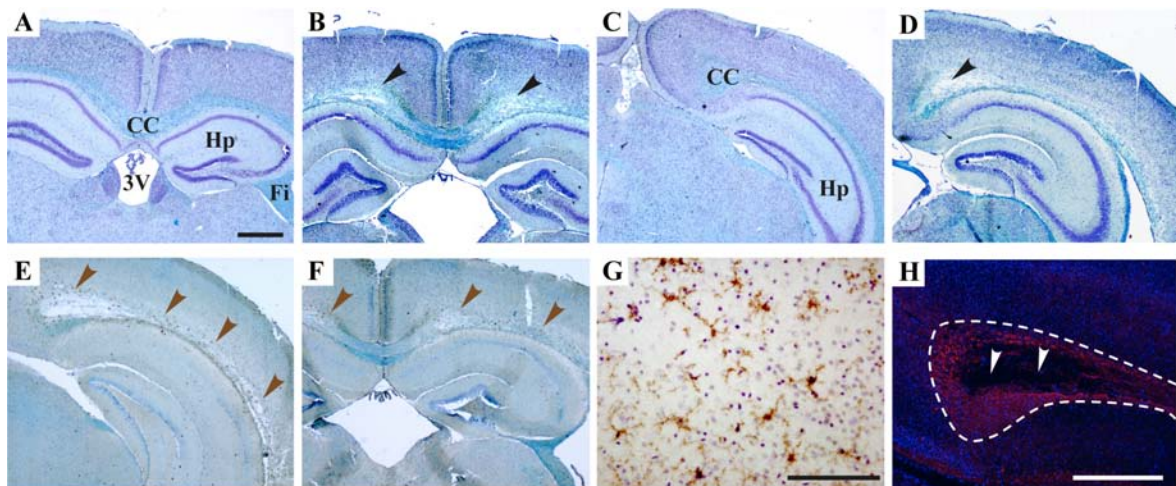
Figure 13. Chronic cuprizone treatment causes severe demyelination in the CC. Six-week old C57BL/6J mice were given cuprizone (CPZ, 0.2% w/w) in their diet for 12 weeks and then were euthanized and brain paraffin sections were stained with Luxol Fast Blue (LFB) and counterstained with cresyl violet (Klüver-Barrera staining). (A-D) Brain coronal sections from WT mice (A, C) and cuprizone-fed mice (B, D) were stained with Klüver-Barrera at the most rostral (A, B) and caudal areas of the CC (posterior forceps) (C, D). Black arrows indicate patches of demyelination (LFB-negative), similar to that seen in chronic lesions of MS. (E, F) Coronal brain sections of the CC were immunostained against NG2 (OPC marker) and counterstained with Klüver-Barrera. Brown arrows shows patches of demyelination surrounded by high concentration of NG2+ OPCs. (G) Higuer magnification image of these regions showing the OPC NG2^{+} typical stellate morphology. (H) Myelin basic protein (MBP) staining (in red immunofluorescence) of the CC posterior fórceps (white matter borders marked with a dotted line) of a cuprizone-fed mice and DAPI for nuclear staining (in blue fluorescence). White arrows indicate patches of myelin loss (MBP-). Abbreviations: CC, corpus callosum; Fi, fimbria; HP, hipocampus; 3V, third ventricle. Scale bar, 100 μm (A-F, H); 50μm (G).

Although cuprizone-induced demyelination is always most notable in the CC and fimbria, some authors have demonstrated certain degree of demyelination in the cerebellum which would affect the motor function of cuprizone mice (Steelman et al., 2012; Groebe et al., 2009; Skripuletz et al., 2008). In the present study, neither demyelinating patches in the

cerebellum, nor staining differences when compared to the WT mice were detected. However, it was decided to confirm that the motor function was not affected. Thus, rotarod treadmill assay was performed to assess forelimb-hindlimb coordination (Figure 14). As a result, no differences were detected among the cuprizone treated mice and the WT at increasing speeds. On average, both mice were capable of walking until reaching speeds of 10–11 rpm (Figure 14). This corroborated previous observations with the Klüver-Barrera staining, where the white matter of the cerebellum was not affected by the cuprizone treatment. This, together with the fact that the CC is by far the largest fiber tract in the brain, being a common target in MS patients (Ozturk et al., 2001; Warlop, et al., 2008), made that the subsequent analysis were decided to be performed focusing in this structure.
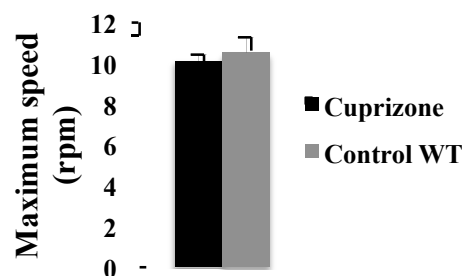
Figure 14. Rotarod assay. C57BL/6J and chronic (12 weeks) cuprizone demyeliated mice were analysed at the same age, for their motor abilities by a rotarod apparatus. The histogram shows the maximum speed achieved by the mice when placed in the rotarod at increasing speeds (4–40 rpm in regular intervals). Control mice n=10, Cuprizone mice n=20. The values are presented as mean ± standard error of the mean (SEM).

4.2 MSCs intraventricular-injection increases the number of OPCs and mature oligodendrocytes in the demyelinated CC

One of the objectives of this study was to assess whether intraventricular injected MSCs were capable of increasing the OPCs numbers in the CC. In order to detect differences regarding the different areas of the CC, and therefore to obtain a more precise data, the 3D structure of the CC was analysed separately, naming it from now on as rostral CC (segments where CC fibers are crossing the midline of the brain) (Figure 15A, E, I) and caudal CC (corresponding to the caudal fibers in the posterior forceps) (Figure 15B-D, F-H, J-K). The average cell number per section was calculated by counting labelled cells in 5 non-overlapping, randomly selected, medial to lateral bilaterally distributed files per section at 40X magnification in the rostral CC and 3 non-overlapping, randomly selected, medial to lateral distributed files per section at 40X magnification in each hemisphere of

the caudal CC forceps (Figure 15M). The oligodendrocyte numbers were calculated at different stages of differentiation (detected by specific markers) within the CC over time (30-60-90 days after MSC-intraventricular transplantations). A significant increase was observed ($P<0.05$) in the number of OPCs (NG2$^+$, PDFGR-α^+) in the CC of the MSC-treated group compared with the SHAM, as early as 2 months after transplantation, as well as a significant raise ($P<0.05$) in the number of mature oligodendrocytes (CC1$^+$) 3 months after the injection at the caudal forceps of the CC (Figure 15N). This effect in oligodendrocyte cell lineage at the demyelinated white matter, may be due to the a paracrine effect of trophic signals, which likely stimulate the differentiation of NSPCs of the SVZ toward OPCs, their migration toward the demyelinated lesions in the CC and their final differentiation in mature oligodendrocytes; as well as the local induction of the same effect in pre-existing OPC in the nearer areas.
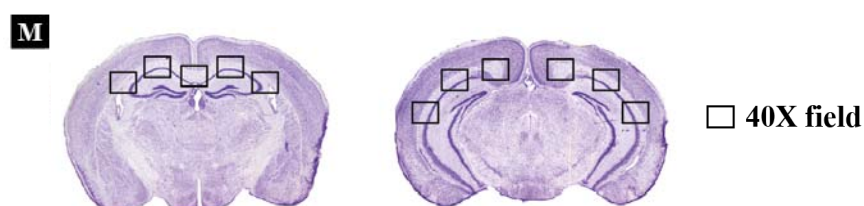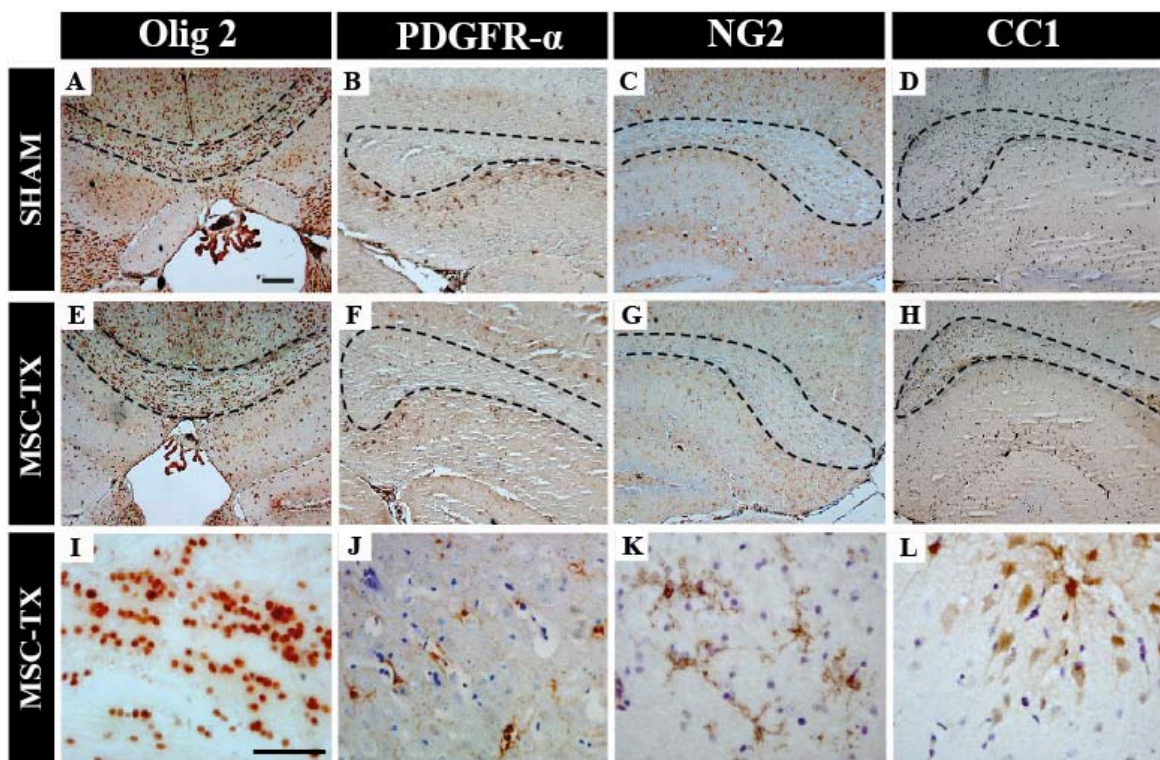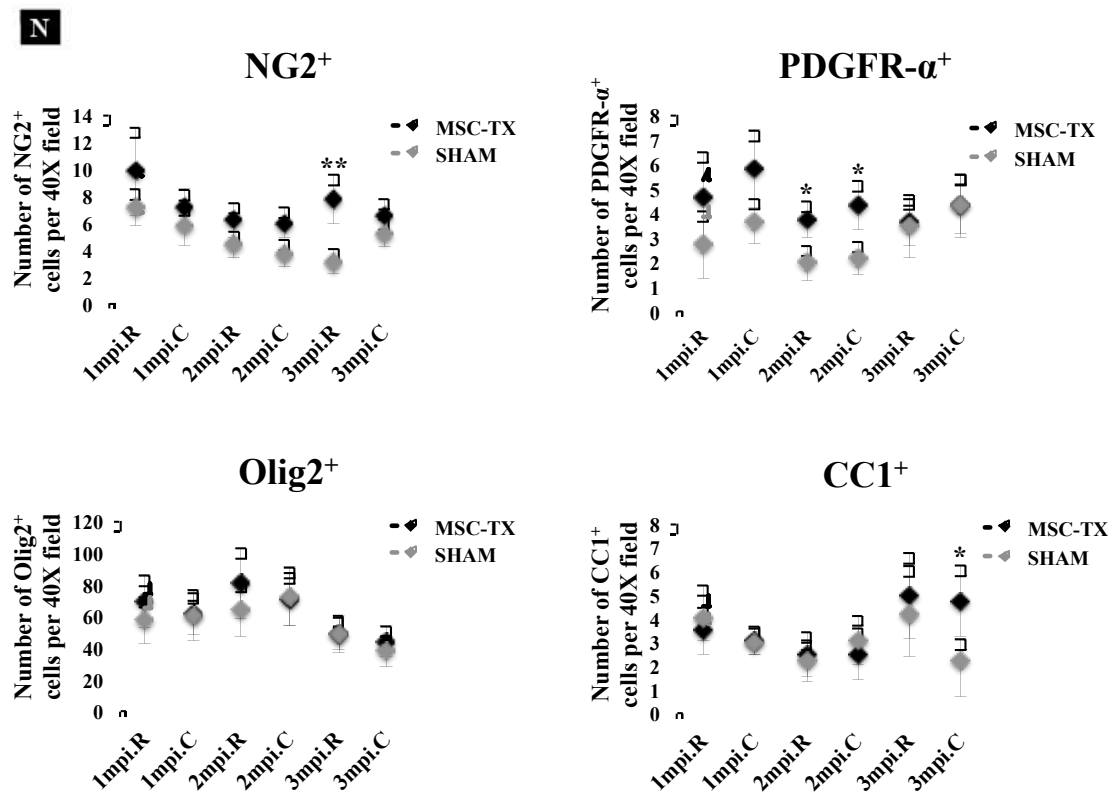
Figure 15. Quantification of OPCs and mature oligodendrocytes in the CC. (A-H) Immunostained brain coronal sections of the CC of stem cell-treated mice and SHAM for different OPC (PDGFR-α, NG2), mature oligodendrocyte (CC1) and the oligodendrocyte lineage marker (Olig 2), and conterstained with cresyl violet. For better visibility borders of CC are illustrated with a dotted line. (I-L) Close-up images of the same coronal sections representing the typical morphology shown with each marker. (M) Schematic representation of mice brain sections containing the most rostral (midline-crossig) and caudal (non midline-crossing) CC. Quantification was performed in each 40X field within the CC of consecutive coronal brain slides as represented in the images. Adapted from Allen Brain Atlas (http://www.brain-map.org). (N) Quantification of OPCs and mature oligodendrocytes at different months after MSC-transplantation demonstrated an increase of OPCs (NG2+ and PDGFR-α+) in the stem cell treated group as early as two months and of mature oligodendricytes (CC1+) in the most caudal CC. Statistically significant compared to SHAM (* $P<0.05$, ** $P<0.01$). n=4 per group for each time point. All data are reported as mean ± standard error of the mean (SEM). Scale bar, 100 μm (A-H); 50μm (I-L).

4.3 MSCs intraventricular-injection stimulates remyelination of the CC over time

In order to elucidate if the increase of oligodendrocytes over time correlated with a real increase of myelin content in the CC, and also to track *in vivo* the location of the MSC, bone marrow-derived MSC were pre-incubated *in vitro* with iron nanoparticles and stereotaxic-guided intraventricularly injected into both LVs. In this manner, it was possible to track *in vivo* the grafted cells by magnetic resonance imaging (MRI) as well as to

analyse the myelin content at different time points (0-15-30-60-90 days), without the need of sacrifice different experimental mice at different time points. To our knowledge, this is the first time that the remyelinating process has been studied over time, with the advantage of being able to quantify the myelin density in the same individual mouse at different time points before and after transplantation. First, it was observed that the cuprizone-treated mice were clearly demyelinated when compared with the WT (Figure 16A, B) and that up to 3 months after the injection the MSCs were still detectable, confined within the CSF of the lateral and diencephalic ventricles, appearing cellular masses as black spots due to the contrast provided by the iron nanoparticles (Figure 16C, D). Second, as early as 2 months after transplantation, a significantly higher level of myelin density content was observed in the cell-treated group when compared with themselves at earlier time points as well as compared to the sham controls ($P<0.05$) (Figure 16E).
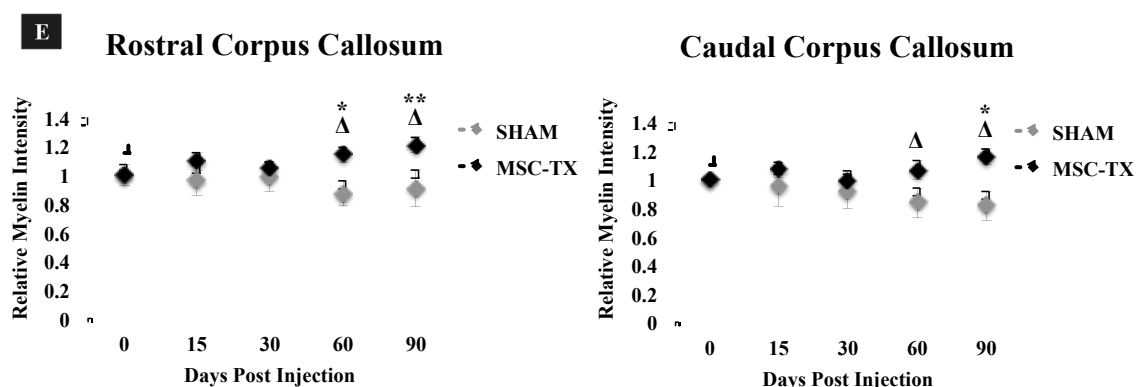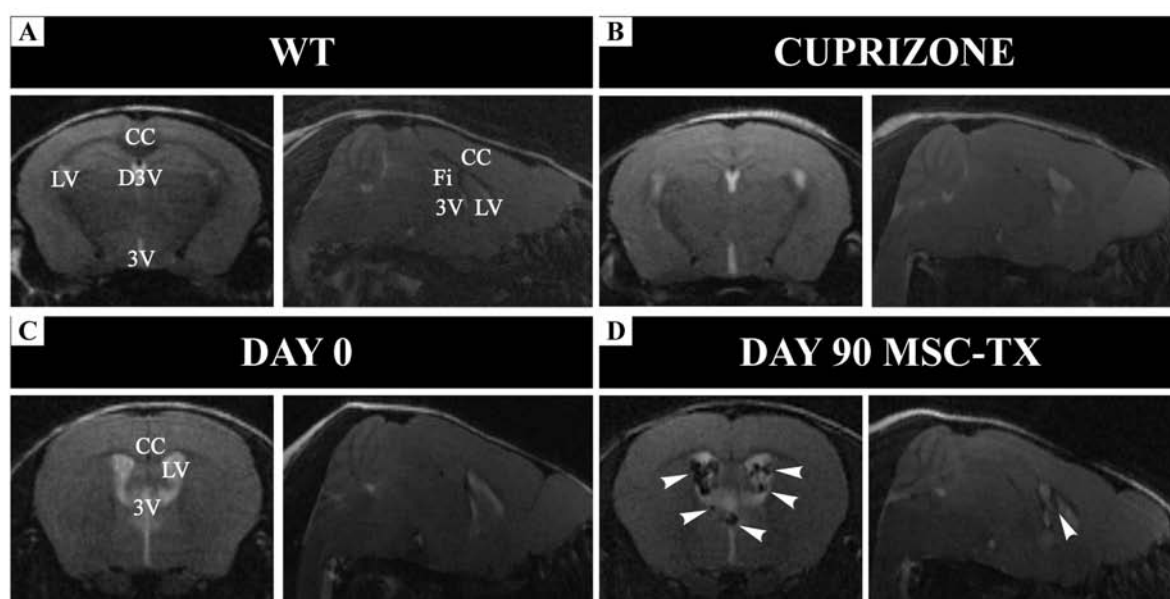
Figure 16. Magnetic resonance imaging (MRI) and *in vivo* myelin content quantification. Representative brain T2-weighted images of WT (A) and chronic cuprizone treated mice (B) in coronal and sagital planes. Myelinated structures appear in black, grey matter in grey and CSF in white. The CC of the cuprizone treated mice shows a lighter grey color, corresponding with the demyelinated state. Representative images at Day 0 before MSC transplantation (C) and 90 days after the injection (D). 90 days after the injection the MSCs are homogenously distributed and confined within the CSF of the ventricles. Arrows show the MSC appearing as black spots due to the contrast provide by the iron nanoparticles. (E) Quantification of the myelin density content showed as early as 2 months after transplantation, a significant increase in the cell-treated group when compared with themselves previously on time as well as with the sham-treated group. Statistically significant compared to SHAM (* P<0.05, ** P<0.01) and compared to Day 0 (Δ P<0.05). n=6 in each treatment group. All data are reported as mean ± standard error of the mean (SEM). Abbreviations: CC, corpus callosum; D3V, dorsal third ventricle; Fi, fimbria; LV, lateral ventricle; 3V, third ventricle.

Myelin content was also measured by IHC. Myelin basic protein staining was performed and z-stacks of the CC were obtained in the confocal microscope. All z-stacks were subsequently converted into 3D volumes by using the Imaris software. In this way, all the tissue stained for MBP could be measured in a more realistic and precise way, as relative myelin volume, rather than using conventional approaches. In Figure 17A, MBP immunostaining is shown in MSC and SHAM groups in both rostral and caudal CC. Typical Imaris 3D reconstruction from MBP immunostained z-stacks is shown in Figure 17B. In this case, although there is more MBP immunostaining in MSCs transplants than in control animals, no significant differences in myelin content were found between the SHAM and the MSC transplanted group (Figure 17C).

C
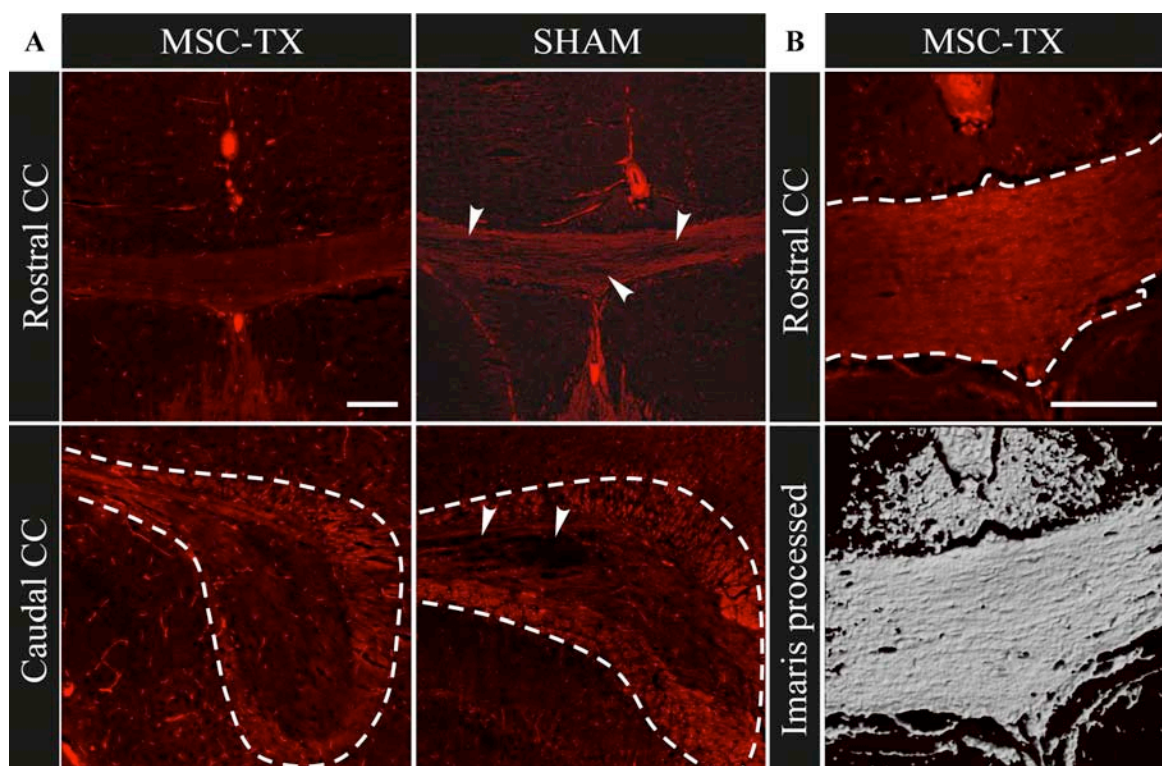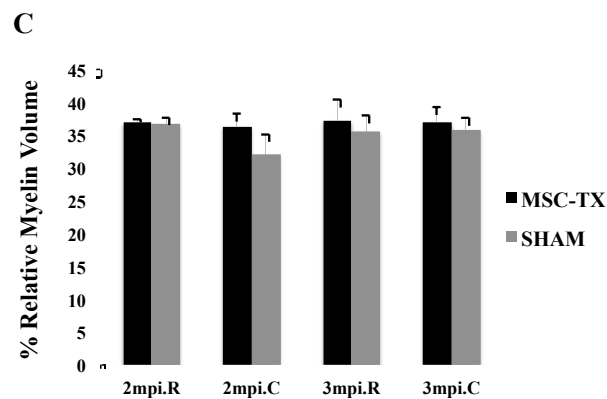
Figure 17. Imaris 3D reconstructions and *in vitro* myelin content quantification. (A) Representative brain images of rostral and caudal CC in both MSC transplanted (MSC-TX) and SHAM group, immunostained for MBP. Arrows indicate some patches of demyelination. For better visibility borders of caudal CC are illustrated with a dotted line. (B) Example of MBP immunostained CC and Imaris software 3D reconstruction of the same section. (C) Quantification of the myelin volumen by the Imaris software at 2 and 3 months post-injection in the rostral and caudal CC. No significant differences were found between groups at any time point, despite the demyelination patches present in the SHAM group. MSC-TX n=5, SHAM n=8. All data are reported as mean ± standard error of the mean (SEM). Scale bar, 50 μm (A); 50μm (B).

4.4 Grafted MSCs does not affect the number of astrocytes in the CC

Reactive astrocytes contribute to the formation of glial scarring, through the secretion of chondroitin sulphate proteoglycans (CSPGs), and this may results in axonal regeneration impairment. Although these cells have long been considered detrimental to the repair of an injured spinal cord, there is some controversy, as other studies have shown that astrocytes can support spinal cord repair (Renault-Mihara et al., 2008). For these reasons, and regardless their role, it was considered relevant to analyse whether intraventricular injections of MSCs was affecting the accumulation of astrocytes in the CC, which may be directly or indirectly inhibiting or promoting the remyelinating process. To this end, IHC analysis and quantification of astrocyte accumulation in the CC was conducted. In Figure 18A, GFAP+ astrocytes were observed in both MSC and SHAM mice. Astrocyte quantification showed no significant differences in the number of GFAP+ astrocytes between the MSC transplanted and SHAM groups in both rostral and caudal CC (Figure 18B).
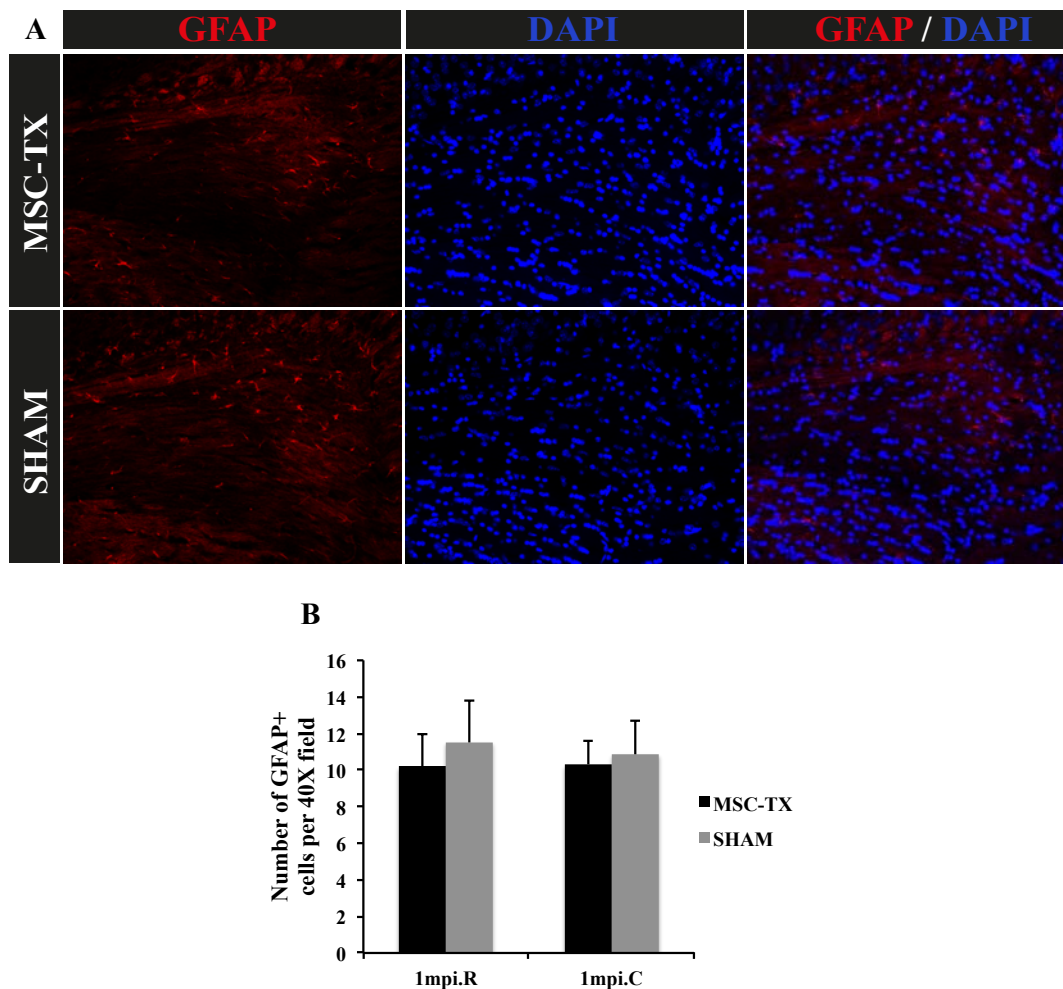
Figure 18. Astroglial activation in the CC. (A) Representative brain images of the CC in both MSC transplanted (MSC-TX) and SHAM group, immunostained for GFAP. Arrows indicate GFAP$^+$ astrocytes. (B) Quantification of astrocytes within the CC one month after MSC-transplantation. No significant differences were found between groups at this time point in both rostral and caudal CC. n=4 in each treatment group. All data are reported as mean ± standard error of the mean (SEM). Scale bar, 50 μm (A).

4.5 Transplanted MSCs remain primarily in the CSF, overexpressing trophic factors genes & with little penetration into the brain parenchyma.

Three months after transplantation, MSCs were still present in the CSF of the ventricles as it was shown by MRI and being consistent with a paracrine mechanism in the observed remyelinating effect. Further experiments were performed in order to histologically map the precise location of the grafted cells, if any had penetrated into the brain parenchyma; and if the cells generated any malformations, tumours, or other structural anomalies. Also, their viability and phenotypic characteristics were studied. To this end, both GFP transgenic mice as well as wild type C57BL/6 were used as donors to obtain the MSCs,

which were injected into C57BL/6 cuprizone-treated mice. IHC analysis (Figure 19A-J) was performed three months post-injection and the CSF of both GFP+ MSC-treated and SHAM group was extracted at the same time point to analyse the presence of the GFP protein by Western blot. First, the results indicated that the MSCs were still present within the CSF of the transplanted mice as shown by the expression of GFP protein (Figure 19M). Moreover, in the histological analysis some GFP+ grafted cells were found attached to the choroid plexus (Figure 19D-E). In particular experimental cases, grafted cells were found penetrating into several brain structures sometimes forming long chains of migrating cells, such as the hippocampus and CC (Figure 19A-C, G), fimbria (Figure 19E) and lateral wall of the SVZ (Figure 19F). In few cases, the grafted MSCs were detected in close contact with blood vessels (Figure 19J), possibly contributing and promoting angiogenesis, as it has been previously described (He et al., 2007). It was also observed in very rare occasions that the MSCs were surrounded by macrophages or microglia CD45+ (Figure 19I, J). In all cases, the regular morphology of the cell body, and the absence of cells with more than one nucleus indicated that there was no sign of trans-differentiation into any type of identifiable neural cell or cell fusion. Moreover, no tumour formations were observed. Similarly, some of the MSCs transplanted cells escaped from the needle path and clearly exert their attracting effect to the OPCs of that area, as the MSCs were mostly found surrounded by OPCs PDGFR-α^+ (Figure 19H).
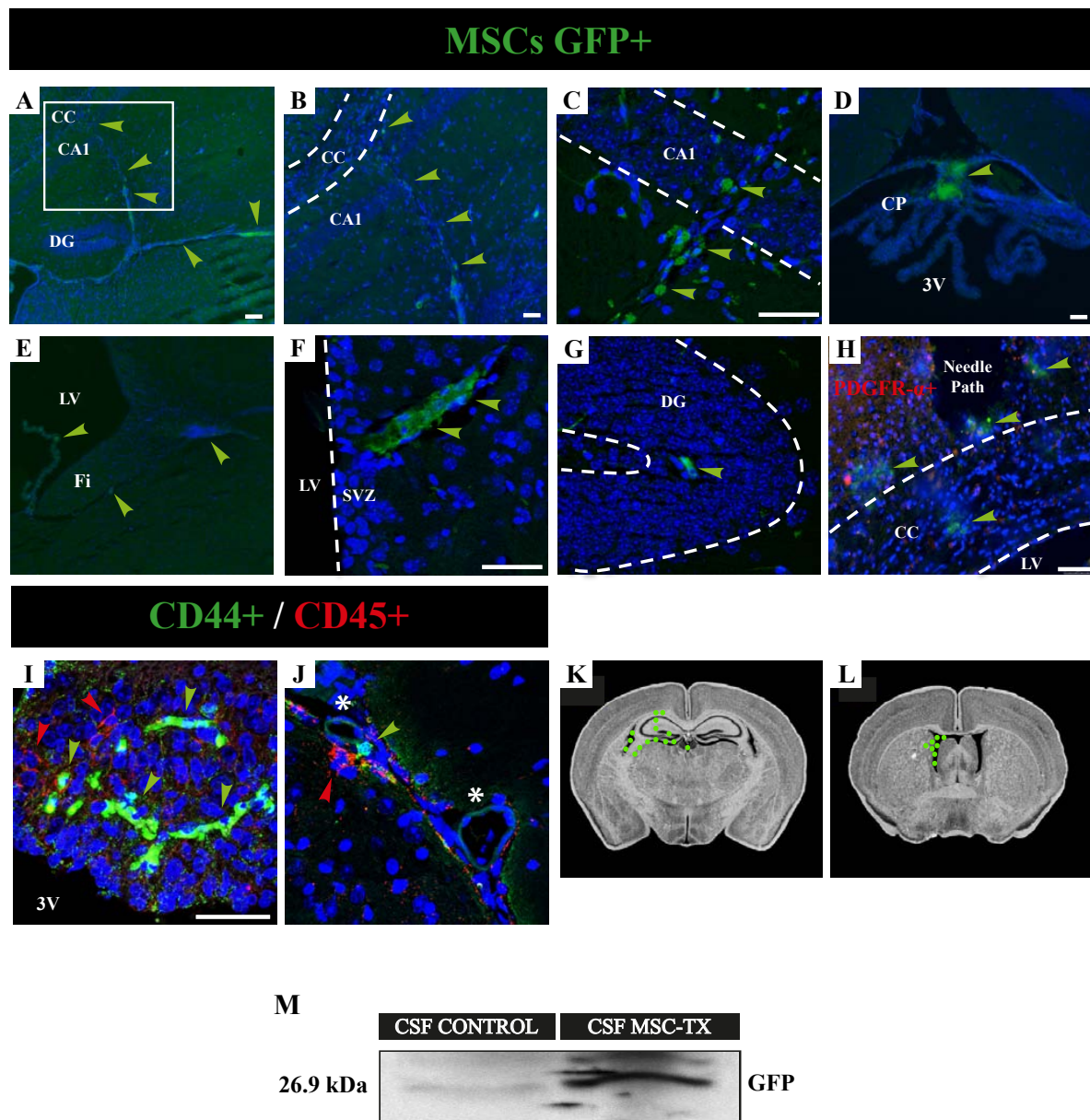
Figure 19. Location of intraventricular transplanted MSCs. MSC obtained from GFP transgenic mice were intraventricular injected in cuprizone treated mice. Immunofluorescence analysis for GFP (green) were performed three months post-injection to detect the MSC location. The GFP+ MSCs were found penetrating into several brain structures such as the hippocampus (HP) (A-C, G), CC (A, B, H), fimbria (E), subventricular zone (F) and attached to the choroid plexus (D, E). (B) Close-up region of a pathway form from the HP to the CC (inset in A). (H) Double immunostaining for GFP (green) and PDGFR-α+ (red). The MSC appear surrounded by OPCs around the needle path as well as within the CC. Arrows indicate the location of MSC. For better visibility borders of CC, CA1, DG and SVZ are illustrated with a dotted line. (I, J) double immunostaining for CD44 (green) and CD45 (red). The MSC CD44+ appear surrounded by few macrophages (CD45 high) or microglia (CD45 low) as well as in close contact with blood vessels (J, asterisk). In all images blue staining corresponds to the nuclei (DAPI). (K-L) Schematic representation of coronal brain sections showing the location of the MSC after transplantation. Adapted from The Mouse Brain Library (http://www.mbl.org). (M) Western Blot analysis of the CSF confirmed the presence of the MSC in the stem cell treated group 3 months post-injection. n=5 in each treatment group. All data are reported as mean ± standard error of the mean (SEM). Abbreviations: CA1, cornus amonis 1; CC, corpus callosum; CP,

choroid plexus; DG, dentate gyrus; Fi, fimbria; SVZ, subventricular zone; 3V, third ventricle. Scale bar, 100 μm (A,E); 50μm (B-D, F-G, H, I-J).

MSCs are known to be the source of multiple immunomodulatory agents and of trophic factors involved in repair and regenerative processes. However, this broad array of secreted factors has been widely analysed *in vitro* and under many different conditions. In this study, the trophic factor content of the CSF was analysed three months after MSC transplantation. To this end, the CSF was extracted from both MSC and SHAM operated mice and subsequently analysed by qPCR for several trophic factors. As a result, PDGF, IGF, NT3, NT4 and FGF2 were greatly overexpressed ($P<0.0001$) in the CSF of the MSC-treated group compared to the SHAM (Figure 20), which are the likely candidates that stimulate the regenerative effects previously observed with the MRI and histology.
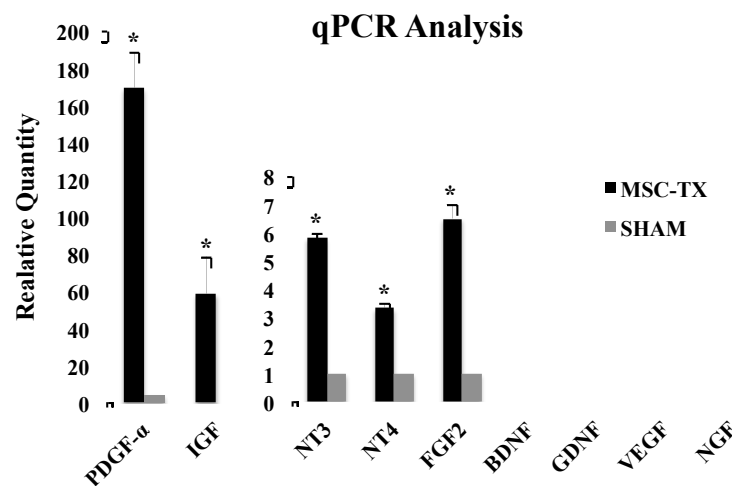
Figure 20. Trophic factor support exert by MSCs. (A) qPCR analysis of the CSF shows the overexpression of some trophic factors such as PDGF, IGF, NT3, NT4 and FGF2 in the MSC-treated group. Other factors such as BDNF, GDNF, VEGF and NGF were not detected. Statistically significant compared to SHAM (* $P<0.0001$). n=5 in each treatment group. All data are reported as mean ± standard error of the mean (SEM).

4.6 MSCs transplantation increases the axonal conduction velocity of the demyelinated fibers in the CC over time

In order to characterize the functional consequences of the neuropathology as well as the observed regenerative effect in the CC of this cuprizone model, compound action potentials (CAP) were recorded in callosal axons (Figure 21). Coronal brain slices with midline-crossing segments of the CC, corresponding to specific Franklin and Paxinos atlas-based plates (see Material and Methods) were used for recording, with a stimuli and two recording electrodes placed as shown in Figure 21A. Two downward phases of the

CAP corresponding to fast- and slow-conducting fibers were observed, probably representing fast depolarization from large, myelinated axons and slower depolarization from non-myelinated axons, respectively. Typical voltage recordings are shown in Figure 21B.

Hence, it was firstly necessary to confirm whether the axonal conduction velocity was affected in the model, therefore comparing the cuprizone treated mice with wild types. It was observed that the cuprizone induced a decrease in the conduction velocity of the fast fibers, whereas the slow fibers, corresponding to the non-myelinated axons presented normal values when compared with WT, as it was expected due to the fact that the cuprizone only affect the oligodendrocytes and thus the myelinated fibers (Figure 21C). Regarding the stem cell-treated mice and the SHAM group, the conduction velocity was recorded 2 and 4 months after MSC transplantation. No significant differences were detected between MSC-treated and SHAM groups at any time point for any type of fibers. However, when the same group of animals were compared over time, the axonal conduction velocity was significantly increased in the MSC group ($P<0.05$). This difference was only observed in the fast conduction fibers, whereas the conduction velocity of the slow fibers did not change (Figure 21D). In conclusion, the electrophysiological analysis corroborate the previous data, indicating that the increase of oligodendrocytes and myelin content over time in the CC, was translated as a final step into a functional recovery, with a slight but significant improvement in the axonal conduction velocity of the MSC-treated group.
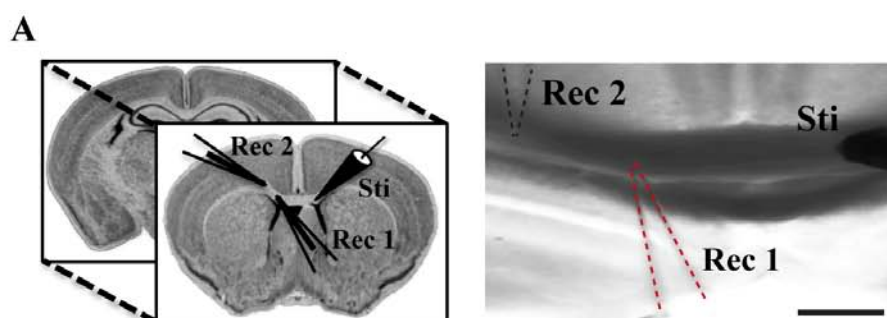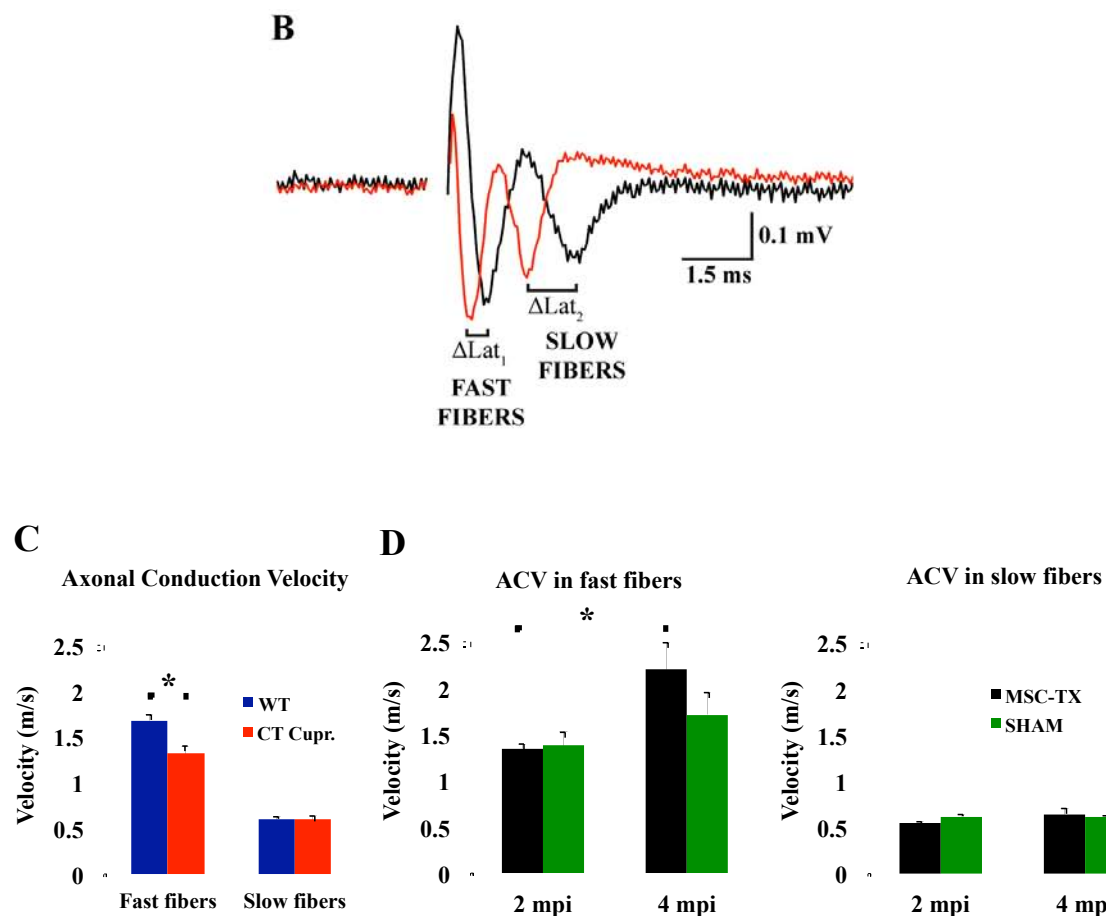
Figure 21. MSCs intraventricular-injection increases axonal conduction velocity over time. (A) Schematic representation of the brain slices corresponding approximately to Plates 25-31 and 40-46 in the atlas of Paxinos and Franklin (2001), and details of the position of the stimuli and two recording electrodes. (B) Typical CC compound action potential (CAP) from recording electrode 1 (red), and recording electrode 2 (black); Two fibers were detected: fast (thicker myelin sheaths) and slow-conducting fibers (thin and/or non-myelin sheaths); ΔLat (difference in latency between both peaks). (C) Histogram depicting the axon conducting velocities in the WT (blue) and the cuprizone mice model (red). The cuprizone produced a significant decrease in the conduction velocity of the fast fibers when compared with the WT. (D) Histogram depicting the axonal conduction velocity over time of MSC treated group (black) and SHAM (green). The conduction velocity of the slow fibers did not change between groups at any time. Statistically significant compared between different time points (* $P<0.05$). n=4 in MSC-TX & CT Cuprizone, n=8 SHAM & WT. All data are reported as mean ± standard error of the mean (SEM). Scale bar, 300 μm (A).

4.7 MSCs transplantation increases myelin thickness, decreasing the g-ratio of callosal axons

Apart from the functionality of the new-formed myelin, it was of vital importance to further assess the integrity of myelination ultrastructure, calculating the axonal diameters, myelin thickness and mean g-ratio of myelinated and unmyelinated axons by EM analysis. To this end, the ratio between the inner axonal area and the outer myelin area, g-ratio, a

gold standard for assessment of demyelination and remyelination in experimental models, was therefore calculated. Three telencephalic areas, enriched in myelinic axons, were studied: *cingulate cortex* (cg), in anterior levels of the telencephalon (from Bregma 1.10 to -0.10 mm) (Figure 22A, C-E), *dorsal hippocampal commissure* (dhc) and *alveus of the hippocampus* (alv), two regions of the posterior levels (Figure 22B, F-K). The results revealed that the stem cell treated group presented a significantly thicker myelin sheat than SHAM control mice in all the regions analysed and consequently lower g-ratio values (Figure 22L-N). In addition to that, significant differences in mean g-ratio when compared to the WT were also observed, since neither the vehicle-control animals nor the MSCs treated reached the WT normal values (Figure 22L-N).
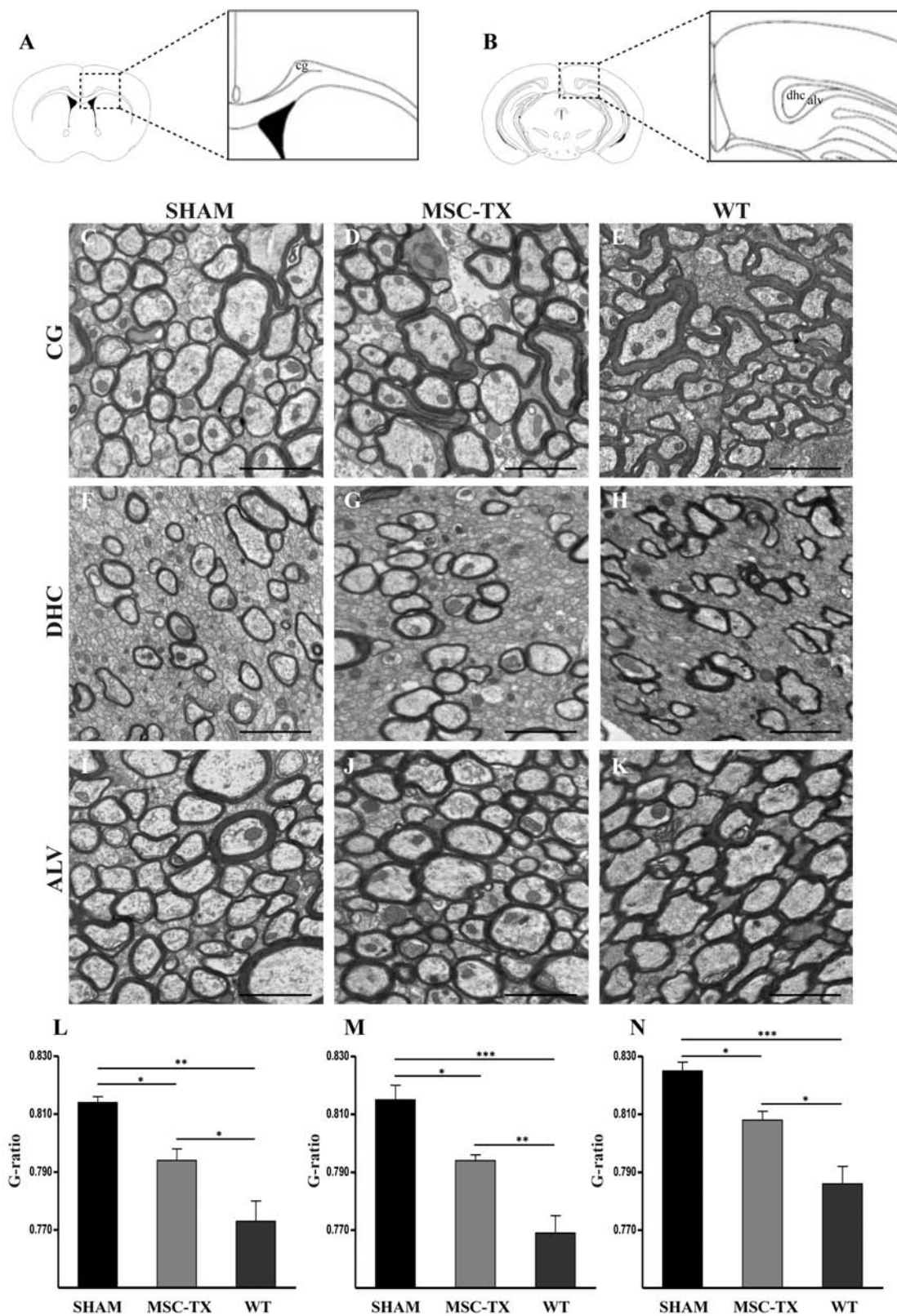
Figure 22. Quantitation of myelin thickness by G-ratio analysis for three telencephalic areas. Coronal section scheme of anterior telencephalic level (A) and posterior telencephalic level (B) with a magnification of these areas. Representative electron micrographs of cingulate cortex (cg) (C-E), dorsal hippocampal commissure (dhc) (F-H) and alveus of the hippocampus (alv) (I-K) in SHAM, MSC-TX and WT mice respectively. The graphs (L-N) show the G-ratio quantification in cg, dhc and alv regions (* P<0.05, **

P<0.001, *** P<0.001). n=4 in each treatment group. All data are reported as mean ± standard error of the mean (SEM). Scale bar, 2 mm (C-K).

4.8 MSCs stimulate the proliferation of the NSPCs in the adult SVZ *in vivo* and activate proliferation and survival signalling routes in NSPCs *in vitro*

The regenerative potential of MSCs transplantation has been demonstrated in previous section of this thesis, with an increase in the number of oligodendrocytes and myelin content that was also proven to be fully functional in terms of increasing axonal conduction velocity. Mammalian neurogenesis in the adult has been demonstrated to be mainly restricted to the SVZ of the LVs and the subgranular zone (SGZ) of the dentate gyrus in the hippocampus (Gonzalez-Perez & Alvarez-Buylla, 2011; Ming & Song, 2011). Also, it has been reported that *in vitro* MSCs are capable of instructing an oligodendrogenic fate decision on adult NSPCs (Rivera et al. 2006). Therefore, based on the previous findings, it was hypothesized that the remyelination observed could be due to the enriched environment created by the MSCs, which would be stimulating through a paracrine effect, the endogenous neurogenesis and possibly an oligodendrogenic fate decision on the NSPCs of the SVZ, which are in direct contact with the CSF through their primary cilia at their apical end. In order to further assess this issue, BrdU incorporating assay was performed just after MSC transplantation. Mice were given BrdU in the drinking water daily for up to two weeks just after transplantations, and sacrificed two weeks later, to analyse the proliferation of the NSPCs (Nestin+) in the adult SVZ (Figure 23A-H). Thus, a significant increase was detected in the number of these cells proliferating in the SVZ of MSC treated mice when compared to SHAM (Figure 23I).
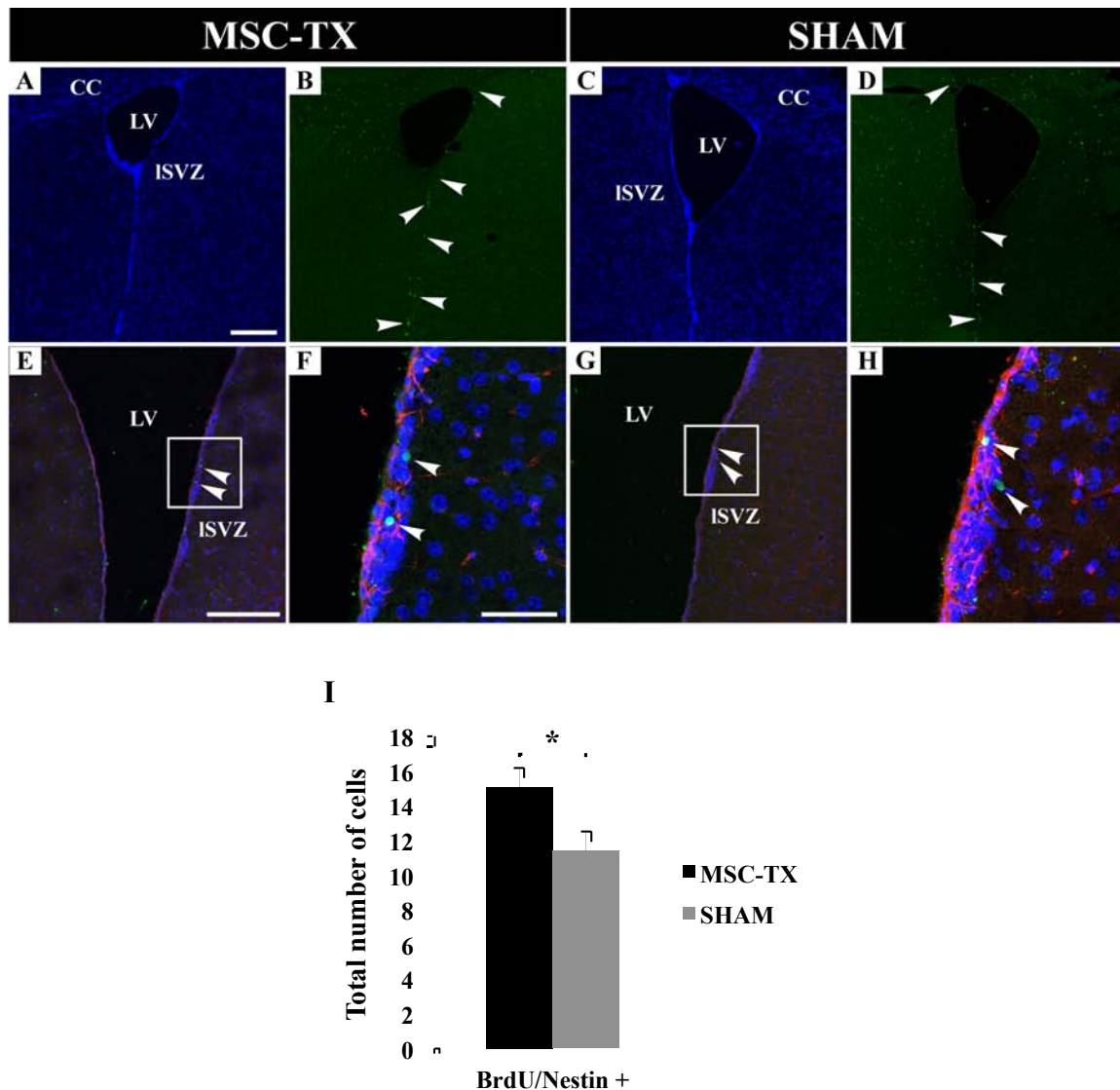
Figure 23. Increased proliferation of NSPCs in the adult SVZ. (A-D) Representative images of proliferating cells within the V-SVZ. Immunostaining for BrdU+ (green) and nuclei (DAPI, blue) is shown. Arrows indicate BrdU+ proliferating cells. (E, G) Representative images of proliferating BrdU/Nestin+ NSPCs in the SVZ. Nestin staining appears in red. (F, H) Close-up regions were the cells are located (inset in E and G respectively). Arrows indicate double immunostained cells. (I) The hisogram shows a significant increase in the total number of BrdU/Nestin+ cells per SVZ of MSC treated mice compared to SHAM. Statistically significant compared to SHAM (* P<0.05). n=6 in each treatment group. All data are reported as mean ± standard error of the mean (SEM). Abbreviations: CC, corpus callosum; lSVZ, lateral subventricular zone; LV, lateral ventricle;. Scale bar, 200 μm (A-D); 200 μm (E,G). 50μm (F, H).

In order to further confirm these observations *in vivo*, the capacity of MSCs to activate survival and proliferation routes *in vitro* was tested. To this end, NSPCs were cultured in the presence of MSC conditioned medium (MSC-CM) and the activation of the PI3K/Akt and MAPK/Erk1/2 signaling pathways was analysed by Western blot. These signal cascades have been shown to be involved in promoting neurogenesis, neuroprotection,

oligodendrocyte fate decision and OPC differentiation as well as inhibiting apoptosis. (Ishii et al., 2013; Xiao et al., 2012; Younes-Rapozo et al., 2009; Hawkins et al. 2006; Pernet et al., 2005; Hayley et al. 2005; Rubinfeld & Seger, 2004; Choi et al. 2003; Brunet et al. 2001; Baron et al., 2000; Leevers et al. 1999). Thus, phospho-AKT and phospo-44/42 MAPK activations were studied at 15, 30 and 60 minutes after adding MSC-CM to the NSPC cultures (Figure 24A), and compared to control cultures where MSC non-CM was added. No differences were observed among incubation times (Figure 24B). The subsequent repetitions of the experiment were conducted, in agreement with this and previous reports (Hu et al., 2012), for 15 minutes after adding the MSC-CM to the NSPC cultures. Hence, both phosphorylated-AKT and phosphorylated-ERK1/2 protein expression levels changed significantly compared to controls (Figure 24C). This observation indicated that MSC-CM was able to activate both routes in NSPC *in vitro*, and therefore corroborated the initial hypothesis.
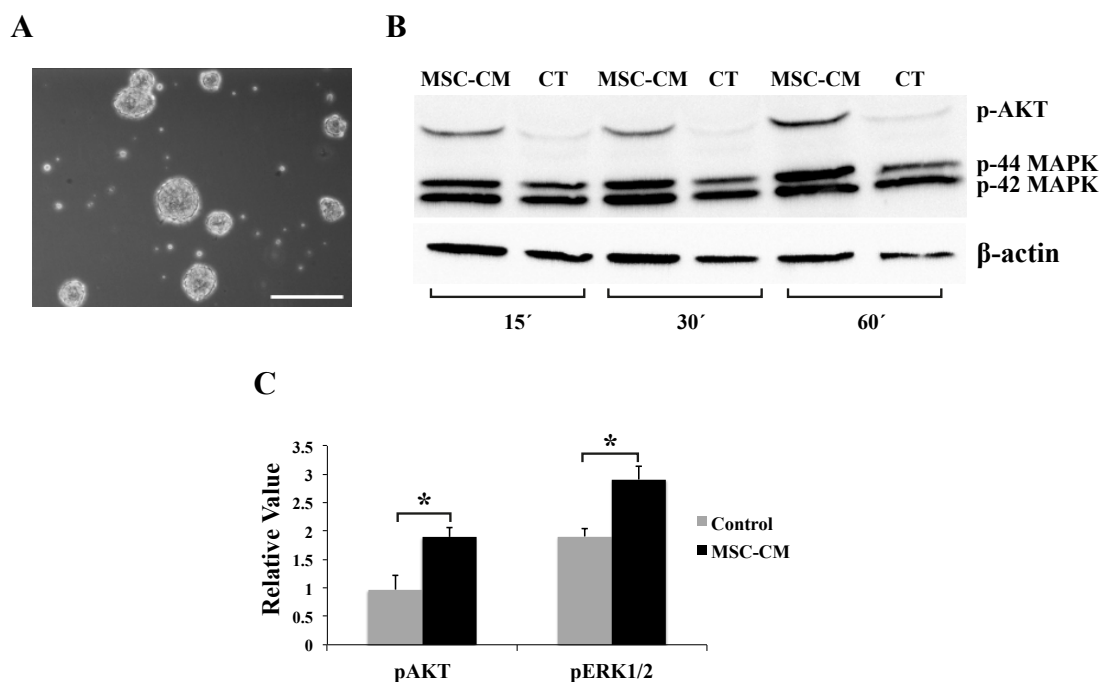
Figure 24. Western blot analysis of the activation of AKT and MAPK pathways induced by MSC conditioned medium. (A) Undifferentiated NSPCs grow in suspension, forming neurospheres just before treatment with MSC-CM. (B) Western Blot images taken in the same gel for p-AKT and p-44/42 MAPK in non-conditioned (CT) and MSC-CM corresponding to different NSPC cultures at 15´, 30´and 60 minutes after exposure to the specidic culture medium. (C) Histogram corresponding to the gel density analysis of CT and MSC-CM for p-AKT and p-44/42 MAPK at 15 minutes after exposure. The mean expression of pAKT and pERK1/2 after normalization is shown as fold induction from the data obtained from four independent experiments. Statistically significant compared to control (* $P<0.05$). n=4 independent experiments. All data are reported as mean ± standard error of the mean (SEM). Scale bar, 500 μm (A).

Finally, to clarify whether the NSPCs of the SVZ, which were proven here to be activated and increased their proliferation, were capable of migrating outside of the SVZ to their final destinations, such as the CC, the V-SVZ was electroporated with a pCX-GFP plasmid. Animals where sacrificed 20 days post electroporation (dpe) and analysed for the expression of both GFP and the neural progenitor cell marker (Nestin). The transfection was successful in all mice, resulting in efficient plasmid uptake and gene expression, which was not limited to the injected LV, but also efficient in the contra-lateral ventricle and in the third ventricle (Figure 25). The electroporation efficiency ranged from 7-15 transfected cells per section, which is lower than the one reported by Barnabé-Heider et al., 2008. Unfortunately, no cells were detected outside from the V-SVZ at the time analysed.
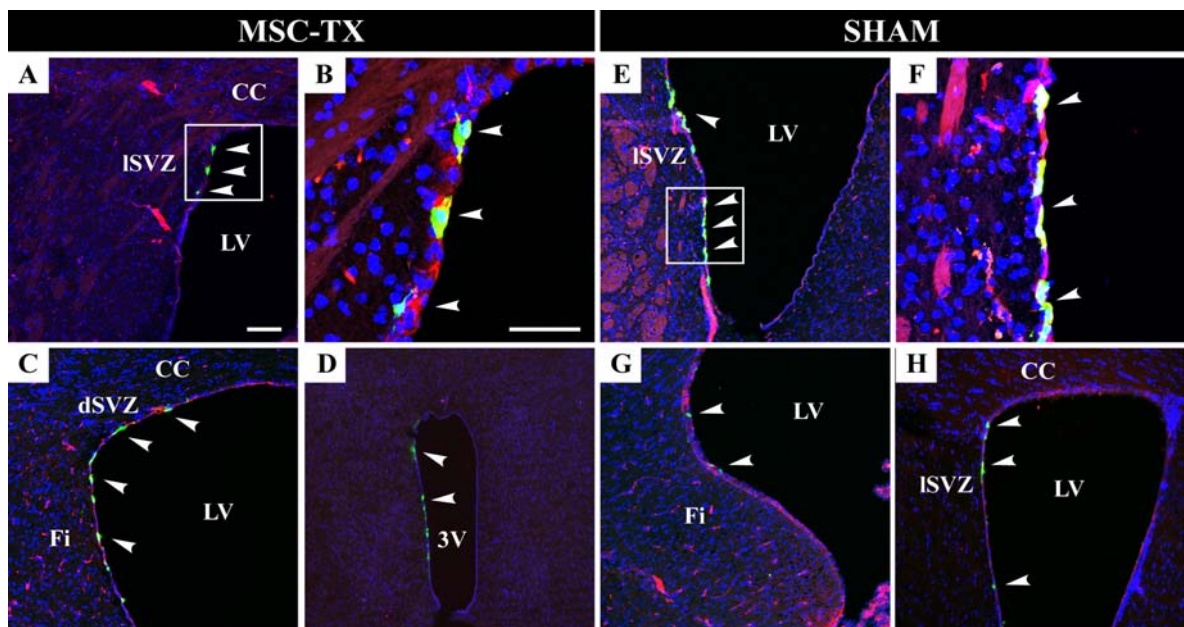
Figure 25. *In vivo* **electroporation of GFP in the adult V-SVZ**. Double immunostaining for GFP+ (green) and Nestin+ (red) is shown in all cases and indicated with arrows. Representative images of GFP/Nestin+ NSPCs found in the SVZ of the LV as well as GFP+ ependymal cells lining the walls of both LV and 3V. (A-D) images correspond to the MSC transplanted group and (E-H) to the SHAM vehicle control group. Abbreviations: dSVZ, dorsal subventricular zone; lSVZ, lateral subventricular zone; Fi, fimbria; 3V, third ventricle; CC, corpus callosum; LV, lateral ventricle. Scale bar, 100 μm (A, C-E, G, H); 50μm (B, F).

Section II

4.9   FGF8 increases proliferation in cultured OPCs

Previous work in our lab have proven that OPCs can be activated and remyelination induced using bone marrow stem cells (Jaramillo-Merchán et al., 2013). These findings may be due to the secretion of certain soluble factors, generally referred to as the MSC secretome. These soluble factors have an enormous potential for the treatment of several diseases, including demyelinating conditions. Harnessing the MSC secretome, will have relevant implications for clinical applications. In this work, it was analysed the effect that a single trophic factor, FGF8, may exert on the activation and differentiation of OPCs.

In order to firstly elucidate the role of FGF8 in terms OPCs proliferation, these were isolated from P0–P2 newborn mice and cultured on poly-L-lysine coated culture dishes. The initial culture was a mixture of astrocytes, OPCs and other cell types, where the OPCs were being mainly detected on top of the astrocytes (Figure 26A). After 7 days of culture, the cells were treated with trypsin and shaken in order to detach the OPCs and replated onto new culture dishes, where they were further expanded using mitogens PDGF-AA and FGF2 (Figure 26B). In this fashion, after an additional 7 days of culture the majority of the cells detected corresponded to OPCs, as indicated in previous publications (Lunn et al., 2007; Yang et al., 2005; Tsang et al., 2004).

To induce OPCs differentiation, the culture medium was changed removing the mitogens and adding fetal bovine serum, resulting in spontaneous differentiation (Figure 26C). Mature oligodendrocytes, identified as cells with many small prolongations, could be detected after 7 days of culture. FGF8 was then added to the culture in the same differentiation medium (Figure 26D). All the analysed cultures were mainly composed of oligodendrocytes, as proved by Olig2 staining (Figure 26E–H). In the cultures with FGF8, an increased number of cells were detected compared to the other treatments, even when the cultures were started with the same initial number of cells. To corroborate that FGF8 induced proliferation, BrdU was incorporated to the culture 24 hours before fixing, and then ICC for BrdU and double stained with NG2+ (an OPC marker) in order to confirm that only oligodendrocytes were counted (Figure 26I–L). The results showed a marked increase in proliferation in the OPC cultures where FGF8 was added, even more than in the

undifferentiated cultures (Figure 26L). This confirmed that FGF8 induced the proliferation of OPCs.
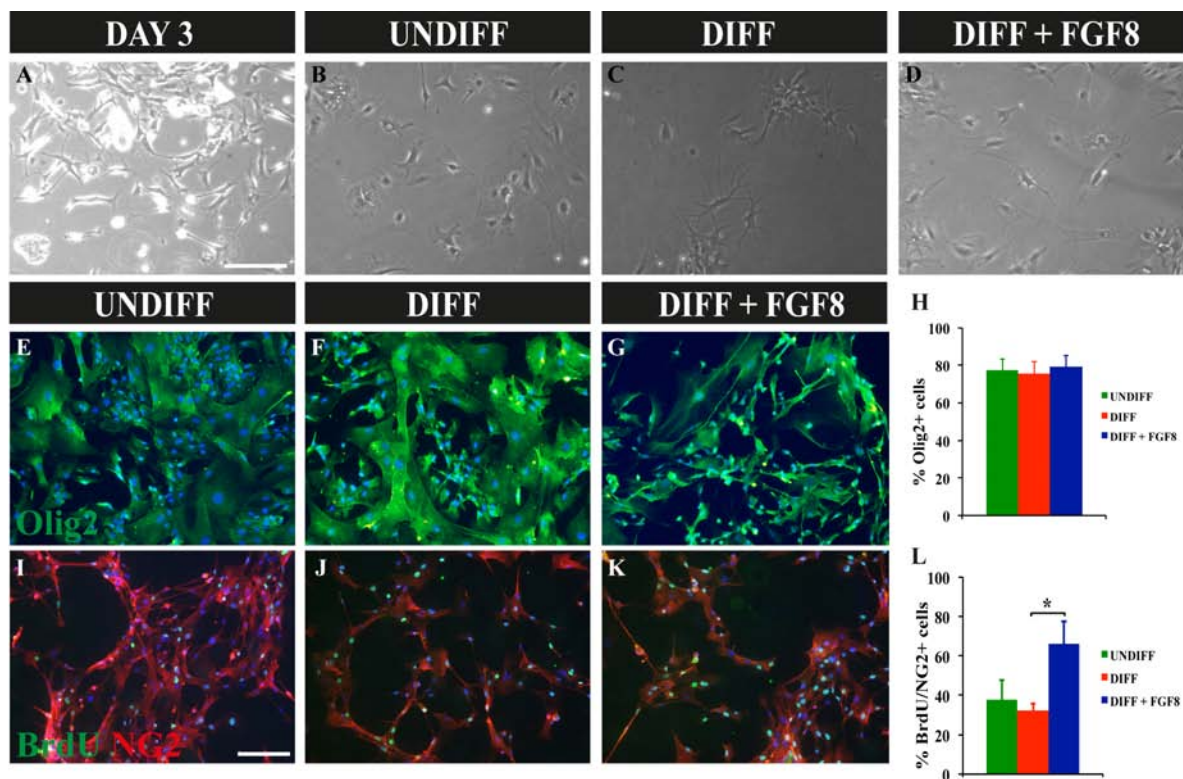
Figure 26. Culture and differentiation of OPCs. (A) OPCs cultured for 3 days after extraction on poly-L-lysine coated culture dishes. Numerous astrocytes are present. (B) OPCs after passaging and expanding in the presence of FGF2 and PDGF-AA, to induce proliferation and maintenance of the OPCs. (C) OPCs cultured in differentiation inducing medium for 7 days. Mature oligodendrocytes appear in the culture. (D) OPCs cultured for 7 days in the differentiating medium and FGF8. All images were taken at 100X magnification. (E–G) Immunocytochemistry of OPCs in undifferentiating medium (E), differentiating inducing medium (F), and in the presence of FGF8 (G), staining for Olig2 (in green) and DAPI for nuclear staining (in blue). (H) Histogram presenting the percentage of Olig2+ cells in the various cultures observed in (E–G). Percentages are with respect to the total number of cells, calculated by DAPI staining. (I–K) ICC of NG2/Brdu+ cell in undifferentiating medium (I), differentiation inducing medium (J), and in the presence of FGF8 (K). (L) Histogram presenting the percentage of NG2/BrdU+ cells in the different cultures, with respect to the total number of cells. (* $P<0.05$). n=4 in each treatment group. All data are reported as mean ± standard error of the mean (SEM). Scale Bar, 150 mm (A–D) and 100 mm (E–G) and (I–K).

4.10 FGF8 upregulates the expression of early OPC markers

This study showed that OPC proliferation was enhanced by FGF8, and therefore it is possible that differentiation might be hampered in turn, as some authors demonstrated that occurred with FGF2 (Fortin et al., 2005; Zhou et al., 2004; Bansal and Pfeiffer, 1997). To confirm this, the immature and OPC markers NG2 and PDGFR-α, oligodendrocyte lineage marker Olig2 and mature oligodendrocyte marker O4 were analysed (Figure 27A).

Differentiated cultures showed a lower percentage of cells positive for PDGFR-α and Olig2 in comparison to the undifferentiated and FGF8 treatments (Figure 27B). As for O4, which begins to be expressed during oligodendrocyte maturation, coinciding with the loss of expression of NG2 and PDGFR-α (Baumann & Pham-dinh, 2001), its expression was increased in the differentiated and FGF8 treatments (Figure 27B). This data was corroborated by qPCR (Figure 27C), indicating that the differentiated treatment resulted in less immature oligodendrocytes and OPCs, coinciding with more mature oligodendrocytes. However, in the case of FGF8, it is interesting to note that there were more immature and mature markers (Figure 27C). Since the composition of both medium only differs in the growth factor, this data seems to indicate that FGF8 induces proliferation, resulting in more OPCs in culture, and does not hamper differentiation, which in turn results in more mature oligodendrocytes in the culture.
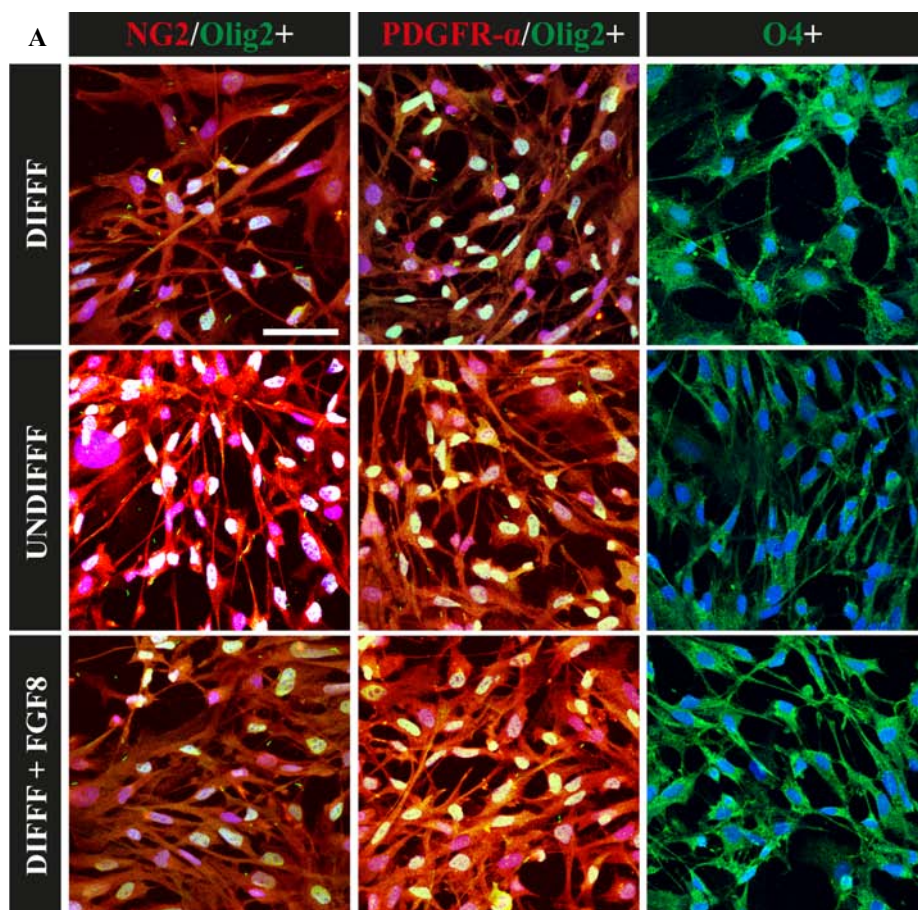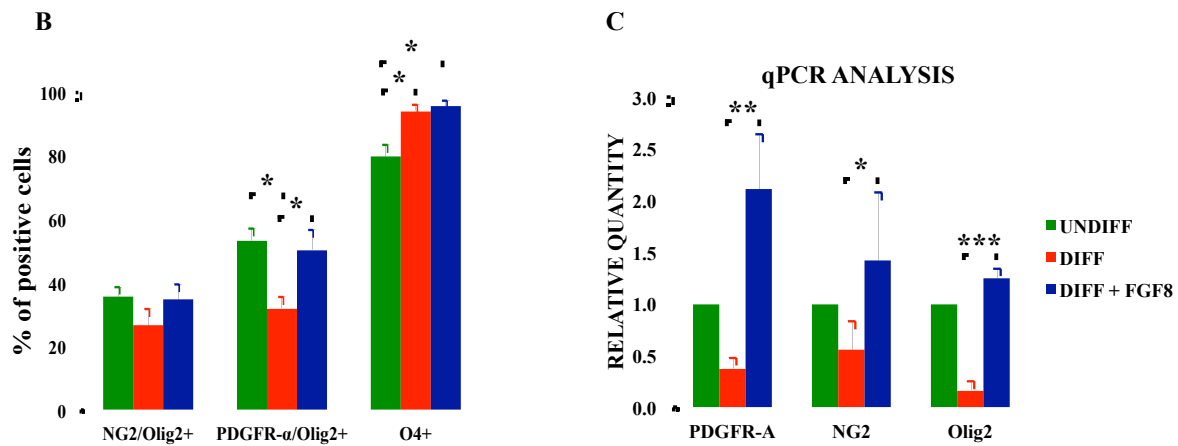
Figure 27. OPCs differentiation with and without FGF8. (A) Immunocytochemistry of NG2/Olig2+, PDGFR-α/Olig2+ and O4+ cells in the undifferentiated, differentiating and FGF8 culture media. In all images, blue staining corresponds to the nuclei (DAPI). (B) Histogram depicting the percentage of cells in the different cell cultures staining for markers analysed in A. Percentages are with respect to the total number of cells. (C) Histogram depicting the results from the quantitative PCR analysis of the different cell cultures. (* P<0.05, ** P<0.01, *** P<0.001). n=4 in each treatment group. All data are reported as mean ± standard error of the mean (SEM). Scale bar indicates 50 mm.

4.11 FGF8 induces the migration of OPCs

Undifferentiated OPCs were placed on matrigel cultures to perform migration assays. To this end, a heparin bead previously soaked in FGF8 solution (500 ng/ml) was placed 0.5 mm away from the cluster of OPCs, while a PBS-soaked bead was used as control (Figure 28A–C). Twenty-four hours afterwards, outgrowths were observed from the OPCs, the majority of which were detected in the direction of the FGF8-soaked bead (Figure 28B). The cultures were maintained and observed after 48 and 72 hours, and the OPCs still migrated towards the heparin bead (Figure 28C). To confirm the attracting effect of FGF8, proximal/distal analysis was performed on the cultures (Figure 28D). The cultures where FGF8-soaked beads were used presented a significantly higher proximal/distal ratio than control cultures where only PBS was used. Specifically, a 2-fold increase in cells was detected near the beads in comparison to more distal areas of the cell clusters (Figure 28D). Therefore, the results indicated a predominantly migrating and attracting effect induced by FGF8. In order to confirm this migrating property, the FGF-receptor inhibitor SU5402 was used in the cultures to counteract the effect of FGF8 (Figure 28E–G). In this case, two beads were used; on one side of the cluster of OPCs, a FGF8-soaked bead was placed, while a bead soaked in the inhibitor was positioned on the other end of the plate. A PBS-soaked bead was used as control of the inhibitor (Figure 28H). After 48 hours of

culture, the side of the OPCs where the SU5402-soaked bead was placed, no cell sprouting or migration was detected (Figure 28F). In the other side of the cluster, closer to the FGF8-soaked bead, numerous cell outgrowths were present (Figure 28G), indicating that the OPCs were stimulated by the FGF8 but the inhibitor managed to halt further migration. In the cases where PBS was used instead of the inhibitor, migration of the OPCs was observed like when FGF8-soaked beads were placed alone (Figure 28H). Overall, the results demonstrated that FGF8 is capable of inducing OPC migration, exerting an attracting effect, which is mediated by the binding of FGF8 to FGF receptors.
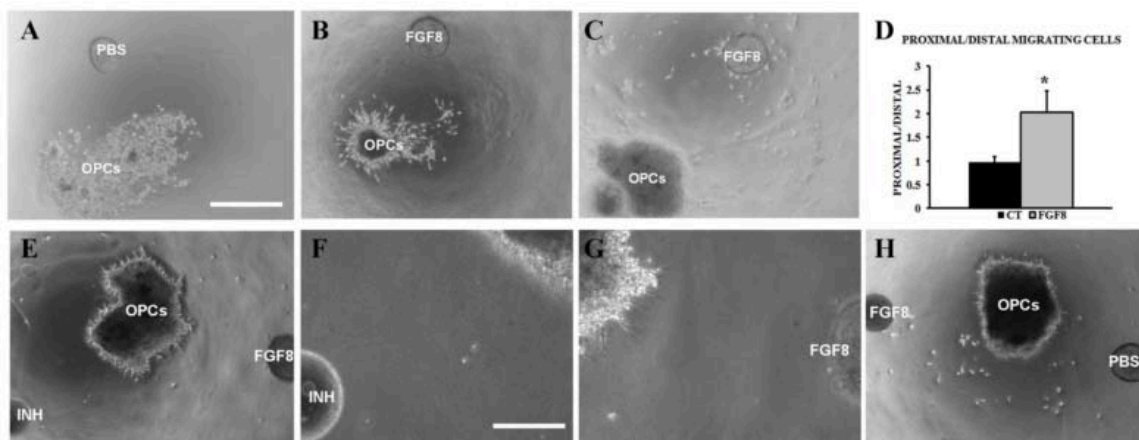
Figure 28. Matrigel cultures of OPCs. (A) OPC matrigel culture where a PBS-soaked bead was placed 0.5 mm away from the cell cluster. Image taken at 40X magnification. (B–C) OPCs where a cluster of cells migrating towards a FGF8-soaked bead can be observed. (D) Histogram depicting the OPC proximal/distal rate in control cultures and where FGF8 was included. (*P<0.01). n=4 in each treatment group. All data are reported as mean ± standard error of the mean (SEM). (E–G) Matrigel cultures where on one side a FGF8-soaked bead was placed and on the other side a FGF8 inhibitor. (F, G) Close-up images of the areas near the inhibitor-soaked bead (F) or near the FGF8-soaked bead (G). (H) OPCs where a FGF8-soaked bead was placed and on the other side a PBS-soaked bead, as control of the inhibitor. Scale bar indicates 500 mm for (A–C, D, H) and 200 mm for (F, G). All images were taken 48 hours after culture.

Chapter V

- DISCUSSION -

Section I

5.1 MSCs intraventricular-injection as a feasible method to boost endogenous oligodendrogenesis & study remyelination within the CC

The adult CNS maintains a certain endogenous potential to repair myelin damage. This regenerative function is, however, insufficient in chronic MS in which progenitor cells either fail to be recruited into lesion sites (Boyd et al., 2013) or experience difficulties with respect to differentiation, as they remain in a quiescent state (Back et al., 2005; Reynolds et al., 2001; Prineas and Connell, 1979). The microenvironment of chronic demyelinated lesions also plays an important role, as it inhibits remyelination (Jadasz et al., 2012). This inefficiency or failure of myelin-forming oligodendrocytes to remyelinate axons and preserve axonal integrity remains a major impediment in the repair of MS lesions and is principally responsible for axonal and neuronal degeneration leading to chronic disability (Trapp and Nave, 2008; Pagani et al., 2005). Current MS treatments mostly focus on reducing the formation of inflammatory lesions within the CNS but do not enhance endogenous myelin repair. Thus, boosting the endogenous oligodendrogenesis, either by targeting stimulatory or inhibitory pathways in resident stem and precursor cells or through appropriate cell therapies as presented in this thesis, will probably lead to the development of significant repair strategies for the demyelinated CNS and complement the currently available immunosuppressive treatments.

In this regard, MSCs represent an attractive source to develop a cell therapy for MS. First, bone marrow-derived MSCs are accessible cells, easy to obtain and therefore minimally invasive. Second, autologous MSCs can be used, avoiding the search for compatible tissue donors. Third, MSCs exert stromal bystander immunomodulatory, neuroprotective and eventually remyelinating effects in the damaged CNS. As commented in the introduction section, different authors have shown that MSCs are capable of releasing a number of trophic factors that *in vitro* induce oligodendrocyte fate decision in NSPCs, OPCs activation/migration and eventually their differentiation toward mature myelinating oligodendrocytes (Cruz-Martinez et al., 2014; Jadasz, et al., 2013; Jaramillo-Merchán et al., 2013; Barhum et al., 2010; Bai et al., 2009; Lu et al., 2009; Gerdoni et al., 2007; Rivera et al., 2006). Moreover, during the last decades, different research groups have studied the therapeutic effect of MSC transplantation into the diseased CNS, demonstrating that MSC

induces regeneration and neuroprotection in the damaged areas of different animal experimental models (Gerdoni et al., 2007; Neuhuber et al., 2005; P. Lu et al., 2005; Zhang et al., 2005; Hofstetter et al., 2002; Dezawa et al., 2001;). In the case of demyelinating diseases, our group (Jaramillo-Merchán et al., 2013) as well as others (Kemp et al., 2011; Gordon et al., 2010; Bai et al., 2009; Lanza et al., 2009; Z. Lu et al., 2009; Rafei et al., 2009a; Rafei et al., 2009b; Zhang et al., 2009, 2006, 2005; Gordon et al., 2008; Kassis et al., 2008; Gerdoni et al., 2007; Zappia et al., 2005) have shown that *in vivo* transplantations of MSCs, increase neuroprotection, modulate neuroinflammation, reduce demyelination and partially enhance functional recovery in some MS models.

There are two principal approaches to transplant cells into the body: local delivery into the tissue and systemic delivery. However, both methods have been shown to be inefficient for long-term engraftment of MSCs. Whereas the loss of locally injected cells can be attributed to wash out, cell death, and rejection via the innate immune system, for systemic delivery (especially intravenous, via tail vein) transplantations have resulted in significantly entrapment of MSCs in the lung (reviewed in Kean et al., 2013). In this context, intraventricular transplantations seem to be an alternative interesting route of MSC administration, which has not attracted so much attention as the others. Kassis and colleagues demonstrated that following intraventricular injection, a small percentage of the transplanted cells expressed several neural markers, suggesting that some level of transdifferentiation is possible (Kassis et al., 2008). Similarly, Barhum and colleagues showed that intraventricular injections of modified MSCs produce neurotrophins, which successfully attenuated EAE development (Barhum et al., 2010). However, a deeper understanding of the phenomenon and the mechanisms activated *in vivo* after the stem cell infusion is necessary. In addition, it was also reported that intravenously and intranasally applied murine and human bone marrow-derived MSCs on cuprizone induced demyelination, had not impact on demyelination or glial activation, as the cells could not cross the intact BBB and therefore enter the CNS (Nessler et al., 2013). Altogether, these studies lead us to hypothesize whether intraventricular transplantation of MSCs in the chronic demyelinated cuprizone model may be a more feasible route of administration in terms of cell survival, engraftment, effect duration and mainly, its potential to stimulate the neurogenic/oligodendrogenic niche of the V-SVZ due to its direct contact with the CSF, and the presence of neurotrophic receptors in the primary cilia of NSPCs (Cuccioli et al., 2015).

As for the mouse model, cuprizone intake produced highly intense and reproducible demyelination of distinct brain regions, among them the CC, which is the most commonly studied region to investigate the mechanism of remyelination (Steelman et al., 2012). Moreover, the major advantage of this model is that permits the study of the processes independently of the participation of peripheric immune cells, as the BBB is intact. However, the cuprizone effect is strain-dependent and can be influenced by a variety of co-factors such as age, genetic background, dose, duration of exposure, and even the method of administration into the diet (Skripuletz et al., 2010a; Adamo et al., 2006; Stidworthy et al., 2003; Love, 1988; Kimberlin et al., 1976; Carlton, 1969). For this reason, it was firstly analysed the demyelinated brain regions of the mice 12 weeks after cuprizone intake. As it was shown in Figure 13, the CC was more homogenously affected among mice than any other region. Moreover, the cerebellum, which was reported by other authors to be affected and therefore the motor function altered, (Steelman et al., 2012; Groebe et al., 2009; Skripuletz et al., 2008) was preserved in our model (Figure 14). This, together with the fact that the CC is by far the largest fiber tract of the brain and its close proximity to the ventricles and SVZ, made that the complete analysis of this work was basically focused on this structure.

5.2 MSCs intraventricular-injection in a chronic demyelinated model, induces remyelination, enhancing the number of oligodendrocytes in the CC

The idea that the adult CNS was fixed, immutable and unable to generate new cells was long believed. However, in the early twentieth century, Santiago Ramón y Cajal published his work on the regeneration of the nervous system following injury (Ramon y Cajal, 1913a). More recent scientific and technological advancements have shown that the CNS has a certain level of regenerative capacity, with a pool of undifferentiated dividing cells within the brain. These cells are mainly located in two major brain regions during adulthood: the SVZ of the frontal horns of the LVs and in the antero-lateral region of the subgranular layer of the hippocampal dentate gyrus (DG) (reviewed in Gonzalez-Perez & Alvarez-Buylla, 2011). For instance, in MS, after myelin damage, resident OPCs and NSPCs located in the neurogenic niches direct their fate into myelin-producing oligodendorcytes. However, repeated episodes of demyelination and remyelination may lead to their exhaustion, being these mechanism of self-renewal and repair either impaired

or insufficient (reviewed in RJ Franklin, 2012). Therefore, to restore the normal brain function in MS the first question to be adressed was whether intraventricular injection of MSCs could enhance the number of recruited oligodendrocytes in the demyelinated CC by modulating the cell fate decision of endogenous NSPCs and/or stimulating resident OPCs to proliferate and/or migrate.

In the first part of this work, it was revealed that MSC transplantations elicits a significant increase in the number of OPCs (NG2^{+}, PDFGR-α[+]) in the CC when compared with the SHAM group, as early as 2 months after transplantation as well as a significant rise in the number of mature oligodendrocytes (CC1^{+}) 3 months after the injection at the most caudal part of the CC (Figure 15). This may be due to the paracrine effect of several trophic factors, which are likely to be stimulating the differentiation of NSPCs of the SVZ towards OPCs, as well as their migration towards the CC and their final differentiation. A similar effect possibly occurs with resident OPCs in the ventricular surface of the CC since it coincides with the dorsal pole of the LV. However, despite these findings it was necessary to confirm that the newly recruited oligodendrocytes were capable of producing myelin and repair the damaged areas. To this end, the same animals were analysed over time in a longitudinal study by magnetic resonance imaging (MRI). This technique has the advantage of allowing the quantification of the myelin density in the same individual mouse at different time points before and after transplantation *in vivo*. As a result, a significantly higher myelin content was detected in the cell-treated group 2 months after transplantation, comparing themselves with respect to the myelin content before transplantation as well as compared to sham controls (Figure 16). These results suggest that the MSCs were not only capable of stimulating the endogenous oligodendrogenic program, increasing the oligodendrocyte numbers within the CC, which actually was not capable to react anymore, but also enhancing the myelin production. Altogether, these data shows that the MSCs may induce indirectly a regenerative/repairing process in the treated brain, either by stimulating resident OPCs or NSPCs located in the SVZ, which would migrate to the CC and remyelinate it as early as 2 months post-transplantation.

In order to further confirm these observations, the myelin content was also analysed by using quantitative measurements of MBP immunostaining. To this end, the Imaris analysis software was used to make 3D reconstructions in combination with MBP immunostaining. Unfortunately, in this case no significant differences were detected (Figure 17). However,

it is necessary to consider that using this second approach to measure the myelin content, different animals are being compared at different time points, as in this case it is necessary to sacrifice the mice for their analysis, rather than comparing the same animal over time which would be far more realistic. Hence, the variability that could exist between individuals, something that does not occur in the case of MRI, may lead to a masking of the differences between both animal groups.

5.3 MSCs do not affect glial activation within the CC

Despite the fact that, in 1904, Müller stated that MS was astrocyte-based disease (Müller, 1904), the majority of the researchers have focused their work on the role of oligodendrocytes. However, everyday there is more evidence suggesting that astrocytes play a vital role regulating de- and remyelination in MS, making the analysis of this cell population in MS of vital importance. Whereas it is well known that in the healthy brain, astrocytes have different functions including metabolic and structural support to neurons, regulation of the extracellular ionic environment, and elimination of excessive levels of neurotransmitters such as glutamate (Sofroniew, 2010), their role in demyelinating diseases is controversial, showing both protective as well as deleterious effects on demyelination (Moore et al., 2011; De Keyser et al., 2010; Renault-Mihara et al., 2008; William et al., 2007). On one hand, reactive astrocytes are suggested to promote inflammation and damage to oligodendrocytes, contributing into the formation of a glial scar, which creates a physical barrier that impairs remyelination as it contains growth inhibitory proteins such as myelin-derived proteins and proteoglycans (Sofroniew, 2010) as well as by enhancing the immune response through expression of cytokines and recruitment of T cells, microglia and macrophages to demyelinating lesions (Skripuletz et al., 2013; De Keyser et al., 2010; Tanuma et al., 2006). On the other hand, they can create a permissive environment and attenuate the inflammatory response for remyelination as they can secrete anti-inflammatory cytokines, such as interleukin 10, TGF-β and interleukin-27, as well as their effect on OPCs migration, proliferation, and differentiation (Nair et al., 2008).

For this reason, it was considered important to analyse whether the injected stem cells influence astroglial activation in the CC. As a result, no difference in the GFAP+ astrocyte numbers was detected between SHAM and MSC-treated mice (Figure 18). This may indicate that although MSCs does not seem to have an obvious effect on the populations of

astrocytes, it cannot be excluded the possibility that, as the injection site is at a distant range from the regions of the brain where astrocytes are more abundant, it may be difficult for the paracrine effect of the MSCs to reach these cells. The SVZ, however, is much closer and thus capable of responding to the stimuli. However, future studies should focus on the mechanisms underlying stem cell-mediated reduction of astrocytic scar in brain lesions, which may be crucial in promoting a pro-neurogenic microenvironment that supports tissue repair.

5.4 MSCs are primarily located in the CSF three months after transplantation, overexpressing several trophic factor encoding genes

Apart from the regenerative potential previously observed, it was considered interesting to assess the location and survival timing of the injected MSCs. Two different approaches were used to address this issue. First, the MSCs were pre-incubated *in vitro* prior to transplantation with iron nanoparticles, and then injected into the LVs. This enables to track *in vivo* their location due to the contrast that they show when analysed by MRI. Second, MSCs extracted from GFP$^+$ mice were injected in the same manner into the cuprizone treated mice, that were then sacrificed at several time points to perform western blot analysis of the CSF, together with histological analysis of the brain tissue. Thus, the MRI images confirmed that 3 months after transplantation the MSCs were still present within the ventricles, and not only in the lateral ones, but homogenously distributed and confined within the CSF, as they can be observed also in the third ventricle in Figure 16D, appearing as black spots. Moreover, the protein analysis confirmed this observation, as when the CSF was extracted at different time points and Western blot analysed, GFP protein expression was detected in the stem cell treated group (Figure 19M). To further confirm the precise location of the MSCs, and whether they were penetrating into the brain parenchyma (as well as discard the appearance of tumors and study the microglial/macrophage activation), IHC analysis were conducted. It was concluded that the vast majority of MSCs were located within the CSF, which cannot be detected by IHC, and only in very rare occasions some were found in the brain parenchyma (Figure 19), with higher numbers attached to the choroid plexus (Figure 19D, E). In a few cases, the MSCs were detected in close contact with blood vessels (Figure 19J), possibly contributing and promoting angiogenesis, as it has been previously described (He et al., 2007). It was also observed in an insignificant number, that the MSCs were surrounded by macrophages or

microglia CD45+, without being phagocyted (Figure 19I, J). In all cases, the regular morphology of the cell body, and the absence of cells with more than one nucleus indicated that there was no sign of transdifferentiation or cell fusion. Finally, we did not observe any signs of malignancy, with a total absence of mass aggregates along the whole brain. Both in our group (Pastor et al., 2012) as well as other authors had previously shown (Giordano et al., 2007; Vitry et al., 2003; Corti et al., 2002) this lack of tumourigenesis when MSC were injected, possibly due to contact inhibition (Javazon, et al., 2004), which is an essential factor to consider in cell therapy.

Similarly, the CSF was also analysed for its content in trophic factors. MSCs are known to be the source of multiple immunomodulatory agents plus trophic factors involved in repair and regenerative processes. This broad array of secreted factors has been widely analysed *in vitro* and under many different conditions. However, in this study it was aimed to analyse the trophic factor expression within the CSF three months after MSC transplantation. As a result, PDGF, IGF, NT3, NT4 and FGF2 were greatly overexpressed ($P<0.0001$) in the CSF of the MSC-treated group compared to the SHAM (Figure 20), which are the likely candidates together with others not analysed, to be responsible for the regenerative effect previously observed.

5.5 MSCs transplantation increases axonal conduction velocity, myelin thickness and reduces g-ratio of callosal axons

In summary, up until now it was proven the activation and maturation of OPCs, which were recruited into the demyelinated CC and it could be correlated with an increase in the myelin content. However, it was crucial to corroborate the functional consequences of this myelin increase, since an excess of myelin and/or oligodendrocytes not capable of placing the new myelin layers around the demyelinated axons could lead to a deregulated process, with a negative effect (reviewed in RJ Franklin, 2002). Thus, it was necessary to address two fundamental questions: 1) It is the new formed-myelin wrapping the axons correctly? and 2) It is this myelin ensheathing the appropriate axons? To this end, the axonal conduction velocity in the CC was analysed by electrophysiological recordings. The first analysis performed was to confirm that the axonal conduction velocity was affected in the cuprizone model. Whereas non-myelinated fibers, presented normal axonal conduction velocity values, as it was expected due to the fact that the cuprizone only affect the oligodendrocytes and thus the myelinated fibers, myelinated axons were affected by the

cuprizone when compared with the WT (Figure 21C). Therefore, the next step was to compare the MSC-treated group with the SHAM, which were analysed 2 and 4 months after transplantation. Interestingly, the data revealed that there was no difference between the MSC-treated and the SHAM animals at any time point in terms of conduction velocity. However, when the animals were compared within the same group over time, the axonal conduction velocity was significant increased in the MSC group. In response to the second question, this difference was only observed in the fast conduction fibers, whereas the conduction velocity of the slow fibers did not change, showing that the remyelination was directed only to the axons that were previously myelinated, instead of aberrantly myelinating the slow, unmyelinated fibers (Figure 21D). This demonstrated that the increase in myelination with MSCs treatment was functionally relevant as it led to improved axon conduction velocity over time. Moreover, the selective effect on the myelinated fibers suggested that the newly activated oligodendrocytes recognized selectively these fibers, reestablishing their function and without developing a disorganized myelinating pattern. Therefore, correct signals to stimulate and enhance myelin formation are still present in chronically demyelinated fibers.

In addition, the integrity of myelination ultrastructure was also studied, calculating the mean g-ratio of myelinated and unmyelinated axons by EM analysis in three telencephalic areas, enriched in myelinic axons. The results revealed that the stem cell treated group presented significantly thicker myelin sheath than SHAM control mice in all the regions analysed and consequently lower g-ratio values (Figure 22L-N). Although, it was also observed that when compared to the WT, neither the vehicle-control animals nor the MSCs treated reached their normal values (Figure 22L-N). This is easy to explain since a characteristic feature of remyelination is that the new myelin sheaths are always thinner and shorter than expected for the diameter of the axon as it was explained in the introduction section (reviewed in RJ Franklin, 2002). In conclusion, the electrophysiological recordings together with the EM analysis indicated that the increase of oligodendrocytes and myelin content over time in the CC, was translated as a final step into a functional recovery.

5.6 MSCs stimulate NSPCs in the adult SVZ, inducing survival and proliferation through PI3K/Akt & MAPK/Erk1/2 activation

In the present work, it was confirmed the regenerative potential of intraventricular

transplanted MSCs into a chronic model of demyelination. However, it was of vital importance to elucidate the mechanism by which the stem cells were exerting this beneficial effect. It is well known, that the V-SVZ harbours the largest population of NSPCs in the adult brain. They are closely associated with ependymal cells and as radial glia during embryonic development, type B1-cell often possesses a single primary cilium that projects into the ventricle (Tramontin et al., 2003). The function of this apical ending has been considered essential for growth factor, morphogen reception and transduction, and therefore for the proliferation, survival and/or differentiation of these quiescent cells (Cuccioli et al., 2015; García-González et al., 2014; Ka-Tong et al., 2013; Nait-Oumesmar et al., 2008). In fact, several studies reported that the CSF flow plays a major role in the proliferation (Owen-Lynch et al., 2003) and directional migration (Sawamoto et al., 2006) of these cells. Furthermore, Cayre and colleagues demonstrated that when the adult SVZ was heterotopically transplanted into WM tracts they massively generate myelinating oligodendrocytes as well as exhibit a migratory potential along these fiber bundles (Cayre et al., 2006). This, together with the data previously obtained in this work, led to hypothesize that both the resident OPCs of the CC and the NSPCs of the SVZ may be responding to the MSCs secreted soluble factors into the CSF, increasing their proliferative rate and eliciting an oligodendrocytic fate decision in the latter ones. These newly generated or activated OPCs would migrate to the damaged areas and remyelinate the affected axons, which was already demonstrated in previous sections.

Therefore, the first aspect to analyse was whether the population of NSPCs located within the V-SVZ were capable of responding to the secreted soluble factors in the CSF. To this end, BrdU proliferating assay was performed, starting immediately after MSCs transplantation. BrdU was added to the drinking water for fifteen days, and mice sacrificed one month post-transplantation. As a result, a significant increase in the percentage of NSPCs (BrdU/Nestin+) was detected, proliferating in the SVZ of MSC-treated mice when compared to the SHAM controls (Figure 23). These results indicate that intraventricular injected MSCs were exerting a paracrine effect in the V-SVZ, which was prone to respond to the soluble factors secreted into the CSF. In order to further confirm this finding, it was also analysed whether the MSCs were capable of activating survival and proliferation routes *in vitro*. To this end, NSPCs were cultured in the presence of MSC-CM and the activation of the PI3K/Akt and MAPK/Erk1/2 signaling pathways was analysed by Western blot.

The PI3K/AKT pathway regulates a diverse array of cellular functions, such as cell growth, survival, proliferation, and movement (Hawkins et al. 2006; Brunet et al. 2001; Leevers et al. 1999). In the mammalian brain, apart from its functions in neuronal survival and differentiation (Frebel and Wiese, 2006), several studies have implicated this pathway in synaptic plasticity, learning, and memory, showing that activation of PI3K/AKT was necessary for the expression of long-term potentiation (LTP) in the dentate gyrus (Kelly & Lynch 2000) and CA1 region of the hippocampus (Raymond et al. 2002; Sanna et al. 2002). On the other hand, ERK1/2, the mitogen-activated protein (MAP) kinase family members, is classically implicated in the regulation of various cellular functions (Rubinfeld & Seger, 2004). Emerging evidences have indicated that ERK1/2 signalling is involved a variety of neural cellular processes including cell proliferation and survival, neoplastic transformation, neural plasticity and differentiation (Ishii et al., 2013; Xiao et al., 2012; Pernet et al., 2005). More importantly, it was shown that the pharmacological blockade of ERK1/2 activation leads to fewer oligodendrocytes with mature phenotypes, suggesting the implication of the ERK1/2 pathway in oligodendrocyte differentiation (Younes-Rapozo et al., 2009; Baron et al., 2000). Moreover, activation of the MAPK/ERK pathway could inhibit apoptosis by inducing the phosphorylation of Bax (a proapoptotic protein) as well as enhancing the expression of antiapoptotic Bcl-2 (Hayley et al. 2005; Choi et al. 2003). As a result, it was observed that the expression of phosphorylated-AKT and phosphorylated-ERK1/2 protein was significantly enhanced in the MSC-CM treated NSPCs compared to controls (Figure 24C). This data proved that the soluble factors secreted by the MSCs were capable of stimulating both *in vivo* and *in vitro* the activation of NSPCs and increased their proliferation, suggesting a neurogenic and neurprotective effect as well as possibly promoting an oligodendrocytic fate decision on these cells, therefore corroborating the initial hypothesis.

Finally, the question remained as to which cells were responsible for the remyelinating effect observed in this study. Thus, to clarify whether the NSPCs from the adult SVZ were capable of migrate to the CC once activated to differentiate toward the oligodendrocyte lineage, the V-SVZ was electroporated with the pCX-GFP plasmid. Animals where sacrificed 20 days post electroporation (dpe) and analysed for the expression of both GFP and the neural progenitor cell marker Nestin. Despite the successful transfection in all mice, resulting in efficient plasmid uptake and gene expression (Figure 25), unfortunately

any GFP+ cell was detected outside of the V-SVZ cytoarchitecture. Although many possible explanations exist, the fact that this type of plasmids provides only transient GFP short-term expression is a remarkable limitation. This require that the animals are sacrificed less than 3 weeks after transplantation, while the first remyelinating effects within the CC were observed only at 2 months post-transplantation. For this reason, other approaches such as viral vectors or transgenic mice lines could be considered in the future to address this issue and obtain stable, long-term expression of GFP in these specific populations of cells. In conclusion, the results suggest that the NSPCs of the SVZ are likely to increase the numbers of OPCs in the CC, which in turn functionally remyelinate the damaged axons. However, the increase in myelin content could also be derived from resident OPCs in the CC which would be being activated, as the ventricular surface of the CC coincide with the dorsal pole of the LV, where the MSCs are creating a trophic factors-enriched CSF.

Section II

5.7 FGF8 activates proliferation and migration in mouse post-natal OPCs, without impairing their differentiation

In this work, it was proven that FGF8 is capable of activating post-natal mouse (OPCs) *in vitro*. Proliferation, migration and finally differentiation of OPCs to mature oligodendrocytes were observed *in vitro*, indicating that this process is not hampered. Oligodendrocytes are known to express various FGF receptors, mainly several subtypes of FGFR1, FGFR2 and FGFR3 (Bansal et al., 1996). Many studies have focused on the expression of these receptors, as well as on the effect of FGFs on the cells, which varies throughout its lineage. For example, FGF2, when combined with PDGF-AA, is known to induce proliferation of OPCs (McKinnon et al., 1990; Bogler et al., 1990), while mature oligodendrocytes, in the presence of this growth factor, revert to a progenitor state (Grinspan et al., 1993; Fressinaud et al., 1995). This indicates a negative effect in terms of differentiation and myelin production using FGF2. On the other hand, another work has shown that OPCs cultured in the presence of FGF8 expressed significantly more MBP compared to FGF2 (Fortin et al., 2005), revealing a distinct effect of these two at-first similar growth factors. That study also shown that in oligodendrocyte cultures, while FGF2 downregulated mature oligodendrocyte markers and induced a reverted state, this was not observed with FGF8. In the current work, we have further revealed that FGF8 is not only capable of inducing a proliferative effect on OPCs in culture (Figure 26), but is also capable of attracting these cells (Figure 28) and allowing their differentiation to myelinating oligodendrocytes (Figure 27). Thus, while FGF2 is useful in inducing OPC proliferation at the handicap of blocking differentiation, FGF8 seems to possess similar properties without this impediment.

The mouse model used in this study, where cuprizone was added to the mice diet, results in a chronic, irreversible demyelinating model similar to the lesions observed in MS. If the cuprizone is removed prematurely (before 12 weeks), remyelination is spontaneously activated, which occurs in two phases: OPCs proliferation and colonization of the demyelinated area, and differentiation towards immature oligodendrocytes that bind to the demyelinated axons and mature to myelinating oligodendrocytes. This process is regulated by the coordinated expression of soluble factors (Chari et al., 2007). The remyelinating process observed by early cuprizone removal also occurs naturally *in vivo*. OPCs are

expressed throughout the adult CNS, and are capable of differentiating to mature oligodendrocytes when a demyelinating lesion occurs (Menn et al., 2006). However, in the chronic phase of MS, there is a multiple dysfunction in the activation of OPCs, which affects the remyelinating process (Sim et al., 2002). This may be due either to the absence of nearby OPCs or to their quiescence, which make them unable to react. Regardless of the reason, the lack of soluble factors that activate the migration and differentiation of OPCs may be one of the primary reasons for this failed response. Thus, for a therapeutic approach to be effective it must be capable of stimulating the quiescent OPCs, as well as of inducing their migration to the damaged area and their final differentiation. This work demonstrates that FGF8 may be used to this end. In conclusion, FGF8 is a morphogenetic factor that may be used to induce post-natal migration, proliferation and differentiation of OPCs. This property makes it a candidate factor to treat demyelinating disorders as an alternative therapy.

Chapter VI

- CONCLUSIONS -

Section I

Intraventricular-injection of bone marrow-derived MSCs in the cuprizone chronically demyelinated model:

1. Increases the number of both OPCs and mature oligodendrocytes in the CC over time, without affecting the number of astrocytes.

2. Promotes remyelination in the CC, with a functional recovery, increasing the conduction velocity of the myelinated fibers in the callosal axons over time.

3. Increases the myelin sheath thickness and therefore decreases the g-ratio of the newly-formed myelin layers.

4. Overexpress several trophic factor-encoding genes in the CSF, which stimulates the proliferation of NSPCs in the adult SVZ.

5. MSC-CM activates both PI3K/AKT and MAPK/ERK signalling pathways in NSPCs *in vitro*, routes that participate in processes of proliferation, differentiation, movement and survival.

Section II

1. FGF8 activates post-natal mouse OPCs, inducing proliferation without impairing their differentiation to mature oligodendrocytes.

2. FGF8 stimulates OPCs migration, exerting an attractant effect, which is mediated by the binding of FGF8 to its FGF receptors.

BIBLIOGRAPHY

Aarum, J., Sandberg, K., Haeberlein, S. L., Persson, M. A. (2003). Migration and differentiation of neural precursor cells can be directed by microglia. Proc Natl Acad Sci USA 100: 15983–15988

Adamo, A.M., Paez, P.M., Escobar Cabrera, O.E., Wolfson, M., Franco, P.G., Pasquini, J.M., et al. (2006). Remyelination after cuprizone-induced demyelination in the rat is stimulated by apotransferrin. Exp. Neurol. 198, 519–529.

Allen, N. J., & Barres, B. A. (2009). Neuroscience: Glia - more than just brain glue. Nature 457, 675-677.

Angeles, W. L., Affairs, V., & Foundation, C. C. (2002). Premyelinating oligodendrocytes in chronic lesions of multiple sclerosis, 346(3), 165–173.

Azim, K., Raineteau, O., & Butt, A. M. (2012). Intraventricular injection of FGF-2 promotes generation of oligodendrocyte-lineage cells in the postnatal and adult forebrain. Glia, 60(12), 1977–90.

Bachelin, C., Lachapelle, F., Girard, C., Moissonnier, P., Serguera-Lagache, C., Mallet, J. et al. (2005). Efficient myelin repair in the macaque spinal cord by autologous grafts of Schwann cells. Brain : A Journal of Neurology, 128(Pt 3), 540–9.

Bai, L., Lennon, D. P., Caplan, A. I., DeChant, A., Hecker, J., Kranso, J. et al., (2012). Hepatocyte growth factor mediates mesenchymal stem cell–induced recovery in multiple sclerosis models. Nature Neuroscience, 15(6), 862–70.

Bai, L., Lennon, D. P., Eaton, V., Maier, K., Caplan, A. I., Miller, S. D., & Miller, R. H. (2009). Human bone marrow-derived mesenchymal stem cells induce Th2-polarized immune response and promote endogenous repair in animal models of multiple sclerosis. Glia, 57(11), 1192–203.

Bakker, D.A., Ludwin, S. K. (1987). Blood-brain barrier permeability during Cuprizone-induced demyelination. Implications for the pathogenesis of immune-mediated demyelinating diseases. J Neurol Sci 78: 125-137.

Bansal R, Pfeiffer S. E. (1997). FGF-2 converts mature oligodendrocytes to a novel phenotype. J Neurosci Res 50:215–228.

Bansal R, Kumar M, Murray K, Morrison RS, Pfeiffer SE. (1996). Regulation of FGF receptors in the oligodendrocyte lineage. Mol and Cell Neurosci 7: 263– 275.

Barhum, Y., Gai-Castro, S., Bahat-Stromza, M., Barzilay, R., Melamed, E., & Offen, D. (2010). Intracerebroventricular transplantation of human mesenchymal stem cells induced to secrete neurotrophic factors attenuates clinical symptoms in a mouse model of multiple sclerosis. Journal of Molecular Neuroscience : MN, 41(1), 129–37.

Barnabé-Heider, F., Meletis, K., Eriksson, M., Bergmann, O., Sabelström, H., Harvey, M., et al. (2008). Genetic manipulation of adult mouse neurogenic niches by in vivo electroporation. Nature Methods, 5(2), 189–96.

Barnett, S. C., Alexander, C. L., Iwashita, Y., Gilson, J. M., Crowther, J., Clark, L., et al. (2000). Identification of a human olfactory ensheathing cell that can effect transplant-mediated remyelination of demyelinated CNS axons. *Brain : A Journal of Neurology*, *123 (Pt 8)*, 1581–1588.

Baron, W., Metz, B., Bansal, R., Hoekstra, D., de Vries, H. (2000). PDGF and FGF-2 signaling in oligodendrocyte progenitor cells: regulation of proliferation and differentiation by multiple intracellular signaling pathways. Mol Cell Neurosci 15: 314–329.

Baumann, N., & Pham-dinh, D. (2001). Biology of Oligodendrocyte and Myelin in the Mammalian Central Nervous System, 81(2), 871–928.

Blakemore, W. F. & Crang, A. J. (1985). The use of cultured autologous Schwann cells to remyelinate areas of persistent demyelination in the central nervous system. J. Neurol. Sci. 70, 207–223.

Blunt, a. G., Lawshe, a., Cunningham, M. L., Seto, M. L., Ornitz, D. M., & MacArthur, C. a. (1997). Overlapping Expression and Redundant Activation of Mesenchymal Fibroblast Growth Factor (FGF) Receptors by Alternatively Spliced FGF-8 Ligands. Journal of Biological Chemistry, 272(6), 3733–3738.

Bogler, O., Wren, D., Barnett, S.C., Land, H., Noble, M. (1990). Cooperation between two growth factors promotes extended self-renewal and inhibits differentiation of oligodendrocyte-type-2 astrocyte (O-2A) progenitor cells. Proc Natl Acad Sci USA 87: 6368–6372.

Bottcher, T., Niehrs, C. (2005). Fibroblast growth factor signaling during early vertebrate development. Endocr Rev 26: 63–77.

Boyd, A., Zhang, H., & Williams, A. (2013). Insufficient OPC migration into demyelinated lesions is a cause of poor remyelination in MS and mouse models. *Acta Neuropathologica*, *125*, 841–859.

Boyd, J. G., Skihar, V., Kawaja, M., & Doucette, R. (2003). Olfactory ensheathing cells: historical perspective and therapeutic potential. Anatomical Record. Part B, New Anatomist, 271(1), 49–60.

Brinkmann, V., Billich, A., Baumruker, T., Heining, P., Schmouder, R., Francis, G., et al. (2010). Fingolimod (FTY720): discovery and development of an oral drug to treat multiple sclerosis. *Nature Reviews. Drug Discovery*, *9*(11), 883–897.

Brunet, A., Datta, S. R., Greenberg, M. E. (2001). Transcription-dependent and -independent control of neuronal survival by the PI3K-Akt signaling pathway. Curr Opin Neurobiol 11:297–305

Brüstle, O. (1999). Embryonic Stem Cell-Derived Glial Precursors: A Source of Myelinating Transplants. Science, 285(5428), 754–756.

Bryant, M. R., Marta, C. B., Kim, F. S., Bansal, R. (2009). Phosphorylation and lipid raft association of fibroblast growth factor receptor-2 in oligo- dendrocytes. GLIA 57:935–946.

Bunge, R. P. (1968). Glial cells and the central myelin sheath. Physiol Rev 48: 197–210.

Caplan, A. I., & Correa, D. (2011). The MSC: an injury drugstore. Cell Stem Cell, 9(1), 11–5.

Carlton, W. W. (1969). Spongiform encephalopathy induced in rats and guinea pigs by cuprizone. Exp. Mol. Pathol. 10, 274–287

Cayre, M., Bancila, M., Virard, I., Borges, A., & Durbec, P. (2006). Migrating and myelinating potential of subventricular zone neural progenitor cells in white matter tracts of the adult rodent brain. *Molecular and Cellular Neurosciences*, *31*(4), 748–58.

Chandran, P., Upadhyay, J., Markosyan, S., Lisowski, A., Buck, W., Chin, C.-L., et al. (2012). Magnetic resonance imaging and histological evidence for the blockade of cuprizone-induced demyelination in C57BL/6 mice. Neuroscience, 202, 446–53.

Chandran, S., Kato, H., Gerreli, D., Compston, A., Svendsen, C.N., et al. (2003). FGF-dependent generation of oligodendrocytes by a hedgehog-independent pathway. Development 130: 6599–6609.

Chari DM (2007) Remyelination in multiple sclerosis. Int Rev Neurobiol 79: 589–620.

Chari, D. M., & Blakemore, W. F. (2002). Efficient recolonisation of progenitor-depleted areas of the CNS by adult oligodendrocyte progenitor cells. Glia, 37(4), 307–13.

Chari, D. M., Huang, W. L., & Blakemore, W. F. (2003). Dysfunctional Oligodendrocyte Progenitor Cell (OPC) Populations May Inhibit Repopulation of OPC Depleted Tissue. Journal of Neuroscience Research, 79(3), 787–793.

Choi, I. J., Kim, J. S., Kim, J. M., Jung, H. C., Song, I. S. (2003). Effect of inhibi- tion of extracellular signal-regulated kinase 1 and 2 pathway on apoptosis and bcl-2 expression in Helicobacter pylori-infected AGS cells. Infect Immun 71:830–837

Christen, B., Slack, J. M. (1999). Spatial response to fibroblast growth factor signalling in Xenopus embryos. Development 126: 119–25.

Constantinescu, C. S., Farooqi, N., O'Brien, K., & Gran, B. (2011). Experimental autoimmune encephalomyelitis (EAE) as a model for multiple sclerosis (MS). British Journal of Pharmacology, 164(4), 1079–106.

Corson, L., Yamanaka, Y., Lai, K., Rossant, J. (2003). Spatial and temporal patterns of ERK signaling during mouse embryogenesis. Development 130: 4527–4537.

Corti, S., Locatelli, F., Donadoni, C., Strazzer, S., Salani, S., Del Bo, R., et al. (2002). Neuroectodermal and microglial differentiation of bone marrow cells in the mouse spinal cord and sensory ganglia. *Journal of Neuroscience Research*, *70*(July), 721–733.

Crawford, D. K., Mangiardi, M., Song, B., Patel, R., Du, S., Sofroniew, M. V, et al. (2010). Oestrogen receptor beta ligand: a novel treatment to enhance endogenous functional remyelination. Brain : A Journal of Neurology, 133(10), 2999–3016.

Cross, a H., & Naismith, R. T. (2014). Established and novel disease-modifying treatments in multiple sclerosis. Journal of Internal Medicine, 275(4), 350–63.

Crossley, P.H. & Martin, G.R. (1995). The mouse Fgf8 gene encodes a family of polypeptides and is expressed in regions that direct outgrowth and patterning in the developing embryo. Development 121: 439–451.

Crossley, P.H., Martinez, S., Martin, G.R. (1996). Midbrain development induced by FGF8 in the chick embryo. Nature 380: 66–68.

Cruz-Martinez, P., Martinez-Ferre, A., Jaramillo-Merchán, J., Estirado, A., Martinez, S., & Jones, J. (2014). FGF8 Activates Proliferation and Migration in Mouse Post-Natal Oligodendrocyte Progenitor Cells. PloS One, 9(9), 1-8.

Cruz-Martinez, P., Pastor, D., Estirado, A., Pacheco-Torres, J., Martinez, S., Jones, J. (2014). Stem cell injection in the hindlimb skeletal muscle enhances neurorepair in mice with spinal cord injury. Regenerative medicine *9*, 579–591.

Cuccioli, V., Bueno, C., Belvindrah, R., Lledo, P.-M., & Martinez, S. (2015). Attractive action of FGF-signaling contributes to the postnatal developing hippocampus. *Hippocampus*, *25*(4), 486–499.

Darlington, P.J., Boivin, M.N., Bar-Or, A. (2011). Harnessing the therapeutic potential of mesenchymal stem cells in multiple sclerosis. Expert Rev Neurother. Sep;11(9):1295-303.

De Keyser, J., Laureys, G., Demol, F., Wilczak, N., Mostert, J., & Clinckers, R. (2010). Astrocytes as potential targets to suppress inflammatory demyelinating lesions in multiple sclerosis. *Neurochemistry International*, *57*(4), 446–450.

De Riccardis, L., Rizzello, A., Ferramosca, A., Urso, E., De Robertis, F., Danieli, A., et al. (2015). Bioenergetics profile of CD4+ T cells in relapsing remitting multiple sclerosis subjects. *Journal of Biotechnology*, *202*, 31–39.

Dezawa, M., Takahashi, I., Esaki, M., Takano, M., & Sawada, H. (2001). Sciatic nerve regeneration in rats induced by transplantation of in vitro differentiated bone-marrow stromal cells. European Journal of Neuroscience, 14(11), 1771–1776.

Duncan, I.D., Aguayo, A. J., Bunge, R.P., Wood, P.M. (1981). Transplantation of rat Schwann cells grown in tissue culture into the mouse spinal cord. J. Neurol. Sci. 49, 241–252.

Einstein, O., Fainstein, N., Vaknin, I., Mizrachi-Kol, R., Reihartz, E., Grigoriadis, N. et al. (2007). Neural precursors attenuate autoimmune encephalomyelitis by peripheral immunosuppression. Annals of Neurology, 61(3), 209–18.

Einstein, O., Grigoriadis, N., Mizrachi-Kol, R., Reinhartz, E., Polyzoidou, E., Lavon, I. et al. (2006). Transplanted neural precursor cells reduce brain inflammation to attenuate chronic experimental autoimmune encephalomyelitis. Experimental Neurology, 198(2), 275–84.

El-Akabawy, G., & Rashed, L. A. (2015). Beneficial effects of bone marrow-derived mesenchymal stem cell transplantation in a non-immune model of demyelination. *Annals of Anatomy - Anatomischer Anzeiger*, *198*, 11–20.

Eriksson, A.E., Cousens, L.S., Weaver, L.H., Matthews, B.W. (1991). Three-dimensional structure of human basic fibroblast growth factor. Proc Natl Acad Sci USA 88: 3441–3445.

Fletcher, J. M., Lalor, S. J., Sweeney, C. M., Tubridy, N., & Mills, K. H. G. (2010). T cells in multiple sclerosis and experimental autoimmune encephalomyelitis. Clinical and Experimental Immunology, 162(1), 1–11.

Fortin, D., Rom, E., Sun, H., Yayon, A., Bansal R. (2005). Distinct fibroblast growth factor (FGF)/FGF receptor signaling pairs initiate diverse cellular responses in the oligodendrocyte lineage. J Neurosci 25: 7470–7479.

Franklin, K., & Paxinos, G. (2001). The mouse brain: in stereotaxic coordinates. San Diego: Academic Press.

Franklin, R. J. M., Gilson, J. M., Franceschini, I. A. & Barnett, S. C. (1996). Schwann cell-like myelination following transplantation of an olfactory bulb-ensheathing cell line into areas of demyelination in the adult CNS. Glia 17, 217–224.

Franklin, R. J. M. (2002). Why does remyelination fail in multiple sclerosis? Nature Reviews. Neuroscience, 3(9), 705–14.

Franklin, R. J. M., & Ffrench-Constant, C. (2008). Remyelination in the CNS: from biology to therapy. Nature Reviews. Neuroscience, 9(11), 839–55.

Franklin, R. J. M., & Hinks, G. L. (1999). Mini-Review Understanding CNS Remyelination : Clues From Developmental and Regeneration Biology, 213(July), 207–213.

Franklin, R. J. M., & Kotter, M. R. (2008). The biology of CNS remyelination: the key to therapeutic advances. Journal of Neurology, 255 Suppl , 19–25.

Franklin, R. J. M., ffrench-Constant, C., Edgar, J. M., & Smith, K. J. (2012). Neuroprotection and repair in multiple sclerosis. Nature Reviews. Neurology, 8(11), 624–34.

Frebel, K., Wiese, S. (2006). Signalling molecules essential for neuronal survival and differentiation. Biochem Soc Trans 34:1287–1290

Fressinaud, C., Vallat, J.M., Labourdette, G. (1995). Basic fibroblast growth factor down-regulates myelin basic protein gene expression and alters myelin compaction of mature oligodendrocytes in vitro. J Neurosci Res 40: 285–293.

Friedenstein, A.J., Chailakhjan, R.K., Lalykina, K.S. (1970). The development of fibroblast colonies in monolayer cultures of guinea-pig bone marrow and spleen cells. Cell Tissue Kinet. 3, 393–403.

Friedenstein, A.J., Gorskaj, J.F., Kulagina, N.N. (1976). Fibroblast precur- sors in normal and irradiated mouse hematopoietic organs. Exp. Hematol. 4, 267–274.

Friedenstein, A.J., Petrakova, K.V., Kurolesova, A.I., Frolova, G.P. (1968). Heterotopic of bone marrow. Analysis of precursor cells for osteogenic and hematopoietic tissues. Transplantation 6, 230–247.

Furusho, M., Kaga, Y., Ishii, A., Hebert, J.M., Bansal R. (2011). Fibroblast growth factor signaling is required for the generation of oligodendrocyte progenitors from the embryonic forebrain. J Neurosci 31: 5055–5066.

García-González, D., Murcia-Belmonte, V., Esteban, P. F., Ortega, F., Díaz, D., Sánchez-Vera, I., et al. (2014). Anosmin-1 over-expression increases adult neurogenesis in the subventricular zone and neuroblast migration to the olfactory bulb. *Brain Structure & Function*. doi:10.1007/s00429-014-0904-8

Gerdoni, E., Gallo, B., Casazza, S., Musio, S., Bonanni, I., Pedemonte, E., et al. (2007). Mesenchymal stem cells effectively modulate pathogenic immune response in experimental autoimmune encephalomyelitis. Annals of Neurology, 61(3), 219–27.

Giordano, A., Galderisi, U., & Marino, I. R. (2007). From the laboratory bench to the patient´s bedside: and update on clinical trials with mesenchymal stem cells. *Journal of Cellular Physiology*, 211, 27-35.

Goebbels, S., Oltrogge, J. H., Kemper, R., Heilmann, I., Bormuth, I., Wolfer, S., Wichert, S. P., Möbius, W., Liu, X., Lappe-Siefke, C., Rossner, M.J., Groszer, M., Suter, U., Frahm, J., Boretius, S., Nave, K. A. (2010) Elevated phosphatidylinositol 3,4,5-trisphosphate in glia triggers cell-autonomous membrane wrapping and myelination. J Neurosci. Jun 30;30(26):8953-64

Goldenberg, M. M. (2012). Multiple sclerosis review. P & T : A Peer-Reviewed Journal for Formulary Management, 37(3), 175–84.

Gonzalez-Perez, O., & Alvarez-Buylla, A. (2011). Oligodendrogenesis in the subventricular zone and the role of epidermal growth factor. Brain Research Reviews, 67(1-2), 147–56.

Gordon, D., Pavlovska, G., Glover, C.P., Uney, J.B., Wraith, D., Scolding, N.J. (2008) Human mesenchymal stem cells abrogate experimental allergic encephalomyelitis

after intraperitoneal injection, and with sparse CNS infi ltration. Neurosci Lett 448: 71-3.

Gordon, D., Pavlovska, G., Uney, J.B., Wraith, D., Scolding, N.J. (2010) Human Mesenchymal Stem Cells Infiltrate the Spinal Cord, Reduce Demyelination, and Localize to White Matter Lesions in Experimental Autoimmune Encephalomyelitis. J Neuropathol Exp Neurol.

Goridis, C., & Rohrer, H. (2002). Specification of catecholaminergic and serotonergic neurons. Nature Reviews Neuroscience 3: 531-541.

Gotoh, N. (2008) Regulation of growth factor signaling by FRS2 family docking/ scaffold adaptor proteins. Cancer Sci 99: 1319–1325.

Graeber, M.B., Li, W., & Rodriguez, M.L. (2011). Role of microglia in CNS inflammation. FEBS Lett 585, 3798-3805.

Greer, J. M. (2013). Autoimmune T-cell reactivity to myelin proteolipids and glycolipids in multiple sclerosis. Multiple Sclerosis International, 2013, 151427.

Griffiths, I., Klugmann, M., Anderson, T., Yool, D., Thomson, C., Schwab, M.H., Schneider, A., Zimmermann, F., McCulloch, M., Nadon, N., et al. (1998). Axonal swellings and degeneration in mice lacking the major proteolipid of myelin. Science 280, 1610-1613.

Grinspan, J.B., Stern, J.L., Franceschini, B., Pleasure, D. (1993). Trophic effects of basic fibroblast growth factor (bFGF) on differentiated oligodendroglia: a mechanism for regeneration of the oligodendroglial lineage. J Neurosci Res 36: 672–680.

Groebe, A., Clarner, T., Baumgartner, W., Dang, J., Beyer, C., & Kipp, M. (2009). Cuprizone treatment induces distinct demyelination, astrocytosis, and microglia cell invasion or proliferation in the mouse cerebellum. Cerebellum (London, England), 8(3), 163–74.

Groves, A. K. et al. (1993). Repair of demyelinated lesions by transplantation of purified O-2A progenitor cells. Nature 362, 453–455.

Gudi, V., Gingele, S., Skripuletz, T., & Stangel, M. (2014). Glial response during cuprizone-induced de- and remyelination in the CNS: lessons learned. Frontiers in Cellular Neuroscience, 8(March), 73.

Hammang, J. P., Archer, D. R. & Duncan, I. D. (1997). Myelination following transplantation of EGF- responsive neural stem cells into a myelin-deficient environment. Exp. Neurol. 147, 84–95.

Hardy, R. & Reynolds, R. (1991). Proliferation and differentiation potential of rat forebrain oligodendroglial progenitors both in vitro and in vivo. Development 111: 1061–1080.

Hartline, D.K., & Colman, D.R. (2007). Rapid conduction and the evolution of giant axons and myelinated fibers. Current biology : CB 17, R29-35.

Hawkins, P. T., Anderson, K. E., Davidson, K., Stephens, L. R. (2006) Signalling through Class I PI3Ks in mammalian cells. Biochem Soc Trans 34:647–662

Hayley, S., Poulter, M.O., Merali, Z., Anisman, H. (2005). The pathogenesis of clinical depression: stressor- and cytokine-induced alterations of neuroplasticity. Neuroscience 135:659–678

He, Q., Wan, C., & Li, G. (2007). Concise review: multipotent mesenchymal stromal cells in blood. *Stem Cells*, *25*, 69–77.

Hibbits, N., Pannu, R., Wu, T. J., Armstrong, R. C. (2009). Cuprizone demyelination of the corpus callosum in mice correlates with altered social interaction and impaired bilateral sensorimotor coordination. ASN Neuro, 1(3), 153–164.

Hofstetter, C. P., Schwarz, E. J., Hess, D., Widenfalk, J., El Manira, a, Prockop, D. J., & Olson, L. (2002). Marrow stromal cells form guiding strands in the injured spinal cord and promote recovery. Proceedings of the National Academy of Sciences of the United States of America, 99(4), 2199–204.

Homs, J., Pagès, G., Ariza, L., Casas, C., Chillón, M., Navarro, X., & Bosch, A. (2014). Intrathecal administration of IGF-I by AAVrh10 improves sensory and motor deficits in a mouse model of diabetic neuropathy. Molecular Therapy — Methods & Clinical Development, 1(November 2013), 7.

Honmou, O., Felts, P. A., Waxman, S. G. & Kocsis, J. D. (1996). Restoration of normal conduction properties in demyelinated spinal cord axons in the adult rat by transplantation of exogenous Schwann cells. J. Neurosci. 16, 3199–3208.

Hu, J.-G., Wang, Y.-X., Wang, H.-J., Bao, M.-S., Wang, Z.-H., Ge, X., et al. (2012). PDGF-AA mediates B104CM-induced oligodendrocyte precursor cell differentiation of embryonic neural stem cells through Erk, PI3K, and p38 signaling. *Journal of Molecular Neuroscience : MN*, *46*(3), 644–53.

Hu, X., & Beeton, C. (2010). Detection of functional matrix metalloproteinases by zymography. *Journal of Visualized Experiments : JoVE*, (November), 1–5.

Hutton, S. R. & L, H, Pevny. (2008). Isolation, Culture, and Differentiation of Progenitor Cells from the Central Nervous System. Cold Spring Harbor Protocols , 11: 5077.

Imaizumi, T., Lankford, K. L., Waxman, S. G., Greer, C. A. & Kocsis, J. D. (1998). Transplanted olfactory ensheathing cells remyelinate and enhance axonal conduction in the demyelinated dorsal columns of the rat spinal cord. J. Neurosci. 18, 6176–6185.

Irvine, K. A., & Blakemore, W. F. (2008). Remyelination protects axons from demyelination-associated axon degeneration, 1464–1477.

Ishii, A., Furusho, M., Bansal, R. (2013). Sustained activation of ERK1/2 MAPK in oligodendrocytes and schwann cells enhances myelin growth and stimulates oligodendrocyte progenitor expansion. J Neurosci 33: 175–186.

Itoh, N., Ornitz, D.M. (2004). Evolution of the FGF and FGFR gene families. Trends in Genetics 20: 563–569.

Jadasz, J. J., Aigner, L., Rivera, F. J., Küry, P. (2012). The remyelination Philosopher's Stone: stem and progenitor cell therapies for multiple sclerosis. Cell and Tissue Research, 349(1), 331–47.

Jaramillo-Merchán, J., Jones, J., Ivorra, J. L., Pastor, D., Viso-León, M. C., Armengól, J. A., et al. (2013). Mesenchymal stromal-cell transplants induce oligodendrocyte progenitor migration and remyelination in a chronic demyelination model. Cell Death & Disease, 4, e779.

Javazon, E. H., Beggs, K. J., & Flake, A. W. (2004). Mesenchymal stem cells: Paradoxes of passaging. *Experimental Hematology*, *32*, 414–425.

Jones, J., Estirado, A., Redondo, C., Pacheco-Torres, J., Sirerol-Piquer, M.-S., Garcia-Verdugo, J. M., & Martinez, S. (2014). Mesenchymal Stem Cells Improve Motor Functions and Decrease Neurodegeneration in Ataxic Mice. *Molecular Therapy*, *23*(1), 130–138

Jones, J., Estirado, A., Redondo, C., Bueno, C., Martinez, S. (2012). Human adipose stem cellconditioned medium increases survival of Friedreich's ataxia cells submitted to oxidative stress. Stem Cells Dev. 21(15), pp. 2817-2826.

Jones, J., Jaramillo-Merchán, J., Bueno, C., Pastor, D., Viso-León, M., & Martínez, S. (2010). Mesenchymal stem cells rescue Purkinje cells and improve motor functions in a mouse model of cerebellar ataxia. Neurobiology of Disease, 40(2), 415–23.

Kandel, E. R., J. H. Schwartz, & T. M. Jessell. (2000). Principles of neural science. New York: McGraw- Hill, Health Professions Division.

Kassis, I., Grigoriadis, N., Gowda-Kurkalli, B., Mizrachi-Kol, R., Ben-Hur, T., Slavin, S., et al. (2008). Neuroprotection and immunomodulation with mesenchymal stem cells in chronic experimental autoimmune encephalomyelitis. Archives of Neurology, 65(6), 753–61.

Kean, T. J., Lin, P., Caplan, A. I., & Dennis, J. E. (2013). MSCs: Delivery Routes and Engraftment, Cell-Targeting Strategies, and Immune Modulation. Stem Cells International, 2013, 732742.

Kelly, A., Lynch, M. A. (2000). Long-term potentiation in dentate gyrus of the rat is inhibited by the phosphoinositide 3-kinase inhibitor, wortmannin. Neuropharmacology 39:643–651

Kemp, K., Gordon, D., Wraith, D. C., Mallam, E., Hartfield, E., Uney, J., et al. (2011). Fusion between human mesenchymal stem cells and rodent cerebellar Purkinje cells. Neuropathology and Applied Neurobiology, 37(2), 166–78.

Kessaris, N., Fogarty, M., Iannarelli, P., Grist, M., Wegner, M., Richardson, W. D. (2005). Competing waves of oligodendrocytes in the forebrain and postnatal elimination of an embryonic lineage, (December), 1–7.

Kimberlin, R. H., Collis, S. C., Walker, C. A. (1976). Profiles of brain glycosidase activity in cuprizone-fed Syrian hamsters and in scrapie-affected mice, rats, Chinese hamsters and Syrian hamsters. J. Comp. Pathol. 86, 135–142

Kipp, M., Clarner, T., Dang, J., Copray, S., Beyer, C. (2009). The cuprizone animal model: new insights into an old story. Acta Neuropathologica, 118(6), 723–36.

Kondo, A., Nakano, T., Suzuki, K. (1987). Blood-brain barrier permeability to horseradish peroxidase in twitcher and cuprizone-intoxicated mice. Brain Res 425: 186-190.

Kotter, M. R., Li, W.-W., Zhao, C., Franklin, R. J. M. (2006). Myelin impairs CNS remyelination by inhibiting oligodendrocyte precursor cell differentiation. The Journal of Neuroscience : The Official Journal of the Society for Neuroscience, 26(1), 328–32.

Kouhara, H., Koga, M., Kasayama, S., Tanaka, A., Kishimoto, T., et al. (1994). Transforming activity of a newly cloned androgen-induced growth factor Oncogene 9: 455–462.

Krampera, M., Marconi, S., Pasini, A., Galiè, M., Rigotti, G., Mosna, F. et al., (2007). Induction of neural-like differentiation in human mesenchymal stem cells derived from bone marrow, fat, spleen and thymus. Bone, 40(2), 382–90.

Lachapelle, F., Gumpel, M., Baulac, M., Jacque, C., Duc, P., Baumann, N. (1984). Transplantation of CNS fragments into brain of shiverer mutant mice: extensive myelination by implanted oligodendrocytes. I. Immunohistochemical studies. Dev. Neurosci. 6, 325–334.

Lanza, C., Morando, S., Voci, A., Canesi, L., Principato, M. C., Serpero, L. D., et el. (2009). Neuroprotective mesenchymal stem cells are endowed with a potent antioxidant effect in vivo. Journal of Neurochemistry, 110(5), 1674–84.

Lee, X., Yang, Z., Shao, Z., Rosenberg, S.S., Levesque, M., et al. (2007). NGF regulates the expression of axonal LINGO-1 to inhibit oligodendrocyte differentiation and myelination. J Neurosci 27: 220–225.

Leevers, S. J., Vanhaesebroeck, B., Waterfield, M. D. (1999). Signalling through phosphoinositide 3-kinases: the lipids take centre stage. Curr Opin Cell Biol 11:219–225

Levine, J.M., Reynolds, R., & Fawcett, J.W. (2001). The oligodendrocyte precursor cell in health and disease. Trends Neurosci 24, 39-47.

Lindvall, O., & Kokaia, Z. (2010). Review series Stem cells in human neurodegenerative disorders — time for clinical translation?, 120(1).

Love, S. (1988). Cuprizone neurotoxicity in the rat: morphologic observations. J. Neurol. Sci. 84, 223–237 10.1016/0022-510X(88)90127-X

Love, S. (2006). Demyelinating diseases. Journal of Clinical Pathology, 59(11), 1151–9.

Lu, P., Jones, L. L., & Tuszynski, M. H. (2005). BDNF-expressing marrow stromal cells support extensive axonal growth at sites of spinal cord injury. Experimental Neurology, 191(2), 344–60.

Lu, Z., Hu, X., Zhu, C., Wang, D., Zheng, X., & Liu, Q. (2009). Overexpression of CNTF in Mesenchymal Stem Cells reduces demyelination and induces clinical recovery in experimental autoimmune encephalomyelitis mice. Journal of Neuroimmunology, 206(1-2), 58–69.

Lubetzki, C., Demerens, C., Zalc, B. (1997). Signaux axonaux et myelino- genese dans le systeme nerveux central. Medecine/Sciences 13: 1097–1105.

Lublin FD, Reingold SC. Defining the clinical course of multiple sclerosis: results of an international survey. Neurology 1996;46:907–911.

Lucchinetti, C., Bru, W., Parisi, J., Scheithauer, B., Rodriguez, M., Lassmann, H. (1999). A quantitative analysis of oligodendrocytes in multiple sclerosis lesions A study of 113 cases, 2279–2295.

Lucchinetti, C., Brück, W., Parisi, J., Scheithauer, B., Rodriguez, M., Lassmann, H. (2000). Heterogeneity of multiple sclerosis lesions: implications for the pathogenesis of demyelination. Annals of Neurology, 47(6), 707–17.

Lunn, J.S., Fishwick, K.J., Halley, P.A., Storey, K.G. (2007). A spatial and temporal map of FGF/Erk1/2 activity and response repertoires in the early chick embryo. Dev Biol 302: 536–552

Macarthur, C. A., Lawshé, A., Xu, J., Santos-ocampo, S., Heikinheimo, M., Chellaiah, A. T., Ornitz, D. M. (1995). FGF-8 isoforms activate receptor splice forms that are expressed in mesenchymal regions of mouse development, 3613, 3603–3613.

Mahad, D., Ziabreva, I., Lassmann, H., Turnbull, D. (2008). Mitochondrial defects in acute multiple sclerosis lesions. Brain : A Journal of Neurology, 131(Pt 7), 1722–35.

Maki, T., Liang, A. C., Miyamoto, N., Lo, E. H., Arai, K. (2013). Mechanisms of oligodendrocyte regeneration from ventricular-subventricular zone-derived progenitor cells in white matter diseases. Frontiers in Cellular Neuroscience, 7(December), 275.

Martinez-Ferre, A., Martinez, S. (2009). The development of the thalamic motor learning area is regulated by Fgf8 expression. J Neurosci 29: 13389–13400.

McKernan, R., McNeish, J., Smith, D. (2010). Pharma's developing interest in stem cells. Cell Stem Cell, 6(6), 517–20.

McKinnon, R.D., Matsui, T., Dubois-Dalcq, M., Aaronson, S.A. (1990). FGF modulates the PDGF-driven pathway of oligodendrocyte development. Neuron 5: 603–614.

Meirelles, L. D. S., Fontes, A. M., Covas, D. T., Caplan, A. I. (2009). Mechanisms involved in the therapeutic properties of mesenchymal stem cells. Cytokine & Growth Factor Reviews, 20(5-6), 419–27.

Menn, B., Garcia-Verdugo, J. M., Yaschine, C., Gonzalez-Perez, O., Rowitch, D., Alvarez-Buylla, A. (2006). Origin of oligodendrocytes in the subventricular zone of the adult brain. The Journal of Neuroscience : The Official Journal of the Society for Neuroscience, 26(30), 7907–18.

Miller, D., Barkhof, F., Montalban, X., Thompson, A., Filippi, M. (2005). Clinically isolated syndromes suggestive of multiple sclerosis, part I: natural history, pathogenesis, diagnosis, and prognosis. The Lancet. Neurology, 4(5), 281–8.

Miller, R. H., & Mi, S. (2007). Dissecting demyelination. Nature Neuroscience, 10(11), 1351–4.

Miller, R.H. & Fyffe-Maricich, S.L. (2010). Restoring the balance between disease and repair in multiple sclerosis: insights from mouse models. Dis. Model. Mech. 3, 535–539.

Miller, S. D., Karpus, W. J., Davidson, T. S. (2010). Experimental autoimmune encephalomyelitis in the mouse. Current Protocols in Immunology / Edited by John E. Coligan., et al. Chapter 15(3), Unit 15.1.

Miller, S. D., Vanderlugt, C. L., Begolka, W. S., Pao, W., Yauch, R. L., Neville, K. L., Katz-Levy, Y., Carrizosa, A., Kim, B. S. (1997). Persistent infection with Theiler's virus leads to CNS autoimmunity via epitope spreading. Nat. Med. 3, 1133–1136.

Milo, R., & Miller, A. (2014). Revised diagnostic criteria of multiple sclerosis. Autoimmunity Reviews, 13(4-5), 518–24.

Ming, G.-L., & Song, H. (2011). Adult neurogenesis in the mammalian brain: significant answers and significant questions. Neuron, 70(4), 687–702.

Miron, V., Cuo, Q., Wegner, C., Antel, J., Bru, W. (2008). Differentiation block of oligodendroglial progenitor cells as a cause for remyelination failure in chronic multiple sclerosis.

Mitew, S., Hay, C.M., Peckham, H., Xiao, J., Koenning, M., et al. (2013). Mechanisms regulating the development of oligodendrocytes and central nervous system myelin. Neuroscience.

Mnguell, J.J., Erices, A., Conget, P. (2001). Mesenchymal stem cells. Exp Biol Med (Maywood) 226: 507-20.

Mohammadi, M., Olsen, S.K., Ibrahimi, O.A. (2005). Structural basis for fibroblast growth factor receptor activation. Cytokine Growth Factor Rev 16: 107–137.

Moore, C. S., Abdullah, S. L., Brown, A., Arulpragasam, A., & Crocker, S. J. (2011). How factors secreted from astrocytes impact myelin repair. *Journal of Neuroscience Research*, *89*, 13–21.

Morello, N., Bianchi, FT., Marmiroli, P., Tonoli, E., Rodriguez Menendez, V., et al. (2011). A role for hemopexin in oligodendrocyte differentiation and myelin formation. PLOS One 6: e20173.

Moyon, S., Dubessy, a. L., Aigrot, M. S., Trotter, M., Huang, J. K., Dauphinot, L., et al. (2015). Demyelination Causes Adult CNS Progenitors to Revert to an Immature State and Express Immune Cues That Support Their Migration. *Journal of Neuroscience*, *35*(1), 4–20.

Nair, a., Frederick, T. J., & Miller, S. D. (2008). Astrocytes in multiple sclerosis: A product of their environment. *Cellular and Molecular Life Sciences*, *65*, 2702–2720.

Nakamura, H., Sato, T., Suzuki-Hirano, A. (2008). Isthmus organizer for mesencephalon and metencephalon. Dev Growth Differ 50: S113–118.

Nave, K.A., & Trapp, B.D. (2008). Axon-glial signaling and the glial support of axon function. Annu Rev Neurosci 31, 535-561.

Nessler, J., Bénardais, K., Gudi, V., Hoffmann, A., Salinas Tejedor, L., Janßen, S., et al. (2013). Effects of murine and human bone marrow-derived mesenchymal stem cells on cuprizone induced demyelination. *PloS One*, *8*(7), e69795.

Neuhuber, B., Timothy Himes, B., Shumsky, J. S., Gallo, G., & Fischer, I. (2005). Axon growth and recovery of function supported by human bone marrow stromal cells in the injured spinal cord exhibit donor variations. Brain Research, 1035(1), 73–85.

Nistor, G. I., Totoiu, M. O., Haque, N., Carpenter, M. K. & Keirstead, H. S. (2005). Human embryonic stem cells differentiate into oligodendrocytes in high purity and myelinate after spinal cord transplantation. Glia 49, 385–396.

Nylander, A., & Hafler, D. A. (2012). Review series Multiple sclerosis, 122(4).

Ornitz, D.M., Xu, J., Colvin, J.S., McEwen, D.G., MacArthur, C.A., et al. (1996). Receptor specificity of the fibroblast growth factor family. J Biol Chem 271: 15292–15297.

Owen-Lynch PJ, Draper CE, Mashayekhi F, Bannister CM, Miyan JA. (2003). Defective cell cycle control underlies abnormal cortical development in the hydrocephalic Texas rat. Brain 126:623–31.

Ozturk, A., Smith, S.A, Gordon-Lipkin, E.M., Harrison, D.M., Shiee, N., Pham, D.L., et al. (2011). MRI of the corpus callosum in multiple sclerosis: association with disability. Mult Scler 16: 166–77.

Parazzini, C., Baldoli, C., Scotti, G., and Triulzi, F. (2002). Terminal zones of myelination: MR evaluation of children aged 20-40 months. AJNR American journal of neuroradiology 23, 1669-1673.

Parmar, M., & Li, M. (2007). Early specification of dopaminergic phenotype during ES cell differentiation. BMC Developmental Biology, 7, 86.

Partanen, J. (2007). FGF signalling pathways in development of the midbrain and anterior hindbrain. J Neurochem 101: 1185–1193.

Pastor, D., Viso-León, M. C., Jones, J., Jaramillo-Merchán, J., Toledo-Aral, J. J., Moraleda, J. M., & Martínez, S. (2012). Comparative effects between bone marrow and mesenchymal stem cell transplantation in GDNF expression and motor function recovery in a motorneuron degenerative mouse model. Stem Cell Reviews, 8(2), 445–58.

Paul, G., & Anisimov, S. V. (2013). The secretome of mesenchymal stem cells: potential implications for neuroregeneration. Biochimie, 95(12), 2246–56.

Pernet, V., Hauswirth, W. W., Di Polo, A. (2005). Extracellular signal-regulated kinase 1/2 mediates survival, but not axon regeneration, of adult injured central nervous system neurons in vivo. J Neurochem 93: 72–83.

Peters, A., Palay, S. L., & Webster, H. D. (1991). The Fine Structure ofthe Nervous System: Neurons and their Supporting Cells (New York, Oxford University Press).

Polito, A., & Reynolds, R. (2005). NG2-expressing cells as oligodendrocyte progenitors in the normal and demyelinated adult central nervous system, 707–716.

Purves, D., Augustine, G.J., Fitzpatrick, D., et al. (2001). Increased Conduction Velocity as a Result of Myelination.Neuroscience. 2nd edition. Sunderland (MA): Sinauer Associates.

Rafei, M., Birman, E., Forner, K., & Galipeau, J. (2009). Allogeneic mesenchymal stem cells for treatment of experimental autoimmune encephalomyelitis. Molecular Therapy : The Journal of the American Society of Gene Therapy, 17(10), 1799–803.

Rafei, M., Campeau, P. M., Aguilar-Mahecha, A., Buchanan, M., Williams, P., Birman, E., et al. (2009). Mesenchymal stromal cells ameliorate experimental autoimmune encephalomyelitis by inhibiting CD4 Th17 T cells in a CC chemokine ligand 2-dependent manner. Journal of Immunology (Baltimore, Md. : 1950), 182(10), 5994–6002.

Ramon y Cajal, S. (1913). Estudios sobre la degeneración y regeneración del sistema nervioso. Vol. 1. Madrid: Moya.

Ramon y Cajal, S. (1913). Contribucion al conocimiento de la neuroglia del cerebro humano. Trab Lab Invest Biol (Madrid) 11: 255–315.

Ranganath, S. H., Levy, O., Inamdar, M. S., Karp, J. M. (2012). Harnessing the mesenchymal stem cell secretome for the treatment of cardiovascular disease. Cell Stem Cell, 10(3), 244–58.

Ransohoff, R. M. (2012). Animal models of multiple sclerosis: the good, the bad and the bottom line. Nature Neuroscience, 15(8), 1074–7.

Raymond, C. R., Redman, S. J., Crouch, M. F. (2002). The phosphoinositide 3- kinase and p70 S6 kinase regulate long-term potentiation in hippocampal neurons. Neuroscience 109:531–536

Reifers, F., Böhli, H., Walsh, E.C., Crossley, P.H., Stainier D.Y., et al. (1998). Fgf8 is mutated in zebrafish acerebellar (ace) mutants and is required for maintenance of midbrain-hindbrain boundary development and somitogenesis. Development 125: 2381–2395.

Renault-Mihara, F., Okada, S., Shibata, S., Nakamura, M., Toyama, Y., Okano, H. (2008) Spinal cord injury: Emerging beneficial role of reactive astrocytes' migration. Int. J. Biochem. Cell Biol. 40, 1649–1653.

Rio Hortega, D. P. (1928). Tercera aportacion al conocimiento morfologico e interpretacion funcional de la oligodendroglia. Memor Real Soc Esp Hist Nat 14: 5–122.

Rivera-Quiñones, C., McGavern, D., Schmelzer, J.D., Hunter, S.F., Low, P.A., Rodriguez, M. (1998). Absence of neurological deficits following extensive demyelination in a class I–deficient murine model of multiple sclerosis. Nat. Med. 4, 187–193.

Rivera, F. J., Aigner, L. (2012). Adult mesenchymal stem cell therapy for myelin repair in multiple sclerosis. Biological Research, 45(3), 257–68.

Rivera, F. J., Couillard-Despres, S., Pedre, X., Ploetz, S., Caioni, M., Lois, C. et al. (2006). Mesenchymal stem cells instruct oligodendrogenic fate decision on adult neural stem cells. Stem Cells (Dayton, Ohio), 24(10), 2209–19.

Rivera, F. J., Kandasamy, M., Couillard-Despres, S., Caioni, M., Sanchez, R., Huber, C. et al. (2008). Oligodendrogenesis of adult neural progenitors: differential effects of ciliary neurotrophic factor and mesenchymal stem cell derived factors. Journal of Neurochemistry, 107(3), 832–43.

Rocca, M. a, Anzalone, N., Falini, A, Filippi, M. (2013). Contribution of magnetic resonance imaging to the diagnosis and monitoring of multiple sclerosis. La Radiologia Medica, 118(2), 251–64.

Rubinfeld, H., Seger, R. (2004). The ERK cascade as a prototype of MAPK signaling pathways. MAP Kinase Signaling Protocols. 1–28.

Sanna, P. P., Cammalleri, M., Berton, F., Simpson, C., Lutjens, R., Bloom, F.E., Francesconi, W. (2002). Phosphatidylinositol 3-kinase is required for the expression but not for the induction or the maintenance of long-term potentiation in the hippocampal CA1 region. J Neuro- sci 22:3359–3365

Salem, H. K., & Thiemermann, C. (2010). Mesenchymal stromal cells: current understanding and clinical status. Stem Cells (Dayton, Ohio), 28(3), 585–96.

Sawamoto K,Wichterle H, Gonzalez-Perez O, Cholfin JA, Yamada M, Spassky N, et al. New neurons follow the flow of cerebrospinal fluid in the adult brain. Science 2006;311:629–32.

Sheehan, D., Hrapchak, B. (1980). Theory and Practice of Histotechnology. 2nd ed. Columbus, OH, Battelle Press.

Sim, F. J., Zhao, C., Penderis, J., Franklin, R. J. M. (2002). The age-related decrease in CNS remyelination efficiency is attributable to an impairment of both oligodendrocyte progenitor recruitment and differentiation. The Journal of Neuroscience : The Official Journal of the Society for Neuroscience, 22(7), 2451–9.

Skripuletz, T., Hackstette, D., Bauer, K., Gudi, V., Pul, R., Voss, E., et al. (2013). Astrocytes regulate myelin clearance through recruitment of microglia during cuprizone-induced demyelination. *Brain*, *136*(2012), 147–167.

Skripuletz, T., Bussmann, J. H., Gudi, V., Koutsoudaki, P. N., Pul, R., Moharregh-Khiabani, D., et al. (2010a). Cerebellar cortical demyelination in the murine cuprizone model. Brain Pathol. 20, 301–312

Skripuletz, T., Lindner, M., Kotsiari, A., Garde, N., Fokuhl, J., Linsmeier, F., et al. (2008). Cortical demyelination is prominent in the murine cuprizone model and is strain-dependent. The American Journal of Pathology, 172(4), 1053–61.

Steelman, A. J., Thompson, J. P., & Li, J. (2012). Demyelination and remyelination in anatomically distinct regions of the corpus callosum following cuprizone intoxication. Neuroscience Research, 72(1), 32–42.

Steinman, L. (1996). Multiple Sclerosis : A Coordinated Immunological Attack against Myelin in the Central Nervous System, 85, 299–302.

Stidworthy, M. F., Genoud, S., Suter, U., Mantei, N., Franklin, R. J. (2003). Quantifying the early stages of remyelination following cuprizone-induced demyelination. Brain Pathol. 13, 329–339

Storm, E.E., Garel, S., Borello, U., Hebert, J.M., Martinez, S., et al. (2006). Dose-dependent functions of Fgf8 in regulating telencephalic patterning centers. Development 133: 1831–1844.

Tanaka, A., & Takeda, M. (1992). Cloning and characterization of an androgen-induced growth factor essential for the androgen-dependent growth of mouse mammary carcinoma cells, 89(October), 8928–8932.

Tanuma, N., Sakuma, H., Sasaki, A., & Matsumoto, Y. (2006). Chemokine expression by astrocytes plays a role in microglia/macrophage activation and subsequent neurodegeneration in secondary progressive multiple sclerosis. *Acta Neuropathologica*, *112*, 195–204.

Thisse, B., & Thisse, C. (2005). Functions and regulations of fibroblast growth factor signaling during embryonic development. Developmental Biology, 287(2), 390–402.

Tong, C. K., Han, Y.-G., Shah, J. K., Obernier, K., Guinto, C. D., & Alvarez-Buylla, A. (2014). Primary cilia are required in a unique subpopulation of neural progenitors. *Proceedings of the National Academy of Sciences of the United States of America*, *111*(34), 1–6. doi:10.1073/pnas.1321425111

Tramontin AD,Garcia-Verdugo JM, LimDA, Alvarez-Buylla A. (2003). Postnatal development of radial glia and the ventricular zone (VZ): a continuum of the neural stem cell compartment. Cereb Cortex,13:580–7.

Tsang, M., Dawid, I.B. (2004). Promotion and attenuation of FGF signaling through the Ras-MAPK pathway. Sci STKE 228: pe17.

Turner, N., Grose, R. (2010). Fibroblast growth factor signalling: from development to cancer. Nature Rev Cancer 10: 116–129

Vernerey, J., Macchi, M., Magalon, K., Cayre, M., Durbec, P. (2013). Ciliary neurotrophic factor controls progenitor migration during remyelination in the adult rodent brain. J Neuroscience 33: 3240–3250

Vincze, A., Mazlo, M., Seress, L., Komoly, S., and Abraham, H. (2008). A correlative light and electron microscopic study of postnatal myelination in the murine corpus callosum. Int J Dev Neurosci 26, 575- 584.

Virchow, R. (1846). Ueber das granulirte Aussehen der Wandungen der Gehirnventrikel. Allg Z Psychiat 3: 242–250.

Vitry, S., Bertrand, J. Y., Cumano, A., & Dubois-Dalcq, M. (2003). Primordial hematopoietic stem cells generate microglia but not myelin-forming cells in a neural environment. *The Journal of Neuroscience : The Official Journal of the Society for Neuroscience*, *23*(33), 10724–10731.

Wachs, F.-P., Couillard-Despres, S., Engelhardt, M., Wilhelm, D., Ploetz, S., Vroemen, M., et al. (2003). High Efficacy of Clonal Growth and Expansion of Adult Neural Stem Cells. Laboratory Investigation, 83(7), 949–962.

Waksman, B. H. (1999). Demyelinating disease: evolution of a paradigm. Neurochemical Research, 24(4), 491–5.

Wang, S., Bates, J., Li, X., Schanz, S., Chandler-Militello, D., Levine, C. et al. (2013). Human iPSC-Derived Oligodendrocyte Progenitor Cells Can Myelinate and Rescue a Mouse Model of Congenital Hypomyelination. Cell Stem Cell, 12(2), 252–64.

Wang, X., Li, X., Wang, K., Zhou, H., Xue, B., Li, L., Wang, X. (2004). Forskolin cooperating with growth factor on generation of dopaminergic neurons from human fetal mesencephalic neural progenitor cells. Neuroscience Letters, 362(2), 117–21.

Wang, Z., Colognato, H., Ffrench-constant, C. (2007). Contrasting Effects of Mitogenic Growth Factors on Myelination in Neuron – Oligodendrocyte Co-cultures, 545(December 2006), 537–545.

Warlop, N. P., Fieremans, E., Achten, E., Debruyne, J., & Vingerhoets, G. (2008). Callosal function in MS patients with mild and severe callosal damage as reflected by diffusion tensor imaging. Brain Research, 1226, 218–25.

Waxman, S. G. (1997). Axon-glia interactions: building a smart nerve fiber. CUff BioI 7, R406-410.

Willenbrock, S., Knippenberg, S., Meier, M., Hass, R., Wefstaedt, P., Nolte, I et al. (2012). In vivo MRI of intraspinally injected SPIO-labelled human CD34+ cells in a transgenic mouse model of ALS. In Vivo 26: 31–38.

Williams, A., Piaton, G., Lubetzki C. (2007) Astrocytes—friends or foes in multiple sclerosis? Glia; 55: 1300–12.

Williams, A., Petermann, F., Zalc, B., Lubetzki, C., Curie, M. (2007). Semaphorin 3A and 3F : key players in myelin repair in multiple sclerosis?, 2554–2565.

Windrem, M. S., Roy, N. S., Wang, J., Nunes, M., Benraiss, A., Goodman, R. et al., (2002). Progenitor cells derived from the adult human subcortical white matter disperse and differentiate as oligodendrocytes within demyelinated lesions of the rat brain. Journal of Neuroscience Research, 69(6), 966–75.

Windrem, M. S. et al. (2004). Fetal and adult human oligodendrocyte progenitor cell isolates myelinate the congenitally dysmyelinated brain. Nature Med. 10, 93–97.

Wingerchuk, D. M., & Carter, J. L. (2014). Multiple sclerosis: current and emerging disease-modifying therapies and treatment strategies. Mayo Clinic Proceedings, 89(2), 225–40.

Xiao J, Ferner AH, Wong AW, Denham M, Kilpatrick TJ, et al. (2012) Extracellular signal-regulated kinase 1/2 signaling promotes oligodendrocyte myelination in vitro. J Neurochem 122: 1167–1180.

Yang, Z., Watanabe, M., Nishiyama, A. (2005). Optimization of oligodendrocyte progenitor cell culture method for enhanced survival. J Neurosci Methods 149: 50–56.

Yednock, T.A., Cannon, C., Fritz, L.C., Sanchez-Madrid, F., Steinman, L., Karin, N. (1992). Prevention of experimental autoimmune encephalomyelitis by antibodies against α 4 1 integrin. Nature 356, 63–66.

Younes-Rapozo V, Felgueiras LO, Viana NL, Fierro IM, Barja-Fidalgo C, et al. (2009). A role for the MAPK/ERK pathway in oligodendroglial differentiation in vitro: stage specific effects on cell branching. Int J Dev Neurosci 27: 757–768.

Zappia, E., Casazza, S., Pedemonte, E., Benvenuto, F., Bonanni, I., Gerdoni, E., et al. (2005). Mesenchymal stem cells ameliorate experimental autoimmune encephalomyelitis inducing T-cell anergy. Blood, 106(5), 1755–61.

Zhang, J., Brodie, C., Li, Y., Zheng, X., Roberts, C., Lu, M., et al. (2009). Bone marrow stromal cell therapy reduces proNGF and p75 expression in mice with experimental autoimmune encephalomyelitis. Journal of the Neurological Sciences, 279(1-2), 30–8.

Zhang, S. C., Ge, B. & Duncan, I. D. Adult brain retains the potential to generate oligodendroglial progenitors with extensive myelination capacity. Proc. Natl Acad. Sci. USA 96, 4089–4094 (1999)

Zhang, J., Li, Y., Chen, J., Cui, Y., Lu, M., Elias, S. B., et al. (2005). Human bone marrow stromal cell treatment improves neurological functional recovery in EAE mice. Experimental Neurology, 195(1), 16–26.

Zhang, J., Li, Y., Lu, M., Cui, Y., Chen, J., Noffsinger, L., et al. (2006). Bone marrow stromal cells reduce axonal loss in experimental autoimmune encephalomyelitis mice. Journal of Neuroscience Research, 84(3), 587–95.

Zhou, C.-J., Pinson, K. I., Pleasure, S. J. (2004). Severe defects in dorsal thalamic development in low-density lipoprotein receptor-related protein-6 mutants. The Journal of Neuroscience : The Official Journal of the Society for Neuroscience, 24(35), 7632–9.

Zimmerlin, L., Park, T. S., Zambidis, E. T., Donnenberg, V. S., Donnenberg, A. D. (2013). Mesenchymal stem cell secretome and regenerative therapy after cancer. Biochimie, 95(12), 2235–45.

- APPENDIX -

APPENDIX 1

FGF8 Activates Proliferation and Migration in Mouse Post-Natal Oligodendrocyte Progenitor Cells

Pablo Cruz-Martinez[1], Almudena Martinez-Ferre[1], Jesus Jaramillo-Merchán[1], Alicia Estirado[1], Salvador Martinez[1,2], Jonathan Jones[1]*

1 Neuroscience Institute, University Miguel Hernández (UMH-CSIC), San Juan, Alicante, Spain, 2 IMIB-Hospital Universitario Virgen de la Arrixaca, Universidad de Murcia, Murcia, Spain

Abstract

Fibroblast growth factor 8 (FGF8) is a key molecular signal that is necessary for early embryonic development of the central nervous system, quickly disappearing past this point. It is known to be one of the primary morphogenetic signals required for cell fate and survival processes in structures such as the cerebellum, telencephalic and isthmic organizers, while its absence causes severe abnormalities in the nervous system and the embryo usually dies in early stages of development. In this work, we have observed a new possible therapeutic role for this factor in demyelinating disorders, such as leukodystrophy or multiple sclerosis. In vitro, oligodendrocyte progenitor cells were cultured with differentiating medium and in the presence of FGF8. Differentiation and proliferation studies were performed by immunocytochemistry and PCR. Also, migration studies were performed in matrigel cultures, where oligodendrocyte progenitor cells were placed at a certain distance of a FGF8-soaked heparin bead. The results showed that both migration and proliferation was induced by FGF8. Furthermore, a similar effect was observed in an in vivo demyelinating mouse model, where oligodendrocyte progenitor cells were observed migrating towards the FGF8-soaked heparin beads where they were grafted. In conclusion, the results shown here demonstrate that FGF8 is a novel factor to induce oligodendrocyte progenitor cell activation, migration and proliferation in vitro, which can be extrapolated in vivo in demyelinated animal models.

Introduction

Oligodendrocyte degeneration and subsequent myelin loss is the primary cause of multiple sclerosis and leukodystrophy, among other demyelinating conditions. This may be due to either an autoimmune attack (multiple sclerosis) or metabolic/genetic defects (leukodystrophy) [1–3]. Myelin loss causes irreversible neurological deficits, as the oligodendrocytes are crucial both for the metabolic support of the axons [4] as well as the correct transmission of the nerve impulse. Thus, oligodendrocyte loss implicates neuronal degeneration.

Oligodendrocyte progenitor cells (OPCs) are located throughout the central nervous system, which can be detected by the expression of the proteoglycan NG2 [5,6]. These cells, after an acute demyelinating lesion, are activated and differentiate into mature oligodendrocytes as early as 7 days after the injury [7]. Depending on the type of demyelinating lesions, multiple sclerosis is divided into two phases: acute and chronic. In the acute phase, the nearby OPCs invade the lesion and remyelinate [8,9], while in the chronic phase the migratory and differentiating mechanisms of the progenitors are affected, resulting in sustained and progressive demyelination [10]. This latter phase is partly due to the lack of factors that stimulate regeneration and/or to the presence in the

lesion of molecules that inhibit remyelination [11]. In this case, the stimulation of OPCs to migrate and differentiate by external sources is a viable therapeutic option in order to favor neuronal survival [12].

Previous works in our lab have proven that OPCs may be activated and remyelination induced using bone marrow stem cells [13]. This was due to the secretion of certain soluble factors. In this work, we analyzed the effect that fibroblast growth factor 8 (FGF8) may exert on the activation and differentiation of OPCs. Fibroblast growth factors (FGFs) are a family of soluble protein ligands that play numerous roles during embryonic development, tissue homeostasis and metabolism. There are 22 known members, with different receptor binding affinities and biological functions [14–16]. Depending on the type and receptor, FGFs activate the RAS-MAPK or PI3K-AKT pathway, promoting proliferation, survival and/or motility in various cell types, including oligodendrocytes [17–23].

Of the FGFs members, FGF8 is known to be implicated in early vertebrate brain patterning, and its inhibition causes early embryonic death with absence of the entire mesencephalic and cerebellar primordia [24–28], as well as important thalamic and telencephalic malformations [29,30]. FGF8 is capable of binding to all 4 FGF

receptors, with different affinities among them [31,32]. When the growth factor binds to its receptor, phosphorylation of the Extracellular signal Regulated Kinase 1/2 (ERK1/2) usually occurs, activating the RAS-MAPK intracellular pathway [33–36].

The aim of this study is to analyze if FGF8 may exert an effect on post-natal OPCs, both in vitro and in vivo. As this factor is a known morphogen during embryonic development, the rationale is that FGF8 may be used to induce the mobilization, proliferation, and differentiation of OPCs, as well as possibly remyelination. The results of this work may indicate a possible use for this morphogen in therapies to induce remyelination such as in multiple sclerosis.

Materials and Methods

1 Animal experimentation

All the experiments with animals have been performed in compliance with the Spanish and European Union laws on animal care in experimentation (Council Directive 86/609/EEC), and have been analyzed and approved by the Animal Experimentation Committee of the University Miguel Hernandez and Neuroscience Institute, Alicante, Spain (Reference IN-SM-001-12). All efforts were made to minimize suffering. Mice were bred and maintained in our animal facilities.

2 Oligodendrocyte progenitor cell isolation and culture

The protocol used is similar to previous publications [37–39]. Briefly, the forebrains of newborn mice were removed, diced into 1 mm fragments, digested at 37°C for 20 min with a collagenase (1 mg/ml)/dispase (3 mg/ml) solution and mechanically dissociated. The resulting cellular suspension was then placed on poly-L-lysine coated dishes with the following culture medium: DMEM, 15% FBS, 1% penicillin/streptomycin. After 7–10 days, the culture consisted mainly in astrocytes with a small number of oligodendrocyte progenitor cells (OPCs) growing on top. In order to purify the culture, the cells were trypsinized with 0.05% trypsin and shaken to separate the OPCs from the astrocytes. Cell suspensions were then plated onto uncoated Petri dishes for 1 h to further remove residual contaminating microglia/astrocytes. The cell suspension was then replated in DMEM with 15% FBS, 1% penicillin/streptomycin, 10 ng/ml PDGF-AA and 10 ng/ml FGF2 for 7 days to stimulate the proliferation of OPCs. This resulted in a cell culture of mainly OPCs. Experiments were performed in triplicate (i.e. isolating OPCs from 3 different mice), and a total of 4 independent experiments were performed.

3 Brdu/Proliferation Analysis, Immunocytochemistry and Immunohistochemistry

A standard immunocytochemistry protocol was used. Twenty-four hours before fixing the cells, 1 μg/ml of BrdU was added to the culture to allow its incorporation. Primary antibodies used were anti-BrdU (1:200, Dakocytomation, Denmark), anti-NG2 (1:150, Chemicon), anti-PDGFR-α (1:200, Santa Cruz Biotechnology), anti-Olig2 (1:500, Santa Cruz Biotechnology), anti-O4 (1:1000, Chemicon), anti-MBP (1:100, Oncogene Research Products), and DAPI as nuclear staining. As for secondary antibodies, Alexa Green (1:500, Molecular Probes) was used to stain in green, while for red staining a biotinylated secondary antibody was used (1:200, Vector Laboratories, Burmingham, California) followed by an incubation with streptavidin conjugated with Cy3 (1:500). Samples were visualized and images taken with a Leica fluorescence microscope (Leica DMR, Leica Microsystems).

For immunohistochemical analysis of the in vivo experiments, the mice were anesthetized and perfused using 4% filtered paraformaldehyde (PFA) in phosphate buffer (pH 7.4). The brain was carefully excised and kept in 4% PFA overnight. After fixation, the samples were cryoprotected for 12 hours at 4°C in 15% sucrose, followed by incubation overnight in 30% sucrose. Finally, samples were embedded in Neg −50 Frozen Section Medium (Richard-Allan Scientific, Kalamazoo, Michigan). Twelve micrometer transverse or longitudinal serial sections were obtained using a Microm HM525 cryostat and mounted on seven parallel series and processed for immunohistochemistry. Histological samples were observed under a fluorescence microscope (Leica DM6000D, Leica Microsystems). Micrographs were taken with DFC350/FX and DC500 Leica cameras.

4 Quantitative Real Time PCR

Total mRNA of the cells was isolated using the Trizol protocol (Invitrogen). A total of 5 micrograms of mRNA was reverse-transcribed, and approximately 100 ng of cDNA was amplified by Real Time PCR using Power SYBR Green Master mix (Applied Biosystems). All the samples were run in triplicate using the StepOne Plus Real-Time PCR system (Applied Biosystems) and analyzed with the StepOne Software. Analyses were carried out using the delta C(T) method and calculated relative to GAPDH (forward: AGGT-CGGTGTGAACGGATTTG, reverse: GGGGTCGTTGATGG-CAACA). The results were normalized with respect to the control condition, which presented a value of 1, using the same approach as in our previous report [40]. The following primers were used: PDGFR-α (Forward: TCCATGCTAGACTCAGAAGTCA, Reverse: TCCCGGTGGACACAATTTTTC), NG2 (Forward: GGG-CTGTGCTGTCTGTTGA, Reverse: TGATTCCCTTCAGG-TAAGGCA), Olig2 (Forward: CTAATTCACATTCGGAAG, Reverse: AAAAGATCATCGGGTTCT).

5 Matrigel Cultures

The method used was similar to that previously published [41]. A total of 20,000 oligodendrocyte progenitor cells were re-suspended in 5 μl of D-MEM and 20 μl of matrigel basement membrane matrix (BD Bioscience, 10 ml). D-MEM supplemented with 15% FBS was used as culture medium, as in the differentiation protocol of oligodendrocyte progenitor cells. The re-suspended cells were spread on a tissue culture dish (Becton Dickinson Labware), solidified during 25 min at 37°C and culture medium was added. Afterwards the cell-matrigel was cut in small squares of 125 μm^2 and put on a solidified matrigel drop. Heparin acrylic beads (Sigma) were first rinsed in phosphate-buffered saline (PBS) four to six times and then soaked in FGF8 solution (5000 ng/ml; R&D) at 4°C overnight. The beads were then rinsed three times in PBS and put on the solidified matrigel drop 500 μm from the place where cells-matrigel was located. Control beads were soaked only in PBS and implanted in the same manner. FGF inhibitor (SU5402) was diluted in culture medium to a final concentration of 20 μM and soaked in Affigel blue beads (Bio-Rad), using the same procedure as described for FGF8-soaked beads. Then, 25 ml of a 1:1 matrigel:culture medium mix was added, covering the drop where cells and beads were placed. After 2 h at 37°C, culture medium was added. Finally, 24 h and 48 h afterwards, the migrating and/or non-migrating-cells were observed under a dissecting microscope.

To confirm an FGF8-mediated attracting effect, the proximal/distal rate was calculated in control and FGF8-embedded cultures. This was performed similar to a previous publication [42]. Briefly, the images of the cell clusters were analyzed by imaging software to draw a 45° arc from the cluster towards the beads. The number of cells counted inside this arc (proximal cells) was divided by the number of cells outside the arc (distal cells), obtaining a proximal/distal rate. Values greater or less than 1 indicated more or less cells, respectively, near the bead.
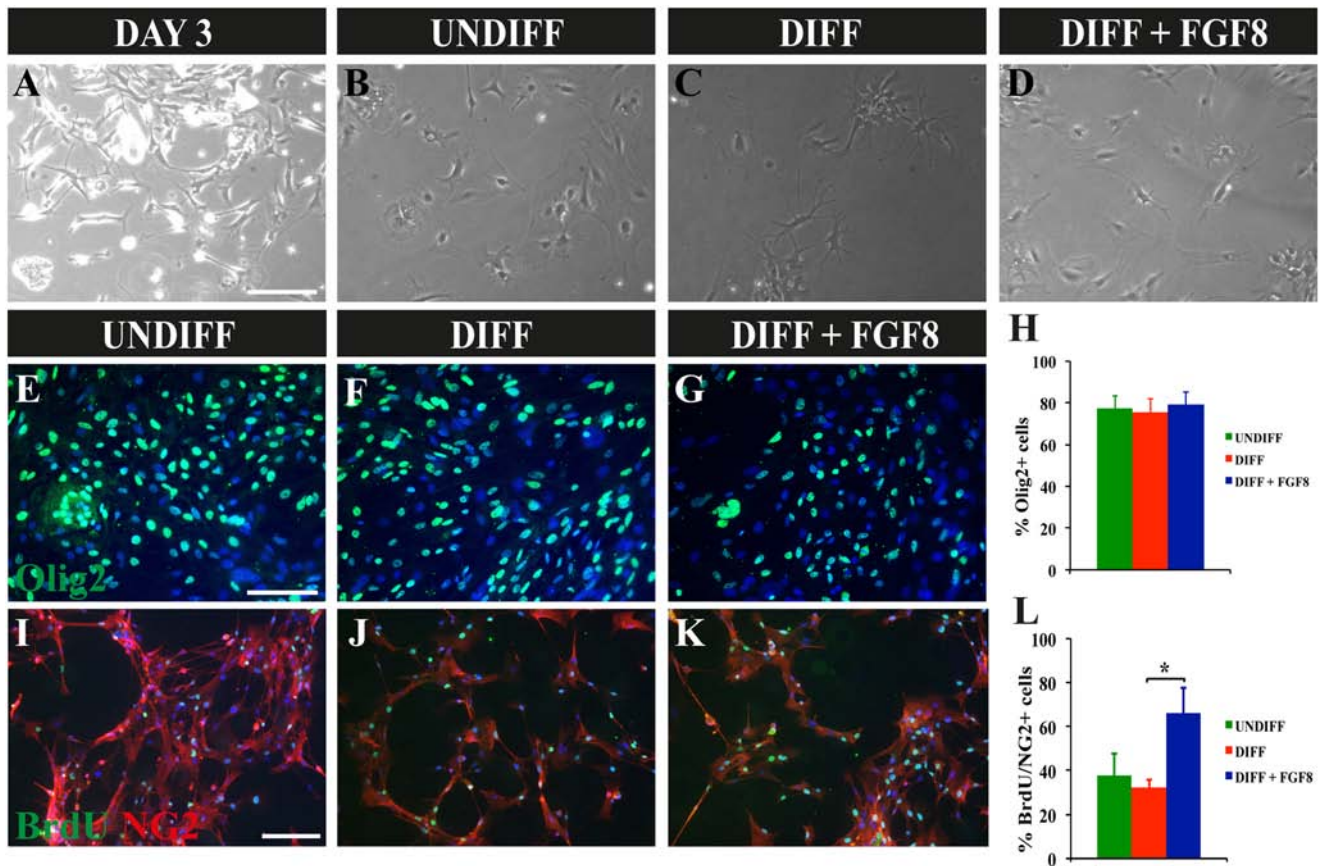
Figure 1. Culture and Differentiation of Oligodendrocyte Progenitor Cells (OPCs). A) OPCs cultured for 3 days after extraction on poly-L-lysine coated culture dishes. Numerous astrocytes are present. B) OPCs after passaging and expanding in the presence of FGF2 and PDGF-AA, to induce proliferation and maintenance of the OPCs. C) OPCs cultured in differentiation inducing medium for 7 days. Mature oligodendrocytes appear in the culture. D) OPCs cultured for 7 days in the differentiating medium and FGF8. All images taken at 100X magnification. E–G) Immunocytochemistry of OPCs in undifferentiating medium (E), differentiation inducing medium (F), and in the presence of FGF8 (G), staining for Olig2 (in green) and DAPI for nuclear staining (in blue). H) Histogram presenting the percentage of Olig2+ cells in the various cultures observed in E–G. Percentages are with respect to the total number of cells, calculated by DAPI staining. I–K) Immunocytochemistry of NG2+/Brdu+ cell in undifferentiating medium (I), differentiation inducing medium (J), and in the presence of FGF8 (K). L) Histogram presenting the percentage of NG2+/BrdU+ cells in the different cultures, with respect to the total number of cells. *p<0.05 (paired t-test), n = 4. Scale Bar indicates 150 μm for A–D and 100 μm for E–G and I–K.
doi:10.1371/journal.pone.0108241.g001

6 Cuprizone Treatment of Mice as an In Vivo Chronic Demyelinating Model

The approach used was similar to our previously published report [13]. Briefly, Four-week old C3H/He mice were given a diet with 0.2% cuprizone (w/w) for 12 weeks ad libitum in order to obtain a chronic version of toxicity-induced demyelination, but with the following changes. Finely-powdered cuprizone (Sigma-Aldrich, St. Louis, MO) was dissolved in 60% tap water (w/v) with 0.5% (w/v) commercialized cane sugar. The cane sugar was added to avoid the weight loss observed in other studies due to the cuprizone treatment. After 12 weeks, the mice were grafted with the FGF8-soaked beads (or culture medium in the case of sham operated group) and returned to normal chow until their sacrifice.

7 FGF8-soaked heparin bead transplantation

The surgical procedure and coordinates used to inject the FGF8-heparin beads was the same as our previous report [13]. Before the surgical procedure, 0.1 mg/kg of buprenorphine (Buprex, Schering-Plough, Madrid, Spain) was injected into the mice. Isoflurane (Esteve Veterinary, Milan, Italy), an inhalational anesthesia, was used, and the mice were placed on a stereotaxic apparatus (Stoelting, Wheat

Lane Wood Dale, IN, USA). The animals were monitored, and anesthesia concentration controlled. After the injection, the incision was sutured and the mice were monitored throughout the whole process of experimentation. A total of 8 cuprizone-treated mice were operated, 4 with FGF8-embedded heparin beads (at 1 mg/ml) and 4 sham controls (where PBS-soaked beads were used). After 1 month, the mice were sacrificed.

To quantify NG2 and MBP immunoreactivity, a similar approach as published in [13] was used. Briefly, images were taken and changed to an 8-bit black and white image. Then, the percentage of illuminated pixels was calculated, and compared between the experimental groups.

8 Statistical Analysis

Statistical significance between control and experimental groups were calculated with Sigmaplot v12.0 software, using the paired t-test and one-way ANOVA test where applicable, establishing the level of significance at p<0.05. Values are measured as mean +/− standard deviation.
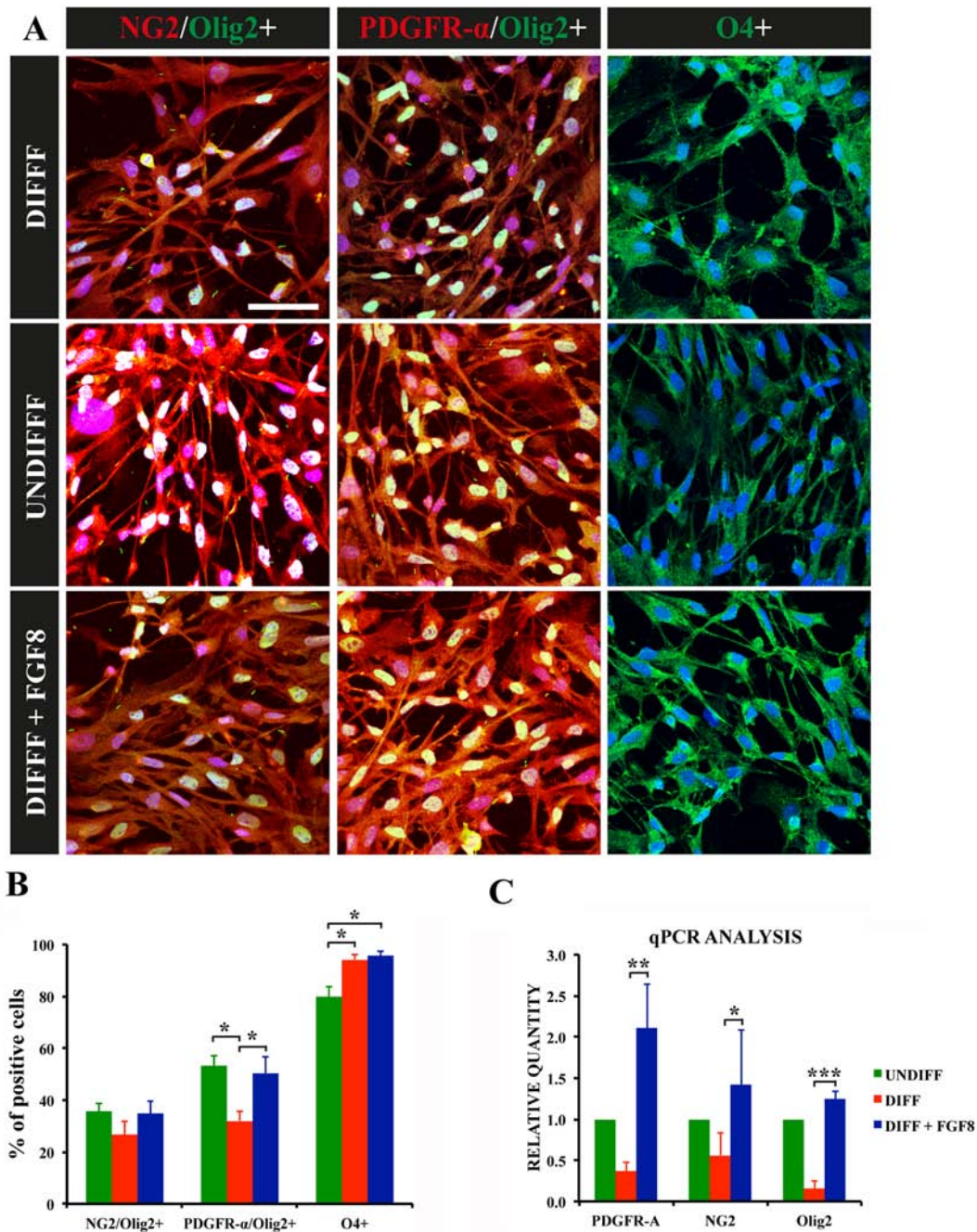
Figure 2. Oligodendrocyte progenitor cell differentiation with and without FGF8. A) Immunocytochemistry of NG2+/Olig2+, PDGFR-A+/ Olig2+ and O4+ cells in the undifferentiated, differentiating and FGF8 culture media. In all images, blue staining corresponds to the nuclei (DAPI). Scale bar indicates 50 μm. B) Histogram depicting the percentage of cells in the different cell cultures staining for markers analyzed in A. Percentages are with respect to the total number of cells. C) Histogram depicting the results from the quantitative PCR analysis of the different cell cultures. *$p <$ 0.05, **$p<0.01$, ***$p<0.001$ (paired t-test in B, one way-ANOVA in C), n = 4.
doi:10.1371/journal.pone.0108241.g002

Results

1 FGF8 Increases Proliferation in Cultured Oligodendrocyte Progenitor Cells (OPCs)

The OPCs were isolated from P0–P2 newborn mice and cultured on poly-L-lysine coated culture dishes. The initial culture was a mixture of astrocytes, OPCs and other cell types, the OPCs being mainly detected on top of the astrocytes (Figure 1A). After 7 days of culture, the cells were treated with trypsin and shaken in

order to detach the OPCs and re-plated onto new culture dishes, where they were further expanded using mitogens PDGF-AA and FGF2 (Figure 1B). In this fashion, after an additional 7 days of culture the majority of the cells detected corresponded to OPCs, as indicated in previous publications [35–37].

In order to induce OPCs differentiation, the culture medium was changed removing the mitogens and adding fetal bovine serum, resulting in spontaneous differentiation (Figure 1C). Mature oligodendrocytes could be detected after 7 days of culture, observed as
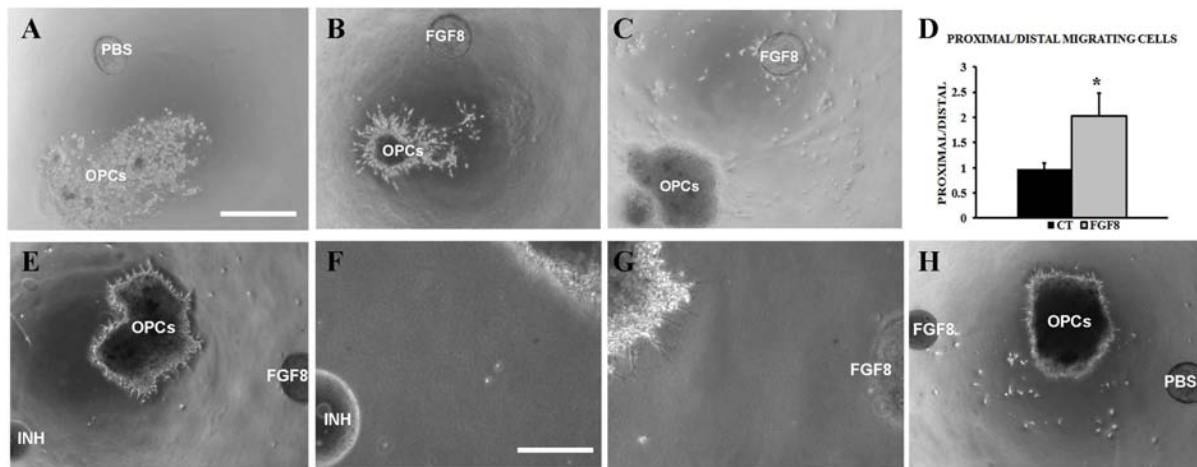
Figure 3. Matrigel cultures of OPCs. A) Oligodendrocyte progenitor cell matrigel culture where a PBS-soaked bead was placed 0.5 mm away from the cell cluster. Image taken at 40X magnification. B–C) OPCs where a cluster of cells migrating towards a FGF8-soaked bead can be observed. D) Histogram depicting the oligodendrocyte progenitor cell proximal/distal rate in control cultures and where FGF8 was included. *p<0.01 (paired t-test, n = 4). (E–G) Matrigel cultures where on one side a FGF8-soaked bead was placed and on the other side a FGF8 inhibitor. (F, G) Close-up images of the areas near the inhibitor-soaked bead (F) or near the FGF8-soaked bead (G). H) OPCs where a FGF8-soaked bead was placed and on the other side a PBS-soaked bead, as control of the inhibitor. Scale bar indicates 500 µm for (A–C, D, H) and 200 µm for (F, G). All images were taken 48 hours after culture.
doi:10.1371/journal.pone.0108241.g003

cells with many small prolongations. In the experimental procedure with FGF8, this factor was added to the culture using the same differentiation medium (Figure 1D). Independently of the treatment, the cultures were mainly composed of oligodendrocytes, as analyzed by Olig2 staining (Figure 1E–H). In the cultures with FGF8, an increased number of cells were detected compared to the other treatments, despite performing the cultures with the same initial number of cells. To corroborate that FGF8 induced proliferation, BrdU was incorporated to the culture 24 hours before fixing, and then immunocytochemistry for BrdU and double-stained with NG2+ (an oligodendrocyte progenitor cell marker) to confirm that only oligodendrocytes were counted (Figure 1I–L). As a result, the oligodendrocyte progenitor cell cultures where FGF8 was added presented a marked increase in proliferation, even more so than in the undifferentiated cultures (Figure 1H). This confirmed that FGF8 induced the proliferation of OPCs.

2 FGF8 Upregulates the Expression of Early Oligodendrocyte Progenitor Cell Markers

As proliferation is enhanced, it is possible that differentiation may be hampered in turn. To confirm this, immature oligodendrocytic and oligodendrocyte progenitor cell markers NG2 and PDGFR-α, oligodendrocyte marker Olig2 and mature oligodendrocyte marker O4 were analyzed (Figure 2A). As a result, the percentage of cells positive for PDGFR-α and Olig2 was lower in the differentiated cultures, compared to the undifferentiated and FGF8 treatments (Figure 2B). As for O4, which begins to be expressed during oligodendrocyte maturation, coinciding with the loss of expression of NG2 and PDGFR-α [43], was increased in the differentiated and FGF8 treatments. This data was corroborated by QPCR (Figure 2C), indicating that the differentiated treatment resulted in less immature oligodendrocytes and OPCs, coinciding with more mature oligodendrocytes.

It is interesting to note that FGF8 treatment presented both more immature and mature markers. The composition of this culture medium was the same medium used for differentiation, except for the growth factor. Therefore, this data seems to indicate that FGF8 induces proliferation, resulting in more OPCs in

culture, and does not hamper differentiation, which in turn results in more mature oligodendrocytes in the culture.

3 FGF8 Induces the Migration of Oligodendrocyte Progenitor Cells

Undifferentiated OPCs were placed on matrigel cultures to perform migration assays. To this end, a heparin bead previously soaked in FGF8 solution (500 ng/ml) was placed 0.5 mm away from the cluster of OPCs, while a PBS-soaked bead was used as control (Figure 3A–C). Twenty four hours afterwards, outgrowths were observed from the OPCs, the majority of which were detected in the direction of the FGF8-soaked bead (Figure 3B). The cultures were maintained and observed after 48 and 72 hours, with similar results (Figure 3C), the OPCs reaching the heparin bead. To confirm the attracting effect of FGF8, proximal/distal analysis was performed on the cultures (Figure 3D). The cultures where FGF8-soaked beads were used presented a significantly higher proximal/distal ratio than control cultures where PBS was used. Specifically, a 2-fold increase in cells was detected near the beads than in distal areas of the cell clusters. Therefore, the results indicated a predominantly migrating, attracting effect induced by FGF8.

In order to confirm this migrating property, the FGF-receptor inhibitor SU5402 was used in the cultures to counteract the effect of FGF8 (Figure 3E–G). In this case, two beads were used, on one side of the cluster of OPCs, a FGF8-soaked bead was placed, while on the other end a bead soaked in the inhibitor. As control of the inhibitor a PBS-soaked bead was used (Figure 3H). As a result, after 48 hours of culture, in the side of the OPCs where the SU5402-soaked bead was placed, no cell sprouting or migration was detected (Figure 3F). In the other side of the cluster, nearest the FGF8-soaked bead, numerous cell outgrowths were present (Figure 3G), indicating that the OPCs were stimulated by the FGF8 but the inhibitor managed to halt further migration. In the cases where PBS was used instead of the inhibitor, migration of the OPCs was observed as in the previous results (Figure 3H).

Overall, the results demonstrated that FGF8 is capable of inducing oligodendrocyte progenitor cell migration, exerting and attracting effect, and is mediated by the binding of FGF8 to FGF receptors.
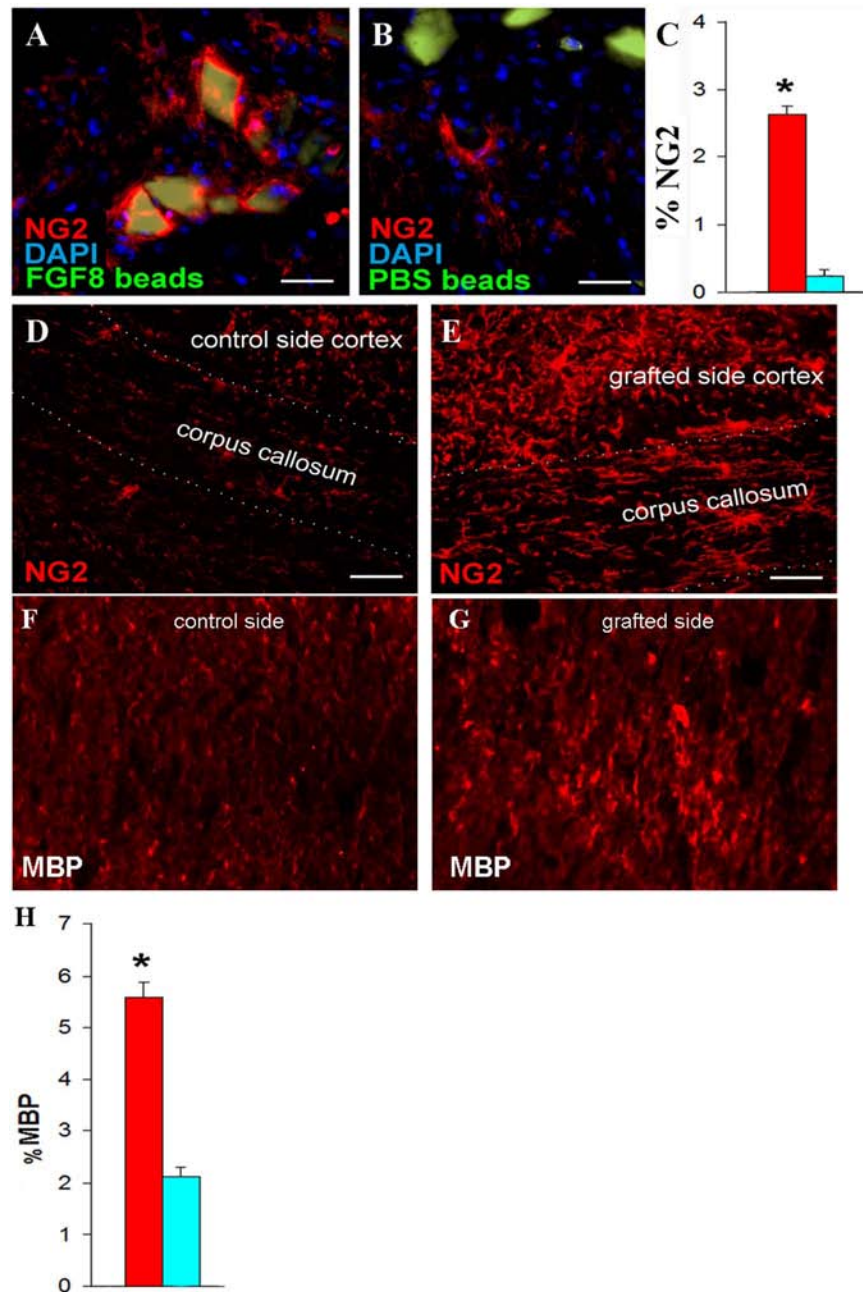
Figure 4. In Vivo Transplantation of FGF8-soaked beads in Chronically Demyelinated Mice. A) FGF8-soaked heparin beads (seen in green) surrounded by NG2-positive cells (in red. B) Control experiment where PBS-soaked beads were transplanted. C) Histogram depicting the percentage of NG2 immunoreactivity in the area injected with the heparin beads. The red bar indicates the percentage in the case FGF8-soaked beads was used, while the blue bar indicates the sham control. D) NG2 immunoreactivity in the corpus callosum and cortex in the area near the PBS-soaked beads. E) NG2 immunoreactivity in the corpus callosum and cortex in the area near the FGF8-soaked beads. F, G) MBP immunoreactivity in the area near the PBS or FGF8-soaked beads, respectively. H) Histogram depicting the percentage of MBP immunoreactivity in the area injected with the PBS- (blue bar) or FGF8- (red bar) soaked heparin beads. Scale bar measures 50 μm. *$p < 0.01$ (paired t-test), $n = 4$.
doi:10.1371/journal.pone.0108241.g004

4 Transplantation of FGF8-Soaked Beads Activates the Migration of Oligodendrocyte Progenitor Cells In Vivo, Exerting an Attracting Effect

In order to confirm if the results observed in vitro can be extrapolated in vivo, as well as analyze if FGF8 may be used as a therapeutic tool in inducing remyelination, mice were treated with cuprizone for 12 weeks to induce a chronic demyelinating condition, similar to previous studies [13,44,45]. Then, FGF8-

soaked heparin beads were grafted on one side of the fimbria closest to the corpus callosum, while in the other side a PBS-soaked bead was grafted. As a result, 1 month after transplantation, an increase in NG2 positive cells was detected in the area where the beads were transplanted, some of which were surrounding the beads (Figure 4A). The side where PBS-soaked beads were used, on the other hand, presented lower NG2

immunoreactivity in the area compared to the group where FGF8-soaked beads were grafted (Figure 4B, C).

Also, both NG2 and MBP (oligodendrocyte progenitor cell and mature oligodendrocyte markers, respectively) immunoreactivity were detected in the corpus callosum near the area where the FGF8-soaked beads were grafted, which was not detected in the side where PBS-soaked beads were used (Figure 4D–H). Thus, FGF8-mediated stimulus was capable of reaching the corpus callosum from the fimbria.

Discussion

In this work, we have proven that FGF8 is capable of activating post-natal mouse oligodendrocyte progenitor cells (OPCs) both in vitro and in vivo. Proliferation and migration of OPCs, as well as their differentiation to mature oligodendrocytes was also observed in vitro, indicating that this process is not hampered.

Oligodendrocytes are known to express various FGF receptors, mainly several subtypes of FGFR1, FGFR2 and FGFR3 [46]. Many works have focused on the study of the expression of these receptors, as well as the effect FGFs have on the cells, which varies throughout its lineage. For example, FGF2, when combined with PDGF-AA, is known to induce proliferation in OPCs [47,48], while mature oligodendrocytes in the presence of this growth factor revert to a progenitor state [49,50]. This indicates a negative effect in terms of differentiation and myelin production using FGF2. On the other hand, another work has shown that OPCs cultured in the presence of FGF8 expressed significantly more MBP compared to FGF2 [51], revealing a distinct effect of these two at-first similar growth factors. This same article also demonstrated that in oligodendrocyte cultures, while FGF2 downregulated mature oligodendrocyte markers and induced a reverted state, this was not observed with FGF8. In our work, we have further demonstrated FGF8 is not only capable of inducing a proliferative effect on OPCs in culture, but is also capable of attracting these cells and allowing their differentiation to myelinating oligodendrocytes. Thus, while FGF2 is useful in inducing OPC proliferation at the handicap of blocking differentiation, FGF8 seems to possess similar properties without this impediment.

The mouse model used in this study, where cuprizone was added to the mices diet, results in a chronic, irreversible demyelinating model similar to the lesions observed in multiple sclerosis. If the cuprizone is removed prematurely (before the 12 weeks), remyelination is spontaneously activated, which occurs in two phases: OPCs proliferation and colonization of the demyelinated area, and differentiation towards immature oligodendrocytes that bind to the demyelinated axons and mature to myelinating oligodendrocytes. This process is regulated by the coordinated expression of soluble factors [52].

The remyelinating process observed by early cuprizone removal also occurs naturally in vivo. OPCs are expressed throughout the adult central nervous system, and are capable of differentiating to mature oligodendrocytes when a demyelinating lesion occurs [6]. However, in the chronic phase of multiple sclerosis, there is a multiple dysfunction in the activation of OPCs, which affects the remyelinating process [53]. This may be due to either an absence of nearby OPCs or that they are quiescent and cannot react. Regardless of the reason, the lack of soluble factors that activate the migration and differentiation of OPCs may be one of the primary reasons for this failed response. Thus, for a therapeutic approach to be effective it must be capable of stimulating the quiescent OPCs, as well as induce their migration to the damaged area. This work demonstrates that FGF8 may be used to this end.

In conclusion, FGF8 is a morphogenetic factor that may be used to induce post-natal migration, proliferation and differentiation of oligodendrocyte progenitor cells. This property makes it a candidate factor that may be used in demyelinating disorders.

Author Contributions

Conceived and designed the experiments: PCM AMF AE JJ SM JJM. Performed the experiments: PCM AMF AE JJ SM JJM. Analyzed the data: PCM AMF AE JJ SM JJM. Contributed reagents/materials/analysis tools: PCM AMF AE JJ SM. Contributed to the writing of the manuscript: JJ SM.

References

1. Steinman L (1996) Multiple sclerosis: a coordinated immunological attack against myelin in the central nervous system. Cell 85: 299–302.
2. Kohler W (2010) Leukodystrophies with late disease onset: an update. Curr Opin Neurol 23: 234–241.
3. Aktas O, Kieseier B, Hartung HP (2010) Neuroprotection, regeneration and immunomodulation: broadening the therapeutic repertoire in multiple sclerosis. Trends Neurosci 33: 140–152.
4. Nave KA (2010) Myelination and support of axonal integrity by glia. Nature 468: 244–252.
5. Nishiyama A, Komitova M, Suzuki R, Zhu X (2009) Polydendrocytes (NG2 cells): multifunctional cells with lineage plasticity. Nat Rev Neurosci 10: 9–22.
6. Menn B, Garcia-Verdugo JM, Yaschine C, Gonzalez-Perez O, Rowitch D, et al. (2006) Origin of oligodendrocytes in the subventricular zone of the adult brain. J Neurosci 26: 7907–7918.
7. Sellers DL, Maris DO, Horner PJ (2009) Postinjury niches induce temporal shifts in progenitor fates to direct lesion repair after spinal cord injury. J Neurosci 29: 6722–6733.
8. Chari DM, Crang AJ, Blakemore WF (2003) Decline in rate of colonization of oligodendrocyte progenitor cell (OPC)-depleted tissue by adult OPCs with age. J Neuropathol Exp Neurol 62: 908–916.
9. Chari DM, Huang WL, Blakemore WF (2003) Dysfunctional oligodendrocyte progenitor cell (OPC) populations may inhibit repopulation of OPC depleted tissue. J Neurosci Res 73: 787–793.
10. Williams A, Piaton G, Aigrot MS, Belhadi A, Théaudin M, et al. (2007) Semaphorin 3A and 3F: key players in myelin repair in multiple sclerosis? Brain 130: 2554–2565.
11. Kuhlmann T, Miron V, Cui Q, Wegner C, Antel J, et al. (2008) Differentiation block of oligodendroglial progenitor cells as a cause for remyelination failure in chronic multiple sclerosis. Brain 131: 1749–1758.
12. Irvine KA, Blakemore WF (2008) Remyelination protects axons from demyelination-associated axon degeneration. Brain 131: 1464–1477.
13. Jaramillo-Merchán J, Jones J, Ivorra JL, Pastor D, Viso-León MC, et al. (2013) Mesenchymal stromal-cell transplants induce oligodendrocyte progenitor migration and remyelination in a chronic demyelination model. Cell Death and Disease 4: e779.
14. Eriksson AE, Cousens LS, Weaver LH, Matthews BW (1991) Three-dimensional structure of human basic fibroblast growth factor. Proc Natl Acad Sci USA 88: 3441–3445.
15. Itoh N, Ornitz DM (2004) Evolution of the FGF and FGFR gene families. Trends in Genetics 20: 563–569.
16. Mohammadi M, Olsen SK, Ibrahimi OA (2005) Structural basis for fibroblast growth factor receptor activation. Cytokine Growth Factor Rev 16: 107–137.
17. Gotoh N (2008) Regulation of growth factor signaling by FRS2 family docking/scaffold adaptor proteins. Cancer Sci 99: 1319–1325.
18. Mitew S, Hay CM, Peckham H, Xiao J, Koenning M, et al. (2013) Mechanisms regulating the development of oligodendrocytes and central nervous system myelin. Neuroscience.
19. Bottcher RT, Niehrs C (2005) Fibroblast growth factor signaling during early vertebrate development. Endocr Rev 26: 63–77.
20. Thisse B, Thisse C (2005) Functions and regulations of fibroblast growth factor signaling during embryonic development. Dev Biol 287: 390–402.
21. Turner N, Grose R (2010) Fibroblast growth factor signalling: from development to cancer. Nature Rev Cancer 10: 116–129.

22. Chandran S, Kato H, Gerreli D, Compston A, Svendsen CN, et al. (2003) FGF-dependent generation of oligodendrocytes by a hedgehog-independent pathway. Development 130: 6599–6609.
23. Furusho M, Kaga Y, Ishii A, Hébert JM, Bansal R (2011) Fibroblast growth factor signaling is required for the generation of oligodendrocyte progenitors from the embryonic forebrain. J Neurosci 31: 5055–5066.
24. Crossley PH, Martin GR (1995) The mouse Fgf8 gene encodes a family of polypeptides and is expressed in regions that direct outgrowth and patterning in the developing embryo. Development 121: 439–451.
25. Crossley PH, Martinez S, Martin GR (1996) Midbrain development induced by FGF8 in the chick embryo. Nature 380: 66–68.
26. Reifers F, Böhli H, Walsh EC, Crossley PH, Stainier DY, et al. (1998) Fgf8 is mutated in zebrafish acerebellar (ace) mutants and is required for maintenance of midbrain-hindbrain boundary development and somitogenesis. Development 125: 2381–2395.
27. Partanen J (2007) FGF signalling pathways in development of the midbrain and anterior hindbrain. J Neurochem 101: 1185–1193.
28. Nakamura H, Sato T, Suzuki-Hirano A (2008) Isthmus organizer for mesencephalon and metencephalon. Dev Growth Differ 50: S113–118.
29. Storm EE, Garel S, Borello U, Hebert JM, Martinez S, et al. (2006) Dose-dependent functions of Fgf8 in regulating telencephalic patterning centers. Development 133: 1831–1844.
30. Martinez-Ferre A, Martinez S (2009) The development of the thalamic motor learning area is regulated by Fgf8 expression. J Neurosci 29: 13389–13400.
31. Ornitz DM, Xu J, Colvin JS, McEwen DG, MacArthur CA, et al. (1996) Receptor specificity of the fibroblast growth factor family. J Biol Chem 271: 15292–15297.
32. Kouhara H, Koga M, Kasayama S, Tanaka A, Kishimoto T, et al. (1994) Transforming activity of a newly cloned androgen-induced growth factor Oncogene 9: 455–462.
33. Christen B, Slack JM (1999) Spatial response to fibroblast growth factor signalling in Xenopus embryos. Development 126: 119–25.
34. Corson L, Yamanaka Y, Lai K, Rossant J (2003) Spatial and temporal patterns of ERK signaling during mouse embryogenesis. Development 130: 4527–4537.
35. Tsang M, Dawid IB (2004) Promotion and attenuation of FGF signaling through the Ras-MAPK pathway. Sci STKE 228: pe17.
36. Lunn JS, Fishwick KJ, Halley PA, Storey KG (2007) A spatial and temporal map of FGF/Erk1/2 activity and response repertoires in the early chick embryo. Dev Biol 302: 536–552.
37. Yang Z, Watanabe M, Nishiyama A (2005) Optimization of oligodendrocyte progenitor cell culture method for enhanced survival. J Neurosci Methods 149: 50–56.
38. Lee X, Yang Z, Shao Z, Rosenberg SS, Levesque M, et al. (2007) NGF regulates the expression of axonal LINGO-1 to inhibit oligodendrocyte differentiation and myelination. J Neurosci 27: 220–225.
39. Morello N, Bianchi FT, Marmiroli P, Tonoli E, Rodriguez Menendez V, et al. (2011) A role for hemopexin in oligodendrocyte differentiation and myelin formation. PLOS One 6: e20173.
40. Jones J, Estirado A, Redondo C, Bueno C, Martínez S (2012) Human adipose stem cell-conditioned medium increases survival of Friedreich's ataxia cells submitted to oxidative stress. Stem Cells Dev 21: 2817–2826.
41. Aarum J, Sandberg K, Haeberlein SL, Persson MA (2003) Migration and differentiation of neural precursor cells can be directed by microglia. Proc Natl Acad Sci USA 100: 15983–15988.
42. Vernerey J, Macchi M, Magalon K, Cayre M, Durbec P (2013) Ciliary neurotrophic factor controls progenitor migration during remyelination in the adult rodent brain. J Neuroscience 33: 3240–3250.
43. Baumann N, Pham-Dinh D (2001). Biology of oligodendrocyte and myelin in the mammalian central nervous system. Physiological Reviews 81: 871–927.
44. Kipp M, Clarner T, Dang J, Copray S, Beyer C (2009) The cuprizone animal model: new insights into an old story. Acta Neuropathol 118: 723–736.
45. Armstrong RC, Le TQ, Flint NC, Vana AC, Zhou YX (2006) Endogenous cell repair of chronic demyelination. J Neuropathol Exp Neurol 65: 245–256.
46. Bansal R, Kumar M, Murray K, Morrison RS, Pfeiffer SE (1996) Regulation of FGF receptors in the oligodendrocyte lineage. Mol and Cell Neurosci 7: 263–275.
47. McKinnon RD, Matsui T, Dubois-Dalcq M, Aaronson SA (1990) FGF modulates the PDGF-driven pathway of oligodendrocyte development. Neuron 5: 603–614.
48. Bogler O, Wren D, Barnett SC, Land H, Noble M (1990) Cooperation between two growth factors promotes extended self-renewal and inhibits differentiation of oligodendrocyte-type-2 astrocyte (O-2A) progenitor cells. Proc Natl Acad Sci USA 87: 6368–6372.
49. Grinspan JB, Stern JL, Franceschini B, Pleasure D (1993) Trophic effects of basic fibroblast growth factor (bFGF) on differentiated oligodendroglia: a mechanism for regeneration of the oligodendroglial lineage. J Neurosci Res 36: 672–680.
50. Fressinaud C, Vallat JM, Labourdette G (1995) Basic fibroblast growth factor down-regulates myelin basic protein gene expression and alters myelin compaction of mature oligodendrocytes in vitro. J Neurosci Res 40: 285–293.
51. Fortin D, Rom E, Sun H, Yayon A, Bansal R (2005) Distinct fibroblast growth factor (FGF)/FGF receptor signaling pairs initiate diverse cellular responses in the oligodendrocyte lineage. J Neurosci 25: 7470–7479.
52. Chari DM (2007) Remyelination in multiple sclerosis. Int Rev Neurobiol 79: 589–620.
53. Sim FJ, Zhao C, Penderis J, Franklin RJ (2002) The age-related decrease in CNS remyelination efficiency is attributable to an impairment of both oligodendrocyte progenitor recruitment and differentiation. J Neurosci 22: 2451–2459.

APPENDIX 2

Regenerative Medicine

Stem cell injection in the hindlimb skeletal muscle enhances neurorepair in mice with spinal cord injury

Aims: To develop a low-risk, little-invasive stem cell-based method to treat acute spinal cord injuries. **Materials & methods:** Adult mice were submitted to an incomplete spinal cord injury, and mesenchymal stem cells injected intramuscularly into both hindlimbs. Behavior tests and MRI of the spinal cord were periodically performed for up to 6 months, along with immunohistochemical analysis. Immunohistochemical and PCR analysis of the muscles were used to detect the grafted cells as well as the soluble factors released. **Results:** The stem cell-treated mice presented significant improvements in their motor skills 5 months after treatment. Spinal cord repair was detected by magnetic resonance and immunohistochemistry. In the hindlimb muscles, the stem cells activated muscle and motor neuron repair mechanisms, due to the secretion of several neurotrophic factors. **Conclusion:** Bone marrow mesenchymal stem cell injection into hindlimb muscles stimulates spinal cord repair in acute spinal cord lesions.

Keywords: bone marrow • intramuscular injection • *in vivo* cell tracking • mesenchymal stem cells • muscle regeneration • neurotrophic factors • spinal cord injury • spinal cord repair

Pablo Cruz-Martinez[‡,1], Diego Pastor[‡,2], Alicia Estirado[1], Jesus Pacheco-Torres[1], Salvador Martinez[1,3] & Jonathan Jones*[,1]

[1]Neuroscience Institute, University Miguel Hernández (UMH-CSIC), San Juan, Alicante, Spain
[2]Sports Research Center, University Miguel Hernández, Elche, Spain
[3]IMIB-Hospital Universitario Virgen de la Arrixaca, University Murcia, Murcia, Spain
*Author for correspondence: jon@umh.es
[‡]Authors contributed equally

Spinal cord injury (SCI) is a severe and debilitating clinical condition that affects thousands of victims around the world annually, many of whom become permanently disabled, and severely affects quality of life [1]. The only clinically proven therapy for SCI is using methylprednisolone, a glucocorticoid that controls the inflammatory process locally and has only a marginal effect on the recovery if used early after injury, and has been associated with important side effects [2–5]. Thus, it is necessary to search for new therapeutic approaches to treat SCI patients, as well as expand existing knowledge on the cellular and molecular aspects of the disorder.

SCI can be separated into two phases: an initial acute phase, which eventually becomes chronic [6,7]. While in the acute phase there are limited autoregenerative capabilities, at the chronic stage the damage is irreversible. Thus, many therapeutic strategies consider treating the initial phase, in order to ameliorate the final outcome. There are numerous strategies currently being investigated, one of them being the use of adult stem cells. The use of adult stem cells, such as those found in the bone marrow including both populations (hematopoietic and mesenchymal stem cells), has been extensively studied in animal models, demonstrating their ability to reduce inflammation, promote remyelination, neuronal regeneration, axonal outgrowth and ultimately functional recovery [8–23]. Furthermore, autologous bone marrow mononuclear cells or pre-isolated and expanded mesenchymal stem cells have been used in initial clinical trials, with a certain degree of functional improvement [24–27]. However, the neurological improvements to date have been modest.

The scientific rationale for the use of bone marrow stem cells in SCI is mainly based on the anti-inflammatory, neuroprotective and/or regenerative properties of the grafted cells. In the first case, mesenchymal stem cells are known to be immunosuppressive [28–31].

Future Medicine part of fsg

This reduces the inflammatory response to the injury and in turn reduces the size of the cavity formed, as well as reducing astrocytic and microglial activation [32].

The neuroprotective and regenerative properties of mesenchymal stem cells mainly derives from their ability to produce and secrete numerous trophic factors, exerting a paracrine effect on the surrounding tissue. For example, the secretion of brain derived neurotrophic factor (BDNF), nerve growth factor (NGF) and vascular endothelial growth factor (VEGF) are known to stimulate neuronal sprouting and axonal outgrowth [33,34]. The expression of other factors such as *ninjurin 1* and 2, *netrin 4*, Neural Cell Adhesion Molecule (NCAM), Robo1 and Robo4 are known to be implicated in neuronal migration and axonal regeneration [33,35]. Furthermore, mesenchymal stem cells are capable of removing potentially damaging debris that appears after a spinal cord lesion, such as matrix metalloproteinases I and MMP2 [36–38]. Thus, mesenchymal stem cell injection is a potentially useful tool for SCI treatment. However, direct, intraspinal stem cell injection poses certain problems. For example, the inflammation and hemorrhage present during the acute phase of a spinal cord lesion may be a dangerous niche for the stem cell engraftment, causing their death before their trophic activity may be in effect. Furthermore, it is very difficult to perform the surgical procedure during this phase, aggravating the injury. Therefore, a less invasive intervention may be necessary to guarantee stem cell survival and subsequent spinal cord regeneration.

One possible method to exert a possible regenerative/repair effect on the damaged spinal cord is to inject bone marrow-derived mesenchymal stem cells into the muscle tissue instead of directly in the spinal cord. This has been performed both by other groups as well as in our lab using amyotrophic lateral sclerosis mouse models [39,40]. In these works, the bone marrow-derived stem cells released neurotrophic factors, such as glial-derived neurotrophic factor (GDNF), which were captured by the axon terminals of the neuromuscular plates and retrogradely transported into the neuronal cell body of the spinal cord. Once in the spinal cord, the soluble factors rescued the degenerating motor neurons by activating antiapoptic proteins and inducing prosurvival mechanisms.

The aim of this current study is to confirm if the same effect observed in the amyotrophic lateral sclerosis models commented on previously can also be extrapolated to spinal cord lesions. To this end, the mesenchymal stem cells will be transplanted into the hindlimb muscles of mice submitted to a thoracic, incomplete lesion, allowing a certain degree of recovery. The results of this work will demonstrate that a simple surgical intervention, such as autologous bone marrow transplantation into skeletal muscle tissue, is capable of enhancing motor neuronal survival, and ultimately the motor function recovery.

Materials & methods
Animal care
All the experiments with animals have been performed in compliance with the Spanish and European Union laws on animal care in experimentation (Council Directive 86/609/EEC), and have been analyzed and approved by the Animal Experimentation Committee of the University Miguel Hernandez and Neuroscience Institute, Alicante, Spain. All efforts were made to minimize suffering. Mice were bred and maintained in our animal facilities. Two- to three-month-old C57/B6 mice were used as experimental mice for the SCI. For the mesenchymal stem cells, the bone marrow of 2- to 3-month-old green fluorescent protein (GFP) transgenic mice were used.

Spinal cord injury
The SCI was induced using a similar approach reported in [41]. Briefly, a laminectomy of the thoracic vertebra segment 9 was performed without damaging the dura-mater. A bilateral clamp, using a laminectomy forceps (Fine Science Tools, Heidelberg, Germany) compressing the sides of the spinal cord but leaving 0.5 mm of space in between, was performed for 30 s on the exposed spinal cord, then removed and skin sutured. Before performing the surgical procedure, 0.1 mg/kg of buprenorphine (Buprex, Schering-Plough, Madrid, Spain) was injected into the mice. Isoflurane (Esteve Veterinary, Milan, Italy), an inhalational anesthesia, was used, and the mice was placed on a stereotaxic apparatus (Stoelting, Wheat Lane Wood Dale, IN, USA). The animal was monitored, and anesthesia concentration was controlled.

For the hindlimb surgical intervention, performed immediately after the spinal cord lesion, the hindlimb muscles were exposed and 10 μl of either culture medium (sham control) or 1 million mesenchymal stem cells (TX-MSC) were injected, in a similar approach as our previous publication [40].

Bone marrow extraction & mesenchymal stem cell culture
Two- to three-month-old GFP-mutant mice were sacrificed by cervical dislocation and the femurs dissected. The procedure used was similar to our previous works [42,43]. Bone marrow was extracted from the femurs and dissociated mechanically to obtain a single-cell suspension. Then, the cells were washed, centrifuged and resuspended in culture medium, which consisted

in D-MEM (Invitrogen) supplemented with 15% FBS (Biochrom AG, Berlin, Germany), and 100 U/ml penicillin/streptomycin (Sigma-Aldrich, St Louis, MO, USA). The cells were then placed in culture flasks to isolate the plastic-adherent cell population. The culture medium was changed twice a week and the cells replated when needed, for a total of 3–4 weeks in culture (passage 4–5) to obtain the necessary cell number.

Behavior tests

Treadmill and footprint tests were performed on a monthly basis similar to our previous work [44]. The tests were performed on a monthly basis for up to 6 months after the surgical intervention. A total of 12 control and 12 experimental mice were used for this test.

The treadmill test consisted of placing the mouse in a lane that pushed the animal to a shock grid (0.4 mA). In this manner, the animal must run to avoid the shock. Each mouse was placed on the treadmill five times, with adequate rests between trials, in order to obtain the average maximum speed.

In the case of the footprint test, the hindlimb paws were painted and the mouse placed on a dark tube with a large dark box in the end. A 60-cm strip of paper was placed under the tube, so that when the animal walked towards the box, its footprints were left on the paper. Stride length was measured as the distance from the tips of the toes of one paw to the following step, and the average of ten distances was calculated per trial.

MRI

For the MRI experiments, mice were anesthetized in an induction chamber with 3–4% isoflurane in medical air and maintained with 1–2% isoflurane during the process. Anesthetized animals were placed in a custom-made animal holder with movable bite and ear bars and positioned fixed on the magnet chair. This allowed precise positioning of the animal with respect to the coil and the magnet and avoided movement artifacts. The body temperature was kept at approximately 37°C using a water blanket and the animals were monitored using a MRI-compatible temperature control unit (MultiSens Signal conditioner, OpSens, Quebec, Canada). Experiments were carried out in a horizontal 7 T scanner with a 30-cm diameter bore (Biospec 70/30v, Bruker Medical, Ettlingen, Germany). The system had a 675 mT/m actively shielded gradient coil (Bruker, BGA 12-S) of 11.4 cm inner diameter. A 1H rat brain receive-only phase array coil with integrated combiner and preamplifier, no tune/no match, in combination with the actively detuned transmit-only resonator (Bruker BioSpin MRI GmbH, Germany) was employed. Data were acquired with a Hewlett-

Packard console running Paravision software (Bruker Medical GmbH, Ettlingen, Germany) operating on a Linux platform.

T2-weighted anatomical images to position the animal were collected in the three orthogonal orientations using a rapid acquisition relaxation enhanced sequence (RARE), applying the following parameters: field of view 40 × 40 mm, 15 slices, slice thickness 1 mm, matrix 256 × 256, effective echo time 56 ms, repetition time 2 s, RARE factor of 8, 1 average and a total acquisition time of 1 min 4 s [45–47].

To quantify the rate of spinal cord repair, the average illuminated pixel density of the lesion in each mouse was calculated and normalized to the average illuminated pixel density of an adjacent region of the spinal cord. The average illuminated pixel density was calculated using image processing software (ImageJ, National Institute of Health [NIH], USA). In this manner, a value of 1 would indicate that the pixel density of the lesion and adjacent spinal cord was the same, while below and above 1 would indicate that the lesion was darker or lighter, respectively. The spinal cord lesion in the MRI was observed as a darkened region, thus, the relative value obtained would be below 1.

Immunohistochemistry

The mice were anesthetized with isoflurane and spinal cords fixed with 4% paraformaldehyde in phosphate buffer (pH 7.4) overnight. After fixation, the spinal cords were placed in Osteosoft (Merck Millipore) solution for 5 days, in order to decalcify the vertebrae. Then, the tissue was placed in paraffin and transverse sections of 16 μm were obtained and mounted on slides. Only the sections where the SCI was performed (at the T9 level) were studied.

First, the tissue samples were permeabilized with 0.25% triton, then incubated at room temperature in PBS with 10% goat serum and 5% bovine albumin to block nonspecific binding of the primary antibody. Afterwards, the slides were incubated overnight with one of the following primary antibodies: mouse or rabbit anti-GFP (1:200, Molecular Probes, OR, USA), mouse anti-Tuj1 (1:1000, Covance Madrid, Spain), rat anti-GFAP (1:500, Calbiochem, Merck Millipore, Billerica, MA, USA), rabbit anti-BDNF (1:200, Santa Cruz Biotechnology, CA, USA), and sheep anti-neurotrophin-3 (NT-3) and anti-neurotrophin-4/5 (NT-4/5) (1:100 in both cases, Chemicon/Millipore, MA, USA). The slides were then incubated with one of the following secondary antibodies: anti-mouse Alexa Fluor 488 (1:500, Molecular Probes, Life Technologies, Madrid, Spain) for GFP, and biotinylated secondary antibodies for the rest (1:200, Vector Laboratories, CA, USA), which were then incubated with

streptavidin conjugated with Cy3 (1:500). For nuclei staining DAPI (Molecular Probes, Life Technologies, Madrid, Spain) was used. In samples where DAB staining was used instead of immunofluorescence, secondary antibodies conjugated with peroxidase were used and the tissue counterstained with cresyl violet (Acros Organics, Belgium). The slides were then analyzed using a Leica fluorescence microscope and images taken using the system's image software (Leica DMR, Leica Microsystems, Barcelona, Spain).

For motor neuron counting, a total of 10 sections were used per mouse and group (sham- and stem cell-treated mice, at 2, 4 and 6 months) staining for Tuj1, a motor neuron marker. The average number of motor neurons per section was calculated per group.

Conventional & real-time, quantitative PCR

Total mRNA of the cells was isolated using the Trizol protocol (Invitrogen Life Technologies, Spain). In the case of standard PCR analysis, the mRNA was reverse-transcribed using the Quantitect Reverse Transcription kit (QIAGEN), processed with the QIAGEN Multiplex PCR kit, and run on the QIAxcel apparatus. For real-time PCR, mRNA was reverse-transcribed to cDNA and amplified using Power SYBR Green Master mix (Applied Biosystems Foster City, CA, USA). The samples were analyzed in triplicate using the StepOne Plus Real-Time PCR system (Applied Biosystems, Foster City, CA, USA). Quantification was performed using the ΔC(T) method relative to GAPDH (forward: AGGTCGGTGTGAACGGATTTG; reverse: GGGGTCGTTGATGGCAACA), and normalized with respect to control conditions, as in previous reports [43]. The primer sequences used were taken from the PrimerBank webpage [57], while the muscle markers were taken from a previous publication [48]: NT4 (forward: TGAGCTGGCAGTATGCGAC; reverse: CAGCGCGTCTCGAAGAAGT), BDNF (forward: TCATACTTCGGTTGCATGAAGG; reverse: GTCCGTGGACGTTTACTTCTTT), NT3 (forward: AGTTTGCCGGAAGACTCTCTC; reverse: GGGTGCTCTGGTAATTTTCCTTA), GFP (forward: CTGCTGCCCGACAACCA; reverse: GAACTCCAGCAGGACGACGACCATGTG), Nnt (forward: GGGTCAGTTGTTGTGGATTTAGC; reverse: GCCTTCAGGAGCTTAGTGATGTT), Snx10 (forward: AGAGGAGTTCGTGAGTGTCTG; reverse: CTTTGGAGTCTTTGCCTCAGC), Ankrd1 (forward: GCTGGTAACAGGCAAAAAGAAC; reverse: CCTCTCGCAGTTTCTCGCT), Rtn4 (forward: TGCCTTCATTGTTTGTCGGG; reverse: TTCCTAGCTGCTGATAGGCGA), Mt2 (forward: GCCTGCAAATGCAAACAATGC; reverse: AGCTGCACTTGTCGGAAGC), Myf5

(forward: AAGGCTCCTGTATCCCCTCAC; reverse: TGACCTTCTTCAGGCGTCTAC), Mef2c (forward: ATCCCGATGCAGACGATTCAG; reverse: AACAGCACACAATCTTTGCCT), Myog (forward: CTGTTTAAGACTCACCCTGAGAC; reverse: GGTGCAACCATGCTTCTTCA).

Statistical analysis

Statistical significance between control and experimental groups was calculated with Sigmaplot v.12.0 software (Systat Software, San Jose, CA, USA), using the one-way ANOVA test, establishing the level of significance at $p < 0.05$. Values are measured as mean ± standard deviation.

Results

Stem cell injection into the hindlimb muscles improves motor functions in mice with SCI.

The mice were submitted to the surgical intervention after SCI and separated into two groups: control mice where only culture medium was injected (sham) and the experimental group which was injected with 106 bone marrow-derived mesenchymal stem cells isolated from GFP-transgenic mice (TX MSC). The culture medium or stem cells, depending on the experimental group, were injected into the quadriceps femoris of the mice, with a total volume of 10 µl in each limb. After the treatment, the mice were analyzed on a monthly basis, submitting them to behavior tests and analyzed by MRI. In the case of the behavior tests, two tests were performed, treadmill and footprint. Since the crushing injury that was performed on the mice resulted in an incomplete lesion of the spinal cord, the mice retained at least part of their hindlimb motor skills. In the case of the sham controls, there was no indication of improvement in either of the two behavior tests performed (Figure 1A). The histograms are represented as the relative value with respect to the scores obtained from each mouse in the first month. The scores obtained from each mouse in the behavior tests vary greatly from each other; thus, to study the progress of the mice, each one is studied individually. To this end, the scores obtained by each mouse in the behavior tests are divided by the initial score (obtained in the first month), obtaining a relative value (as shown in Figure 1A), so that if the scores obtained in the consecutive months were greater than 1, this indicated that the mouse presented improvements in the behavior tests compared to the initial value, and vice versa (i.e., a relative value below 1 indicated that the mice worsened).

In the first analysis of the footprint test, performed 1 month after the surgical intervention, the footprints were mostly incomplete, with the mice mainly dragging one or both hindlimbs throughout the test (Figure 1B).
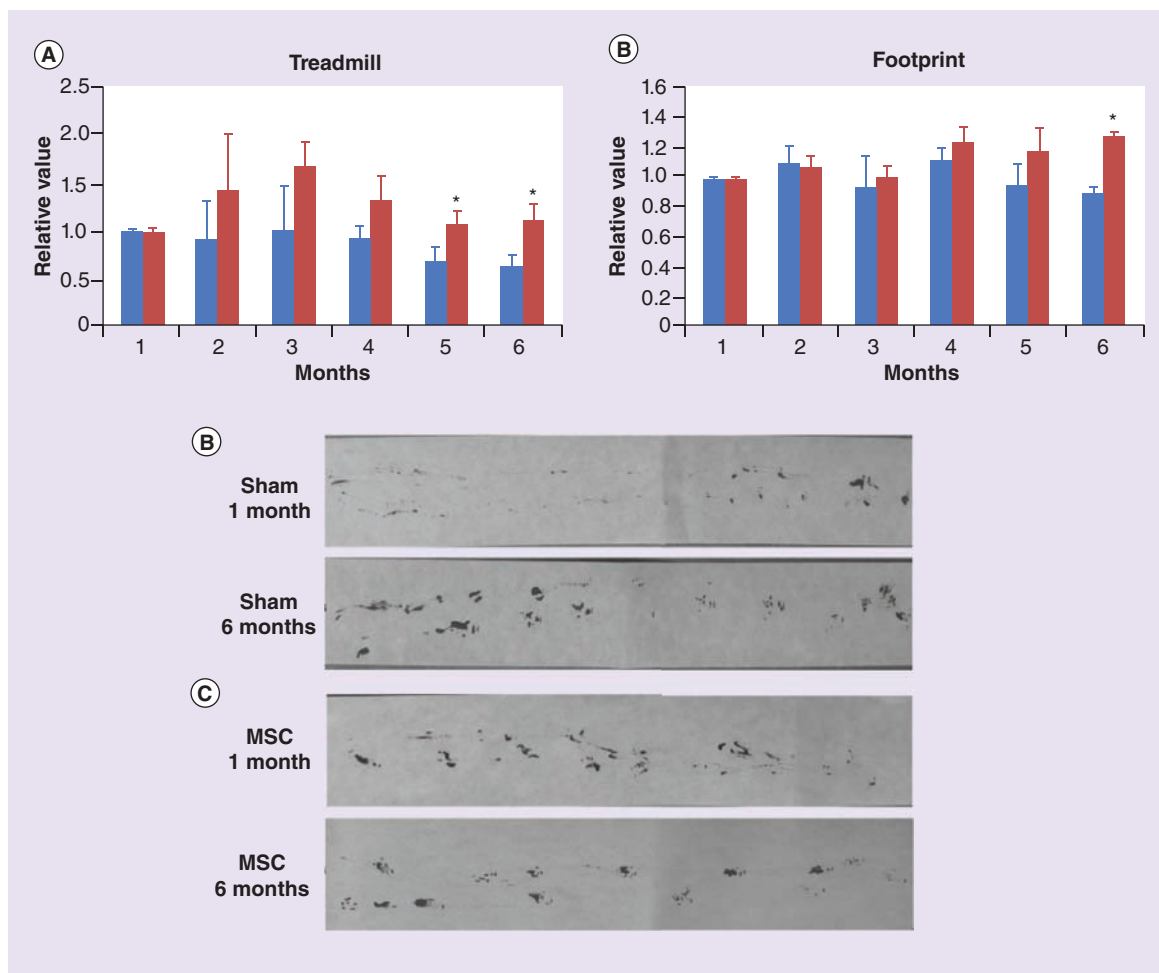
Figure 1. Results of the treadmill and footprint tests. (A) Histograms depicting the results obtained from the treadmill (maximum speed attained) and footprint (stride length) tests. The blue bars represent the sham controls, which were compared with the mesenchymal stem cell-treated group depicted in red (n = 12 in each group). Both groups were compared to the values obtained in the first month analyzed, which was normalized to 1, so that values above and below 1 indicate improvement or loss of motor skills, respectively. **(B & C)** Image taken from a sham control **(B)** and a mesenchymal stem cell-treated mouse **(C)** of the footprint assay at the first and last month of the study. In the first analysis, both groups showed clear loss of proper walking skills, with few complete footprints. At 6 months, the sham control presented a small degree of improvement, while the stem cell-treated mouse presented an almost normal walking ability.
*p < 0.05.
MSC: Mesenchymal stem cell.
For color images please see online www.futuremedicine.com/doi/full/10.2217/rme.14.38

However, 6 months after the intervention, the footprints were more pronounced with a larger number of complete footprints, although the stride length remained unchanged.

In the case of the mice treated with mesenchymal stem cells, there was a significant improvement compared with initial values (scores obtained in the first month of analysis) at 5–6 months after the intervention (Figure 1A & C). This was observed both in the treadmill and the footprint tests. In the latter case, at 1 month postintervention the same paw-dragging and incomplete footprints were observed. However, at 6 months, the footprints were almost as those observed in healthy mice, in terms of the full footprint (palm and fingers), with little to no dragging.

Mesenchymal stem cells accelerate spinal cord repair

MRI was used to analyze the progression of the injury in the spinal cord during the whole time of experimentation, on a monthly basis. The injury could be observed as a darkened region in the spinal cord, corresponding to a thinning of the damaged area (Figure 2A). Initially the images observed in both experimental groups were very similar; however, as the months passed, the spinal cords of the
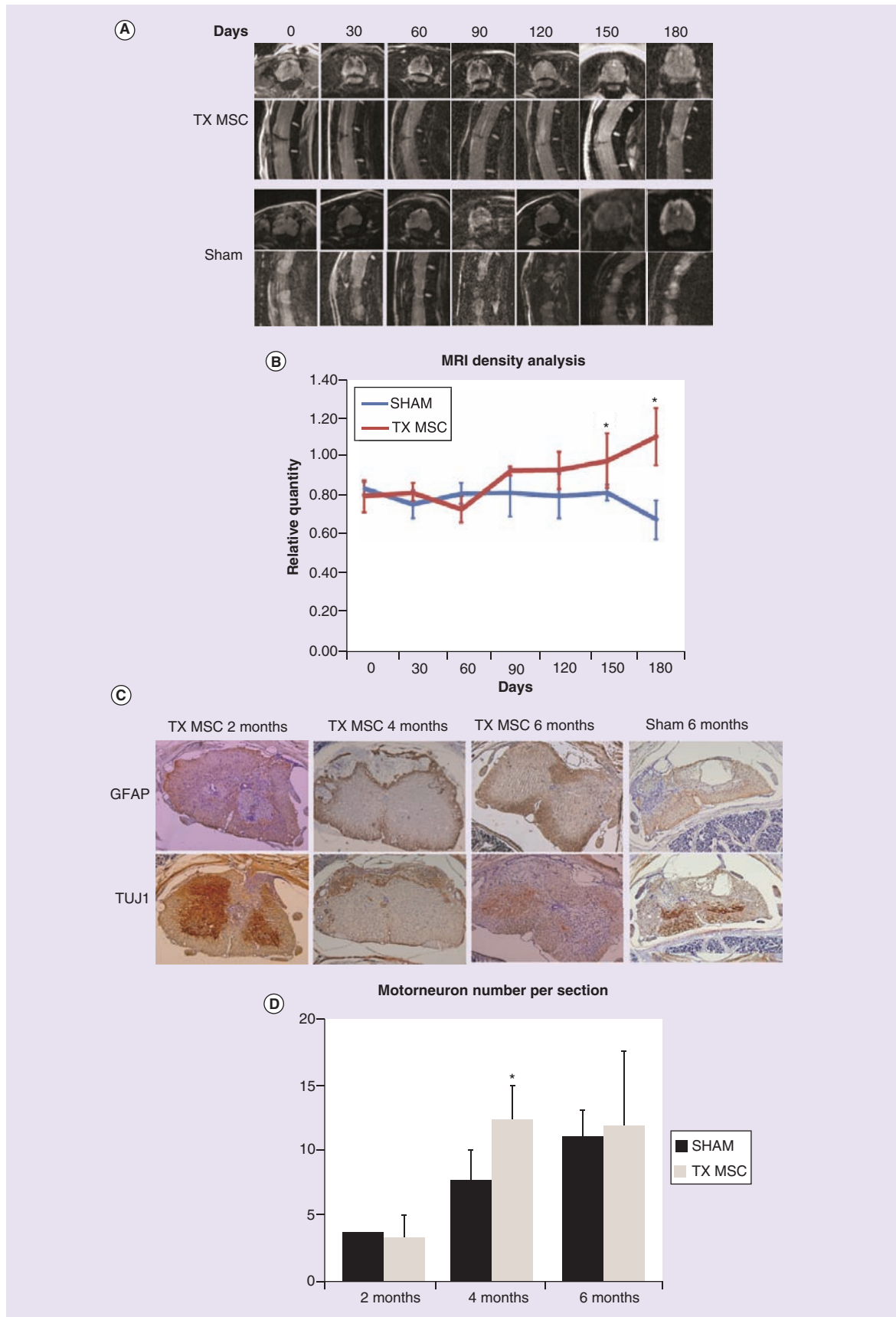
Figure 2. MRI and histological analysis of the spinal cords (see facing page). (A) MRI images taken from a TX MSC and sham control mice, at different time points up to 6 months after the surgical treatment. The top images of each group correspond to horizontal sections and the bottom images to sagittal sections. **(B)** MRI density analysis of the images taken at the different time points. In the histogram, relative quantity is the average illuminated pixel density of the lesion with respect to nearby healthy spinal cord. n = 12 in each group. **(C)** Immunohistochemical images of TX MSC at 2, 4 and 6 months (sham-injected mice also shown at 6 months) after the spinal cord lesion and stem cell injection, staining for GFAP and Tuj1 and counter-stained with violet-cresyl. Images taken at 100×. **(D)** Histogram depicting the number of motor neurons detected (Tuj1+) per section in the sham and treated groups. n = 4 in each group.
*p < 0.05.
TX-MSC: Mesenchymal stem cell treated mice.
For color images please see online www.futuremedicine.com/doi/full/10.2217/rme.14.38

mice treated with mesenchymal stem cells seemed to visually improve, with a progressively smaller darkened/damaged region. To quantify the possible regeneration of the spinal cord, the illuminated pixel density was calculated in the damaged region and normalized with nearby healthy spinal cord of the same mice (Figure 2B). Initially, both sham- and stem cell-treated groups presented similar values. However, the stem cell-treated mice presented progressively higher values after each passing month, these values being significant compared with sham controls at 5 months after the surgical intervention. At 6 months, the average illuminated pixel density values of the lesion compared to the adjacent spinal cord in the stem cell-treated mice were very similar. The values obtained in the sham controls, on the other hand, did not significantly change throughout the whole time of experimentation.

Immunohistochemical analysis was performed at 2, 4 and 6 months postintervention in both sham- and stem cell-treated mice. The spinal cords showed clear signs of mechanical damage in both groups of mice, including posterior horn destruction, the presence of cavities and neuronal cell loss. However histological differences were observed after 6 months between the sham- and stem-cell treated groups (Figure 2C). Whereas the spinal cord remained greatly injured in the sham controls, with little improvement, the stem cell-treated group presented a more normal anatomy.

Furthermore, the number of motor neurons observed per section was calculated in the sham- and stem cell-treated groups at the different time points (Figure 2D). As observed in the MRI analysis, after 4 months of the spinal cord lesion, a significant increase in the number of motor neurons was observed in the stem cell-treated group compared with the sham-treated group, with similar numbers observed after 6 months of the lesion. The sham-treated group presented an increased number of motor neurons at a slower rate, being equal to the stem-cell treated group after 6 months of the lesion. These results seemed to indicate that the stem cell treatment accelerated motor neuron repair.

Neurotrophic factors BDNF, NT3 & NT4 are secreted & released into the muscle tissue by the grafted stem cells

At 2, 4 and 6 months after the surgical intervention, the hindlimb muscles where stem cells were injected were analyzed by PCR to confirm the presence of the grafted cells (Figure 3A). This data was corroborated by immunohistochemistry, where the coexpression of several trophic factors and *GFP* were also evidenced (Figure 3B). Quantitative, real time PCR indicated that the expression of neurotrophic factors *BDNF, NT3* and *NT4* were upregulated in the muscle tissue where stem cells were grafted (Figure 3C). Other factors were also analyzed, but only the three previously mentioned were upregulated compared with sham controls (data not shown). The three factors are known to be implicated in neuronal survival, repair and regeneration, thus they are possible candidate factors that may be retrogradely transported into the motor neurons and inducing the regeneration processes observed in the spinal cord. Our previous works have demonstrated that bone marrow-derived mesenchymal stem cells are capable of producing and secreting *BDNF, NT3* and *NT4*, and can increase their local expression in response to adverse conditions affecting the nervous system [43].

Muscle regeneration & protection is enhanced by stem cell injection

SCI includes motor neuron cell death by direct mechanical and neurotoxic effects derived from posttraumatic hypoxia and inflammation, which eventually causes muscle atrophy in the deinnervated fibers and overall muscle tissue degeneration. Thus, muscle regeneration and survival markers were analyzed in the hindlimb muscle tissues that were treated with mesenchymal stem cells. A total of eight genes were analyzed, comparing wild-type and sham controls of the same ages (Figure 3D). The sham-operated mice presented a significant downregulation of almost all the muscle-regenerating related genes, with the exception of *MEF2C* and myogenin *(MYOG)*. This indicated a significant degenerating process in the muscle tissue and limited regeneration, which lasted throughout the
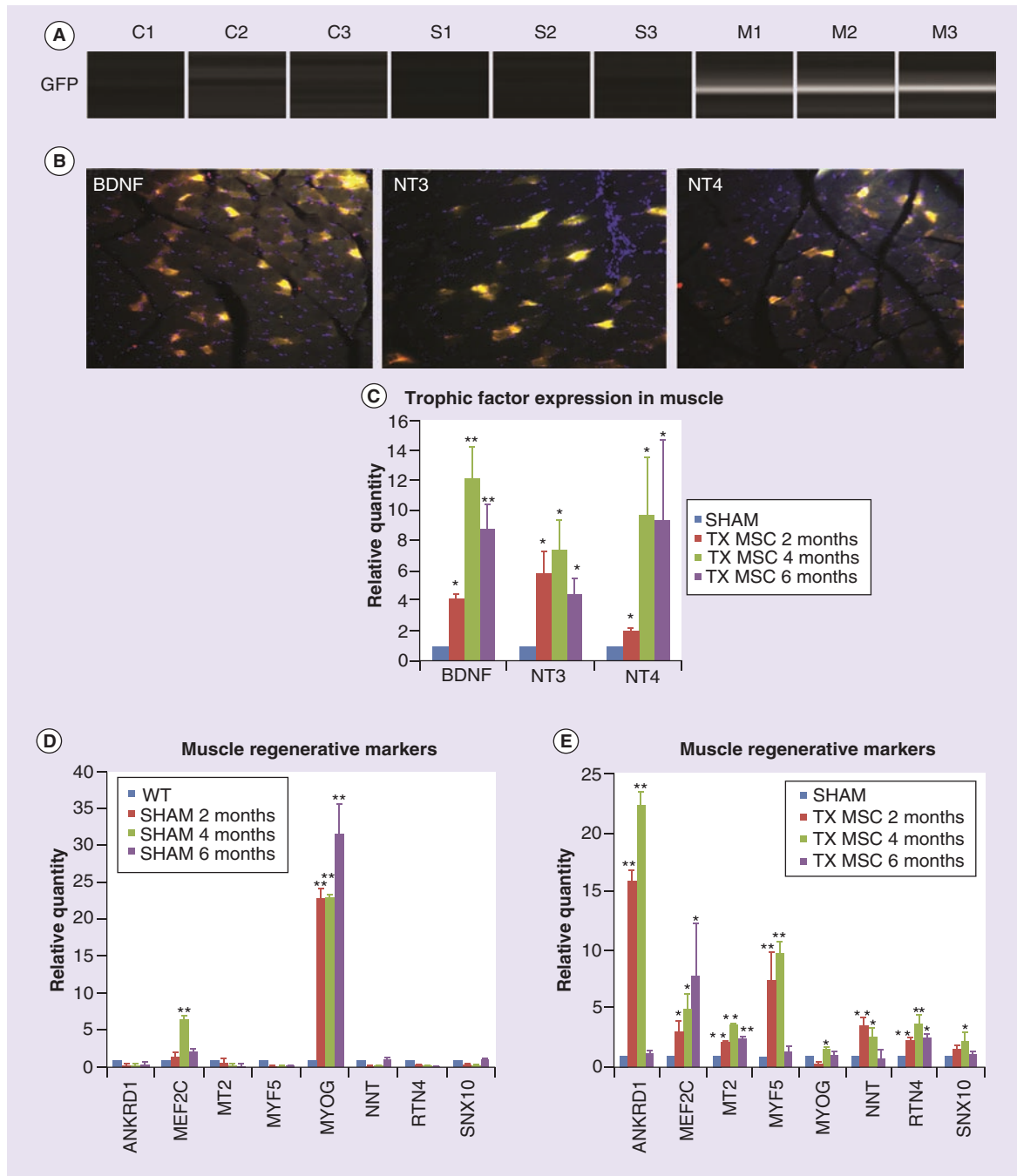
Figure 3. Analysis of the muscle tissue. (A) Conventional PCR of 3 control, 3 sham and 3 mesenchymal stem cell-treated mice analyzed for *GFP* expression, performed 6 months after the surgical intervention in the case of the sham and stem cell-treated groups. **(B)** Immunohistochemical analysis of the hindlimb muscle tissue in mice treated with GFP-expressing mesenchymal stem cells. *GFP* is shown in green, the trophic factors *BDNF, NT3* and *NT4* in red, and nuclei stained with DAPI. Images taken at 100×. **(C)** Quantitative PCR analysis of the expression of trophic factors *BDNF, NT3* and *NT4* in sham and stem cell-treated mice at 2, 4, and 6 months after the surgical intervention. The stem cell-treated groups were compared with the sham-operated group of their respective time point (sham 2 months vs TX MSC 2 months, etc). **(D)** Quantitative PCR analysis of the expression of muscle regeneration markers in wild-type and sham-operated mice at 2, 4 and 6 months after the surgical intervention. **(E)** Quantitative PCR analysis of the expression of muscle regeneration markers in sham- and stem cell-treated mice at 2, 4 and 6 months after the surgical intervention. The stem cell-treated groups were compared to the sham-operated group of their respective time point (sham 2 months vs TX MSC 2 months, etc). n = 4 in each group.
*p < 0.05; **p < 0.01.
For color images please see online www.futuremedicine.com/doi/full/10.2217/rme.14.38

whole time of experimentation. *ANKRD1* is implicated in muscle plasticity; *MEF2C, MYF5* and *MYOG* are implicated in muscle regeneration processes; *MT2* is related to oxidative stress in the muscle and muscle atrophy; nicotinamide nucleotide transhydrogenase (NNT) and *SNX10* are related to muscle metabolism; and finally, *RTN4* is related to deinnervation [48].

However, the expression pattern of these genes greatly differed in the mesenchymal stem cell-treated mice compared with the sham controls (Figure 3E). All the analyzed genes were upregulated compared with sham controls after 2 months of the intervention in the stem cell-treated groups, which continued at 4 months. The increased expression of these genes indicated an induction of regenerative processes in the muscle fibers, which was observed in the muscles where stem cells were injected. At the last time point, 6 months, the expression of almost all the genes analyzed lowered to standard levels (in many cases similar to wild-type values, data not shown), possibly indicating a finalization of the active regenerative process and normalization of the muscular tissue.

Discussion

In this work we have demonstrated that mesenchymal stem cells can accelerate neural regeneration after an acute, incomplete spinal cord lesion when grafted into the skeletal muscle. This in turn allowed the treated mice to significantly improve in their motor skills, obtaining better scores as early as 5 months after injection, while control mice did not present signs of improvement at any moment during the experimental procedure. Previous studies in our laboratory demonstrated this property in a neurodegenerative motor neuron mouse model [40], where the bone marrow stem cells, when transplanted into hindlimb muscles, secreted trophic factors that were captured by the motor end plates and retrogradely transported into the spinal cord. The expression of known soluble factors that are involved in neural regeneration and protection, such as *BDNF, NT3* and *NT4*, were detected by the grafted stem cells. Mesenchymal stem cells are known to upregulate the expression and increase secretion of these trophic factors under adverse conditions, as a paracrine protective effect [43].

One of the aspects that was observed in this work was an increase in the number of motorneurons in the spinal cord throughout the time of experimentation (Figure 2C & D). This was detected both in the sham- and stem cell-treated mice; however, there was a higher number of motor neurons in the stem cell-treated mice compared with the sham controls at 4 months. At 6 months, both groups presented similar values. This observation seems to indicate that the type of injury performed, which is an incomplete lesion by compres-

sion, allows for a certain degree of spontaneous repair in the spinal cord. Indeed, the fact that fewer motor neurons were detected by immunohistochemistry at the earliest time point, 2 months, followed by an increase in number at 4 and 6 months is most probably due to repair mechanisms of damaged motor neurons, and not neurogenesis.

Besides an improvement in motor skills and partial neural recovery, an increase in the expression of molecules involved in muscle regeneration and protection was detected. Spinal cord lesion causes muscle denervation and ultimately muscular atrophy, thus skeletal muscle-protective markers, as well as those implicated in regeneration, are important aspects to consider. The sham-operated mice presented a down-regulation of almost all the genes analyzed related to muscle regeneration, with the exception of *MYOG* and *MEF2C*. This may indicate that the hindlimb muscles were undergoing degenerative processes, quite possibly due to deinnervation. In turn, mesenchymal stem cell-injected mice presented increased levels of expression of all the myo-regenerative genes analyzed, indicating a local effect, besides a direct or indirect effect on the spinal cord.

Several trophic factors were analyzed in the muscle tissue, with *BDNF, NT3* and *NT4* being the most highly expressed. Other factors included epidermal growth factor (EGF), fibroblast growth factor 2 (FGF2), insulin-like growth factor (IGF), GDNF and nerve growth factor (NGF), but none presented increased expression values compared with the sham-operated mice (data not shown). These three trophic factors are known to induce neuroregeneration in the damaged spinal cord both *in vitro* and *in vivo*, and have been linked to motor function improvement [49,50]. Furthermore, there is a previous study demonstrating that retrograde delivery of BDNF from the skeletal muscle by adenovirus-mediated gene delivery exerted a neuroprotective and oligodendrocytic-protective effect in a genetic mouse model of spontaneous spinal cord compression [51]. Our laboratory has also proven that bone marrow stem cells are capable of this effect in another genetic motor neuron degenerative model [40].

There are many published reports demonstrating the beneficial effects of bone marrow-derived stem cells in SCI, even resulting in significant functional recovery [8–23]. In several of these works, the majority of which have been performed in rats, functional recovery was detected as early as 1–2 months after treatment, compared with the 5 months detected in this study. Few of these studies, however, have analyzed the effect of the treatment at the time frame used here, where the mice were studied up to 6 months after treatment. Thus, the long-term effect

of the treatments analyzed in these studies cannot be known. Furthermore, these works have mainly focused on direct stem cell injection into the spinal cord, which is a potentially dangerous surgical intervention that may cause further damage to the tissue. Other methods of administration that have been used include intravenous administration or lumbar puncture [52–54]. These two methods have the advantage of eliminating the risk of further tissue damage, and the cells are capable of migrating to the lesion where they exert their effect. However, these approaches have the disadvantage of low percentage of engraftment, with less than 4% of the cells migrating and integrating into the lesion site [55]. Thus, for these methods to be effective it is necessary to inject a large number of stem cells, which may be a handicap as the stem cells must be harvested and expanded in culture until the appropriate cell number is reached. This is very relevant when considering these approaches be used during the acute stage of the lesion, when repair and regeneration mechanisms are possible.

As previously commented, there are several studies, including from our lab, that have shown that bone marrow-derived stem cells are capable of exerting similar effects when grafted into the hindlimb muscles [39,40], by releasing soluble factors that are captured by the motor-end plates and transported to the motor neuron cell body in the spinal cord. These works, which are a similar approach as with intravenous or intrathecal injections [52–54] without the low level of engraftment, have indicated that this approach is potentially even more effective than direct injection to the spinal cord, as it avoids the potential puncture damage, as well as protects not only the motor neuron but its axonal projection as

well. In this work, of the trophic factors secreted, *BDNF* is of utmost importance as it has been shown to induce nerve growth and overall neuronal survival [18]. In fact, exogenous administration of *BDNF* has been shown to promote regeneration of sensory neurons after SCI [56]. Thus, the mesenchymal stem cells may be acting as a biological pump that releases this trophic factor to the surrounding tissue, which is captured by the motor-end plates and retrogradely transported to motor neurons, and ultimately activating repair/regeneration mechanisms.

In conclusion, bone marrow-derived mesenchymal stem cell injection into the hindlimb muscles in a mouse model of thoracic incomplete, acute SCI is capable of enhancing spinal cord repair, ultimately resulting in motor function improvement 5 months after the surgical treatment. Owing to the relative simplicity and little invasive method of the approach, this is a feasible method to use in the clinic to treat incomplete spinal cord lesions in humans soon after injury, either by using autologous (bone marrow extraction and several weeks of culture to increase stem cell number, or directly by cell-sorting the adequate cell population) or allogeneic-derived stem cells.

Future perspective
Numerous studies demonstrate that bone marrow-derived stem cells present a potentially beneficial effect on SCI. However, in the clinic this has been met with limited success, which is possibly, at least partially, due to the method of administration, as the stem cells have been directly injected into the lesion site. This may cause further damage, hampering their efficacy. Previous results using motor neuron degenerative mouse models have shown that bone marrow

Executive summary

Stem cell injection into the hindlimb muscles improves motor functions in mice with spinal cord injury
- The mice treated with bone marrow-derived mesenchymal stem cells presented significantly better scores in the treadmill (maximum running speed) and footprint (longer stride lengths) tests.
- The non-treated mice, on the other hand, did not improve in any of the tests performed throughout the whole time of experimentation.

Mesenchymal stem cells, when grafted into the muscle tissue of mice with spinal cord injury, release numerous soluble factors that induce repair mechanisms
- The spinal cords of the stem cell-treated mice presented signs of accelerated repair mechanisms, analyzed both by MRI and immunohistochemistry.
- This was due to the release of trophic factors, such as BDNF, NT3 and NT4, which are known to activate prosurvival mechanisms and regeneration.

Muscle regeneration & protection is enhanced by stem cell injection
- After spinal cord injury, there is a deinnervation of the muscles, which ultimately causes muscle atrophy.
- In our experiments, upregulation of muscle regeneration and repair markers was detected in the hindlimbs of the stem cell-treated mice, compared with non-treated sham controls.
- This indicates the presence of a local repair effect of the stem cells in the hindlimb muscles besides the retrograde effect in the motor end plates.

stem cells can exert similar effects when transplanted into the skeletal muscle tissue, by releasing trophic factors that are captured by the motor-end plates that innervate the muscle. The factors then travel retrogradely to the motor neuron cell body, activating prosurvival mechanisms while improving motor functions. The work presented in this study demonstrates that it is possible to extrapolate this surgical method into an acute SCI model. Due to the feasibility of the approach, the little invasive and low risk that it presents, this work may allow, in the next few years, clinical trials administering intramuscularly bone marrow-derived stem cells in acute spinal cord lesions to induce repair and/or regeneration.

Ethical conduct of research

The authors state that they have obtained appropriate institutional review board approval or have followed the principles outlined in the Declaration of Helsinki for all human or animal experimental investigations. In addition, for investigations involving human subjects, informed consent has been obtained from the participants involved.

References

Papers of special interest have been highlighted as:
• of interest; •• of considerable interest

1   Budh CN, Osteraker AL. Life satisfaction in individuals with a spinal cord injury and pain. *Clin. Rehabil.* 21, 89–96 (2007).

2   Bracken MB. Steroids for acute spinal cord injury. *Cochrane Database Syst. Rev.* 1, CD001046 (2012).

3   Bracken MB, Collins WF, Freeman DF *et al.* Efficacy of methylprednisolone in acute spinal cord injury. *J. Am. Med. Assoc.* 251, 45–52 (1984).

4   Bracken MB, Shepard MJ, Collins WF *et al.* Methylprednisolone or naloxone treatment after acute spinal cord injury: 1-year follow-up data. Results of the second national acute spinal cord injury study. *J. Neurosurg.* 76, 23–31 (1992).

5   Bracken MB, Shepard MJ, Collins WF *et al.* A randomized, controlled trial of methylprednisolone or naloxone in the treatment of acute spinal-cord injury. Results of the second national acute spinal cord injury study. *N. Engl. J. Med.* 322, 1405–1411 (1990).

6   Tator CH. Update on the pathophysiology and pathology of acute spinal cord injury. *Brain Pathol.* 5, 407–413 (1995).

7   McDonald JW, Sadowsky C. Spinal-cord injury. *Lancet* 359, 417–425 (2002).

8   Sasaki M, Honmou O, Akiyama Y *et al.* Transplantation of an acutely isolated bone marrow fraction repairs demyelinated adult rat spinal cord axons. *Glia* 35, 26–34 (2001).

9   Akiyama Y, Radtke C, Honmou O, Kocsis JD. Remyelination of the spinal cord following intravenous delivery of bone marrow stromal cells. *Glia* 39, 229–236 (2002).

10 Akiyama Y, Radtke C, Kocsis JD. Remyelination of the rat spinal cord by transplantation of identified bone marrow stromal cells. *J. Neurosci.* 22, 6623–6630 (2002).

11 Chopp M, Zhang XH, Li Y *et al.* Spinal cord injury in rat: treatment with bone marrow stromal cell transplantation. *Neuroreport* 11, 3001–3005 (2000).

•• **First report indicating that bone marrow stem cells can activate repair mechanisms in spinal cord injury models.**

12 Hofstetter CP, Schwarz EJ, Hess D *et al.* Marrow stromal cells form guiding strands in the injured spinal cord and promote recovery. *Proc. Natl Acad. Sci. USA* 99, 2199–2204 (2002).

13 Wu S, Suzuki Y, Ejiri Y *et al.* Bone marrow stromal cells enhance differentiation of co-cultured neurosphere cells and promote regeneration of the injured spinal cord. *J. Neurosci. Res.* 72, 343–351 (2003).

14 Ankeny DP, McTigue DM, Jakeman LB. Bone marrow transplants provide tissue protection and directional guidance for axons after contusive spinal cord injury in rats. *Exp. Neurol.* 190, 17–31 (2004).

15 Koshizuka S, Okada S, Okawa A *et al.* Transplanted hematopoietic stem cells from bone marrow differentiate into neural lineage cells and promote functional recovery after spinal cord injury in mice. *J. Neuropathol. Exp. Neurol.* 63, 64–72 (2004).

16 Ohta M, Suzuki Y, Noda T, Ejiri Y *et al.* Bone marrow stromal cells infused into the rat cerebrospinal fluid promote functional recovery of the injured rat spinal cord with reduced cavity formation. *Exp. Neurol.* 187, 266–278 (2004).

17 Zurita M, Vaquero J. Functional recovery in chronic paraplegia after bone marrow stromal cells transplantation. *Neuroreport* 15, 1105–1108 (2004).

18 Neuhuber B, Timothy-Himes B, Shumsky JS, Gallo G, Fischer I. Axon growth and recovery of function supported by human bone marrow stromal cells in the injured spinal cord exhibit donor variations. *Brain Res.* 1035, 73–85 (2005).

19 Sigurjonsson OE, Perreault MC, Egeland T, Glover JC. Adult human hematopoietic stem cells produce neurons efficiently in the regenerating chicken embryo spinal cord. *Proc. Natl Acad. Sci. USA* 102, 5227–5232 (2005).

20 Sykova E, Jendlova P. Magnetic resonance tracking of implanted adult and embryonic stem cells in injured brain and spinal cord. *Ann. NY Acad. Sci.* 1049, 146–160 (2005).

21 Cízková D, Rosocha J, Vanický I, Jergová S, Cízek M. Transplantation of human mesenchymal stem cells improve functional recovery after spinal cord injury in the rat. *Cell Mol. Neurobiol.* 26, 1167–1180 (2006).

22 Himes BT, Neuhuber B, Coleman C *et al.* Recovery of function following grafting of human bone marrow-derived stromal cells into the injured spinal cord. *Neurorehabil. Neural Repair* 20, 278–296 (2006).

23 Vaquero J, Zurita M, Oya S, Santos M. Cell therapy using bone marrow stromal cells in chronic paraplegic rats: systemic or local administration? *Neurosci. Letts.* 398, 129–134 (2006).

24 Caplan AI. Adult mesenchymal stem cells for tissue engineering versus regenerative medicine. *J. Cell. Physiol.* 213, 341–347 (2007).

25 Syková E, Homola A, Mazanec R *et al.* Autologous bone marrow transplantation in patients with subacute and chronic spinal cord injury. *Cell Transplant.* 15, 675–687 (2006).

26 Deda H, Inci MC, Kürekçi AE *et al.* Treatment of chronic spinal cord injured patients with autologous bone marrow derived hematopoietic stem cell transplantation: 1-year followup. *Cytotherapy* 10, 565–574 (2008).

•• **First report of stem cell transplantation in spinal cord injury human subjects.**

27 Kumar AA, Kumar SR, Narayanan R, Arul K, Baskaran M. Autologous bone marrow derived mononuclear cell therapy for spinal cord injury: a Phase I/II clinical safety and primary efficacy data. *Exp. Clin. Transplant.* 7, 241–248 (2009).

28 Di Nicola M, Carlo-Stella C, Magni M *et al.* Human bone marrow stromal cells suppress T-lymphocyte proliferation induced by cellular or non-specific mitogenic stimuli. *Blood* 99, 3838–3843 (2002).

29 Bartholomew A, Sturgeon C, Siatskas M *et al.* Mesenchymal stem cells suppress lymphocyte proliferation *in vitro* and prolong skin graft survival *in vivo*. *Exp. Hematol.* 30, 42–48 (2002).

30 Jiang XX, Zhang Y, Liu B *et al.* Human mesenchymal stem cells inhibit differentiation and function of monocyte derived dendritic cells. *Blood* 105, 4120–4126 (2005).

31 Corcione A, Benvenuto F, Ferretti E *et al.* Human mesenchymal stem cells modulate B-cell functions. *Blood* 107, 367–372 (2006).

32 Abrams MB, Dominguez C, Pernold K *et al.* Multipotent mesenchymal stromal cells attenuate chronic inflammation and injury-induced sensitivity to mechanical stimuli in experimental spinal cord injury. *Restor. Neurol. Neurosci.* 27, 301–321 (2009).

33 Crigler L, Robey RC, Asawachaicharn A, Gaupp D, Phinney DG. Human mesenchymal stem cell subpopulations express a variety of neuro-regulatory molecules and promote neuronal cell survival and neuritogenesis. *Exp. Neurol.* 198, 54–64 (2006).

• **This report demonstrates that mesenchymal stem cells are capable of promoting neuronal survival and regeneration by releasing neurotrophic factors.**

34 Wright KT, El Masri W, Osman A *et al.* Bone marrow stromal cells stimulate neurite outgrowth over neural proteoglycans (CSPG), myelin associated glycoprotein and Nogo-A. *Biochem. Biophys. Res. Commun.* 354, 559–566 (2007).

35 Phinney DG, Baddoo M, Dutreil M, Gaupp D, Lai WT, Isakova IA. Murine mesenchymal stem cells transplanted to the central nervous system of neonatal versus adult mice exhibit distinct engraftment kinetics and express receptors that guide neuronal cell migration. *Stem Cells Dev.* 15, 437–447 (2006).

36 Son BR, Marquez-Curtis LA, Kucia M *et al.* Migration of bone marrow and cord blood mesenchymal stem cells *in vitro* is regulated by stromal-derived factor-1-CXCR4 and hepatocyte growth factor-c-met axes and involves matrix metalloproteinases. *Stem Cells* 24, 1254–1264 (2006).

37 d'Ortho MP, Will H, Atkinson S *et al.* Membrane-type matrix metalloproteinases 1 and 2 exhibit broad-spectrum proteolytic capacities comparable to many matrix metalloproteinases. *Eur. J. Biochem.* 250, 751–757 (1997).

38 Passi A, Negrini D, Albertini R, Miserocchi G, De Luca G. The sensitivity of versican from rabbit lung to gelatinase A (MMP-2) and B (MMP-9) and its involvement in the development of hydraulic lung edema. *FEBS Letts* 456, 93–96 (1999).

39 Suzuki M, McHugh J, Tork C *et al.* Direct muscle delivery of GDNF with human mesenchymal stem cells improves motor neuron survival and function in a rat model of familial ALS. *Mol. Ther.* 16, 2002–2010 (2008).

• **First report demonstrating that stem cells overexpressing neurotrophic factor GDNF and transplanted in the hindlimb muscles can increase motor neuron survival. The trophic factor is captured by the motor-end plates and retrogradely transported to the motor neuron soma in the spinal cord.**

40 Pastor D, Viso-Leon MC, Botella-López A, Moraleda JM, Jones J, Martinez S. Bone marrow transplantation in hindlimb muscles of motor-neuron degenerative mice reduces neuronal death and improves motor function. *Stem Cells Dev.* 22, 1633–1644 (2013).

• **This work, which is a follow-up of the previous reference, demonstrates that bone marrow stem cells, without further modifications, are capable of exerting a neuroprotective effect on the motor neurons when grafted in the hindlimb muscles.**

41 Curtis R, Green D, Lindsay RM, Wilkin GP. Up-regulation of GAP-43 and growth of axons in rat spinal cord after compression injury. *J. Neurocytol.* 22, 51–64 (1993).

42   Jones J, Jaramillo-Merchán J, Bueno C, Pastor D, Viso-León MC, Martínez S. Mesenchymal stem cells rescue Purkinje cells and improve motor functions in a mouse model of cerebellar ataxia. *Neurobiol. Dis.* 40, 415–423 (2010).

43   Jones J, Estirado A, Redondo C, Martinez S. Stem cells from wildtype and Friedreich's ataxia mice present similar neuroprotective properties in dorsal root ganglia cells. *PLoS ONE* 8, e62807 (2013).

44   Pastor D, Viso-Leon MC, Jones J *et al.* Comparative effects between bone marrow and mesenchymal stem cell transplantation in GDNF expression and motor function recovery in a motorneuron degenerative mouse model. *Stem Cell Rev. Rep.* 8, 445–458 (2012).

45   Hennig J, Friedburg H. Clinical applications and methodological developments of the RARE technique. *Magn. Reson. Imaging* 6, 391–395 (1988).

46   Hennig J, Nauerth A, Friedburg H. RARE imaging: a fast imaging method for clinical MR. *Magn. Reson. Med.* 3, 823–833 (1986).

47   Willenbrock S, Knippenberg S, Meier M *et al. In vivo* MRI of intraspinally injected SPIO-labelled human CD34+ cells in a transgenic mouse model of ALS. *In Vivo* 26, 31–38 (2012).

48   Calvo AC, Manzano R, Atencia-Cibreiro G *et al.* Genetic biomarkers for ALS disease in transgenic SOD1(G93A) mice. *PLoS ONE* 7, e32632 (2012).

49   Gu YL, Yin LW, Zhang Z *et al.* Neurotrophin expressions in neural stem cells grafted acutely to transected spinal cord of adult rats linked to functional improvement. *Cell Mol. Neurobiol.* 32, 1089–1097 (2012).

50   Quertainmont R, Cantinieaux D, Botman O *et al.* Mesenchymal stem cell graft improves recovery after spinal cord injury in adult rats through neurotrophic and pro-angiogenic actions. *PLoS ONE* 7, e39500 (2012).

51   Uchida K, Nakajima H, Hirai T *et al.* The retrograde delivery of adenovirus vector carrying the gene for brain derived neurotrophic factor protects neurons and oligodendrocytes from apoptosis in the chronically compressed spinal cord of twy/twy mice. *Spine* 37, 2125–2135 (2012).

••   **Demonstrates that the expression of neurotrophic factors in the skeletal muscle can induce neuroprotection in a spinal cord injury model by retrograde transport of the factor to the spinal cord.**

52   Corti S, Locatelli F, Donadoni C *et al.* Neuroectodermal and microglial differentiation of bone marrow cells in the mouse spinal cord and sensory ganglia. *J. Neurosci. Res.* 70, 721–733 (2002).

53   Satake K, Lou J, Lenke LG. Migration of mesenchymal stem cells through cerebrospinal fluid into injured spinal cord tissue. *Spine* 29, 1971–1979 (2004).

54   Bakshi A, Barshinger AL, Swanger SA *et al.* Lumbar puncture delivery of bone marrow stromal cells in spinal cord contusion: a novel method for minimally invasive cell transplantation. *J. Neurotrauma* 23, 55–65 (2006).

55   Courtney P, Samdani AF, Betz RR *et al.* Grafting of human bone marrow stromal cells into spinal cord injury: a comparison of delivery methods. *Spine* 34, 328–334 (2009).

56   Song XY, Li F, Zhang FH, Zhong JH, Zhou XF. Peripherally-derived BDNF promotes regeneration of ascending sensory neurons after spinal cord injury. *PLoS ONE* 3, e1707 (2008).

57   PrimerBank. http://pga.mgh.harvard.edu/primerbank